National Library of Canada
Acquisitions and Bibliographic Services Branch
395 Wellington Street
Ottawa, Ontario
K1A 0N4

Bibliothèque nationale du Canada
Direction des acquisitions et des services bibliographiques
395, rue Wellington
Ottawa (Ontario)
K1A 0N4

Your file Votre référence

Our file Notre référence

NOTICE

The quality of this microform is heavily dependent upon the quality of the original thesis submitted for microfilming. Every effort has been made to ensure the highest quality of reproduction possible.

If pages are missing, contact the university which granted the degree.

Some pages may have indistinct print especially if the original pages were typed with a poor typewriter ribbon or if the university sent us an inferior photocopy.

Reproduction in full or in part of this microform is governed by the Canadian Copyright Act, R.S.C. 1970, c. C-30, and subsequent amendments.

AVIS

La qualité de cette microforme dépend grandement de la qualité de la thèse soumise au microfilmage. Nous avons tout fait pour assurer une qualité supérieure de reproduction.

S'il manque des pages, veuillez communiquer avec l'université qui a conféré le grade.

La qualité d'impression de certaines pages peut laisser à désirer, surtout si les pages originales ont été dactylographiées à l'aide d'un ruban usé ou si l'université nous a fait parvenir une photocopie de qualité inférieure.

La reproduction, même partielle, de cette microforme est soumise à la Loi canadienne sur le droit d'auteur, SRC 1970, c. C-30, et ses amendements subséquents.

Canada

UNIVERSITY OF ALBERTA

KINETICS AND MECHANISM OF IODINATION, OXIDATION AND CATALATIC REACTIONS OF PEROXIDASES

by

© WEIMEI SUN

A THESIS

SUBMITTED TO THE FACULTY OF GRADUATE STUDIES AND RESEARCH

IN PARTIAL FULFILMENT OF THE REQUIREMENTS FOR THE DEGREE

OF DOCTOR OF PHILOSOPHY

DEPARTMENT OF CHEMISTRY

EDMONTON, ALBERTA

FALL 1994

National Library
of Canada

Acquisitions and
Bibliographic Services Branch

395 Wellington Street
Ottawa, Ontario
K1A 0N4

Bibliothèque nationale
du Canada

Direction des acquisitions et
des services bibliographiques

395, rue Wellington
Ottawa (Ontario)
K1A 0N4

Your file Votre référence

Our file Notre référence

The author has granted an irrevocable non-exclusive licence allowing the National Library of Canada to reproduce, loan, distribute or sell copies of his/her thesis by any means and in any form or format, making this thesis available to interested persons.

L'auteur a accordé une licence irrévocable et non exclusive permettant à la Bibliothèque nationale du Canada de reproduire, prêter, distribuer ou vendre des copies de sa thèse de quelque manière et sous quelque forme que ce soit pour mettre des exemplaires de cette thèse à la disposition des personnes intéressées.

The author retains ownership of the copyright in his/her thesis. Neither the thesis nor substantial extracts from it may be printed or otherwise reproduced without his/her permission.

L'auteur conserve la propriété du droit d'auteur qui protège sa thèse. Ni la thèse ni des extraits substantiels de celle-ci ne doivent être imprimés ou autrement reproduits sans son autorisation.

ISBN 0-315-95271-7

Canada

Name _____

Dissertation Abstracts International is arranged by broad, general subject categories. Please select the one subject which most nearly describes the content of your dissertation. Enter the corresponding four-digit code in the spaces provided.

_____ SUBJECT TERM

0	4	8	7

SUBJECT CODE

U·M·I

Subject Categories

THE HUMANITIES AND SOCIAL SCIENCES

COMMUNICATIONS AND THE ARTS

- Architecture 0729
- Art History 0377
- Cinema 0900
- Dance 0378
- Fine Arts 0357
- Information Science 0723
- Journalism 0391
- Library Science 0399
- Mass Communications 0708
- Music 0413
- Speech Communication 0459
- Theater 0465

EDUCATION

- General 0515
- Administration 0514
- Adult and Continuing 0516
- Agricultural 0517
- Art 0273
- Bilingual and Multicultural 0282
- Business 0688
- Community College 0275
- Curriculum and Instruction 0727
- Early Childhood 0518
- Elementary 0524
- Finance 0277
- Guidance and Counseling 0519
- Health 0680
- Higher 0745
- History of 0520
- Home Economics 0278
- Industrial 0521
- Language and Literature 0279
- Mathematics 0280
- Music 0522
- Philosophy of 0998
- Physical 0523
- Psychology 0525
- Reading 0535
- Religious 0527
- Sciences 0714
- Secondary 0533
- Social Sciences 0534
- Sociology of 0340
- Special 0529
- Teacher Training 0530
- Technology 0710
- Tests and Measurements 0288
- Vocational 0747

LANGUAGE, LITERATURE AND LINGUISTICS

- Language
  - General 0679
  - Ancient 0289
  - Linguistics 0290
  - Modern 0291
- Literature
  - General 0401
  - Classical 0294
  - Comparative 0295
  - Medieval 0297
  - Modern 0298
  - African 0316
  - American 0591
  - Asian 0305
  - Canadian (English) 0352
  - Canadian (French) 0355
  - English 0593
  - Germanic 0311
  - Latin American 0312
  - Middle Eastern 0315
  - Romance 0313
  - Slavic and East European 0314

PHILOSOPHY, RELIGION AND THEOLOGY

- Philosophy 0422
- Religion
  - General 0318
  - Biblical Studies 0321
  - Clergy 0319
  - History of 0320
  - Philosophy of 0322
- Theology 0469

SOCIAL SCIENCES

- American Studies 0323
- Anthropology
  - Archaeology 0324
  - Cultural 0326
  - Physical 0327
- Business Administration
  - General 0310
  - Accounting 0272
  - Banking 0770
  - Management 0454
  - Marketing 0338
- Canadian Studies 0385
- Economics
  - General 0501
  - Agricultural 0503
  - Commerce-Business 0505
  - Finance 0508
  - History 0509
  - Labor 0510
  - Theory 0511
- Folklore 0358
- Geography 0366
- Gerontology 0351
- History
  - General 0578
  - Ancient 0579
  - Medieval 0581
  - Modern 0582
  - Black 0328
  - African 0331
  - Asia, Australia and Oceania 0332
  - Canadian 0334
  - European 0335
  - Latin American 0336
  - Middle Eastern 0333
  - United States 0337
- History of Science 0585
- Law 0398
- Political Science
  - General 0615
  - International Law and Relations 0616
  - Public Administration 0617
- Recreation 0814
- Social Work 0452
- Sociology
  - General 0626
  - Criminology and Penology 0627
  - Demography 0938
  - Ethnic and Racial Studies 0631
  - Individual and Family Studies 0628
  - Industrial and Labor Relations 0629
  - Public and Social Welfare 0630
  - Social Structure and Development 0700
  - Theory and Methods 0344
- Transportation 0709
- Urban and Regional Planning 0999
- Women's Studies 0453

THE SCIENCES AND ENGINEERING

BIOLOGICAL SCIENCES

- Agriculture
  - General 0473
  - Agronomy 0285
  - Animal Culture and Nutrition 0475
  - Animal Pathology 0476
  - Food Science and Technology 0359
  - Forestry and Wildlife 0478
  - Plant Culture 0479
  - Plant Pathology 0480
  - Plant Physiology 0817
  - Range Management 0777
  - Wood Technology 0746
- Biology
  - General 0306
  - Anatomy 0287
  - Biostatistics 0308
  - Botany 0309
  - Cell 0379
  - Ecology 0329
  - Entomology 0353
  - Genetics 0369
  - Limnology 0793
  - Microbiology 0410
  - Molecular 0307
  - Neuroscience 0317
  - Oceanography 0416
  - Physiology 0433
  - Radiation 0821
  - Veterinary Science 0778
  - Zoology 0472
- Biophysics
  - General 0786
  - Medical 0760

EARTH SCIENCES

- Biogeochemistry 0425
- Geochemistry 0996
- Geodesy 0370
- Geology 0372
- Geophysics 0373
- Hydrology 0388
- Mineralogy 0411
- Paleobotany 0345
- Paleoecology 0426
- Paleontology 0418
- Paleozoology 0985
- Palynology 0427
- Physical Geography 0368
- Physical Oceanography 0415

HEALTH AND ENVIRONMENTAL SCIENCES

- Environmental Sciences 0768
- Health Sciences
  - General 0566
  - Audiology 0300
  - Chemotherapy 0992
  - Dentistry 0567
  - Education 0350
  - Hospital Management 0769
  - Human Development 0758
  - Immunology 0982
  - Medicine and Surgery 0564
  - Mental Health 0347
  - Nursing 0569
  - Nutrition 0570
  - Obstetrics and Gynecology 0380
  - Occupational Health and Therapy 0354
  - Ophthalmology 0381
  - Pathology 0571
  - Pharmacology 0419
  - Pharmacy 0572
  - Physical Therapy 0382
  - Public Health 0573
  - Radiology 0574
  - Recreation 0575
  - Speech Pathology 0460
  - Toxicology 0383
- Home Economics 0386

PHYSICAL SCIENCES

Pure Sciences

- Chemistry
  - General 0485
  - Agricultural 0749
  - Analytical 0486
  - Biochemistry 0487
  - Inorganic 0488
  - Nuclear 0738
  - Organic 0490
  - Pharmaceutical 0491
  - Physical 0494
  - Polymer 0495
  - Radiation 0754
- Mathematics 0405
- Physics
  - General 0605
  - Acoustics 0986
  - Astronomy and Astrophysics 0606
  - Atmospheric Science 0608
  - Atomic 0748
  - Electronics and Electricity 0607
  - Elementary Particles and High Energy 0798
  - Fluid and Plasma 0759
  - Molecular 0609
  - Nuclear 0610
  - Optics 0752
  - Radiation 0756
  - Solid State 0611
- Statistics 0463

Applied Sciences

- Applied Mechanics 0346
- Computer Science 0984
- Engineering
  - General 0537
  - Aerospace 0538
  - Agricultural 0539
  - Automotive 0540
  - Biomedical 0541
  - Chemical 0542
  - Civil 0543
  - Electronics and Electrical 0544
  - Heat and Thermodynamics 0348
  - Hydraulic 0545
  - Industrial 0546
  - Marine 0547
  - Materials Science 0794
  - Mechanical 0548
  - Metallurgy 0743
  - Mining 0551
  - Nuclear 0552
  - Packaging 0549
  - Petroleum 0765
  - Sanitary and Municipal 0554
  - System Science 0790
- Geotechnology 0428
- Operations Research 0796
- Plastics Technology 0795
- Textile Technology 0994

PSYCHOLOGY

- General 0621
- Behavioral 0384
- Clinical 0622
- Developmental 0620
- Experimental 0623
- Industrial 0624
- Personality 0625
- Physiological 0989
- Psychobiology 0349
- Psychometrics 0632
- Social 0451

UNIVERSITY OF ALBERTA

RELEASE FORM

NAME OF AUTHOR: WEIMEI SUN

TITLE OF THESIS: KINETICS AND MECHANISM OF IODINATION, OXIDATION AND CATALATIC REACTIONS OF PEROXIDASES

DEGREE: DOCTOR OF PHILOSOPHY

YEAR OF DEGREE GRANTED: 1994

Permission is hereby granted to THE UNIVERSITY OF ALBERTA LIBRARY to reproduce single copies of this thesis and to lend or sell such copies for private, scholarly or scientific research purposes only.

The author reserves other publication rights, and neither the thesis nor extensive extracts from it may be printed or otherwise reproduced without the author's written permission.

(Signed) weimei Sun

Date: Aug. 30, 1994

This thesis is dedicated to my dear parents.

THE UNIVERSITY OF ALBERTA

FACULTY OF GRADUATE STUDIES AND RESEARCH

The undersigned certify that they have read, and recommend to the Faculty of Graduate Studies and Research for acceptance, a thesis entitled " Kinetics and Mechanisms of Iodination, Oxidation and Catalatic Reactions of Peroxidases" submitted by Weimei Sun in partial fulfilment of the requirements for the degree of Doctor of Philosophy in Chemistry.

H. B. Dunford, Supervisor

G. Kotovych

J. W. Lown

M. Klobukowski

S. Jensen

P. W. Codding, **External Examiner**

Date Aug. 30, 1994

ACKNOWLEDGEMENTS

I wish to express my heartfelt gratitude to my supervisor, Professor H. Brian Dunford, for his invaluable guidance and help throughout my years of Ph. D. studies.

I also wish to acknowledge the Department of Chemistry for teaching and research assistantships. I thank the staff of the general office, purchasing office, and electronics shop of the Department of Chemistry who have been very cooperative throughout my years in the department.

I am grateful to have had the chance to work with Drs. Yuchiong Hsuanyu, Diana Metodiewa, Leah Marquez, Jing Huang and Marica Bakovic and Mr. Hongchang Zhang. I will always remember their kindness, friendship, encouraging support and their willingness to help. My sincere gratitude also goes to Dr. Stephane Alexandre, Mr. Morten Andersen and Ms. Stine Rasmunsen. Their cheerful presence made working in the lab a pleasant experience.

Thanks also goes to Mrs. Jackie Jorgensen for her gracious help and patience. Sincere gratitude is also due to Mr. Qihong Zhong for his gracious help of collecting porcine cerebella from the slaughterhouse and for his assistance with the SDS-PAGE analysis for the NO synthase purification. I must also extend my gratitude to Dr. Richard Schulz for his valuable input during my work of NO synthase purification. I also wish to thank all of my Ph. D. committee members for their helpful advice during my thesis preparation.

Finally, I am deeply grateful for the faithful support of my parents and my sister and brother. In closing, I gratefully acknowledge Prof. Zuyu Luo for her encouragement and understanding throughout all of the years of my studies.

ABSTRACT

The iodination of tyrosine is the first reaction in the biosynthesis of the thyroid hormone thyroxine. Because of this physiological significance, the kinetics and mechanism of the reaction catalyzed by both plant horseradish peroxidase (HRP) and mammalian lactoperoxidase (LPO) were studied using rapid scan spectral analysis and stopped-flow techniques. The difference in the catalytic abilities of the two sources of enzymes was clearly demonstrated by the mechanisms that fit the rate data. In both enzymatic iodination systems, native enzyme (Fe^{III}) reacts with H_2O_2 to form compound I ($Fe^{V}=O$). Compound I oxidizes I^- to become an enzyme-bound hypoiodite (Fe^{III}-O-I^-) from which free HOI is released. The role of HRP is to catalyze the formation of HOI, which reacts with excess I^- to form I_2 and I_3^-. Either I_2 or HOI or both can be the iodinating species (nonenzymatic iodination) in the HRP system. For the mammalian LPO, an LPO-bound hypoiodite, LPO-O-I^-, is an efficient iodinating species and under physiological conditions is probably the only iodinating agent. The overall iodination rate is about 10 times faster for LPO compared to HRP under comparable conditions. Our data show that HOI may be the inorganic iodination reagent. Our results also support the picture of a simple evolutionary progression: from the use of HOI free in solution to the use of the enzyme-bound hypoiodite as the iodinating agent.

The lactoperoxidase compound II (LPO-II)-catalyzed oxidation of Trolox C, a vitamin E water-soluble derivative, was investigated at pH values ranging from 3.0 to 7.0. The oxidation of Trolox C by LPO-II occurs initially by quantitative 1 : 1 binding to a site near the heme. The tighter binding of Trolox C at lower pH facilitates this reaction. A mechanism of Trolox C oxidation by LPO-II has been proposed in which protonation of an amino acid

residue on LPO-II (pK_a = 2.3) is essential. In addition, the ionization of the carboxylic acid group (pK_a = 4.03) on Trolox C accelerates the reaction rate. As an efficient antioxidant, Trolox C is more reactive at low pH values which correlates with the trend in lipid peroxidation. The second order rate constants for the oxidation of Trolox C by LPO-II were determined to be $(4.1 \pm 0.5) \times 10^6$ $M^{-1}s^{-1}$ for protonated Trolox C and $(1.9 \pm 0.3) \times 10^7$ $M^{-1}s^{-1}$ for deprotonated Trolox C.

Chloroperoxidase (CPO) is efficient as a catalase as well as a peroxidase. The catalatic activity of CPO exhibits saturation kinetics under steady state conditions, which is not observed with catalase under similar conditions. Our results indicate the formation of a complex with CPO compound I (CPO-I) and H_2O_2. The dissociation of this complex is the rate-determining step in the overall reaction that generates O_2 from H_2O_2. The demethylation of N,N,N',N'-tetramethyl-*p*-phenylenediamine (TMPD) by CPO was used to determine the peroxidatic activity of CPO. The catalatic activity of CPO was controlled by using a small amount of H_2O_2 compared to TMPD. The mechanism of the peroxidatic reaction catalyzed by CPO is identical to that established for HRP i.e., the modified ping-pong mechanism. However, by using comparable concentrations of H_2O_2 and TMPD, both the peroxidatic and catalatic reactions occur in the reaction system containing H_2O_2, TMPD and CPO. The catalatic activity of CPO is thus demonstrated to be affected by its peroxidatic activity and *vice versa*. In addition, the interaction of catalatic activity with peroxidatic activity is due to the competition of H_2O_2 and TMPD for CPO-I.

The reaction of CPO with HOCl was investigated at pH 6.2, ionic strength 0.11 M using both rapid scan and stopped-flow techniques. CPO-I

formation from CPO and HOCl has a second order rate constant of (4.0 ± 0.1) x 10^6 $M^{-1}s^{-1}$. Before the completion of CPO-I formation, CPO compound II (CPO-II) formation was observed. The presence of Cl^- in the mixture of CPO and HOCl does not affect the CPO-I formation rate but a saturation curve was obtained for CPO-II formation rate *versus* the Cl^- concentration. HOCl can bleach CPO and Cl^- cannot protect the enzyme from the bleaching. In contrast, a large amount of Cl^- can protect the bleaching of myeloperoxidase (MPO) by HOCl. The differences for CPO and MPO are speculated to be due to the different Cl^- binding to the enzymes.

The catalytic activity of HRP on the iodide oxidation was observed not to be inhibited by EDTA at pH from 3.5 to 5.0 and at EDTA concentration from 0 to 30 mM, which is 0 to 300-fold in excess of iodide concentration. Nevertheless, the pseudo-catalatic activity of HRP was inhibited by the presence of EDTA in the system. EDTA reacts with HOI with a second order rate constant of (2.6 ± 0.1) x 10^5 $M^{-1}s^{-1}$ at pH 3.5, ionic strength 0.18 M. The inhibition of EDTA on the pseudo-catalatic activity of HRP is due to its competition with H_2O_2 for HOI.

Nitric oxide synthase (NOS) was purified from porcine cerebella. The purified NOS monomer has a molecular weight of 128 KDa. The effects of EGTA, hematin and calmodulin concentrations on the NOS activity were examined. EGTA inhibits NOS activity and calmodulin enhances the activity. Hematin enhances the NOS activity when its concentration is less than the enzyme concentration but inhibition was observed when a high concentration of hematin was used. More than 70% of the total NOS activity was lost after the storage at -70°C for six days. The low yield and instability of NOS prevent us from doing some kinetic studies on NOS-catalyzed reactions.

TABLE OF CONTENTS

CHAPTER	PAGE
1. INTRODUCTION	
1.1 Peroxidases	1
1.1.1 Definition	1
1.1.2 Active site of peroxidase	2
1.1.3 Reaction of peroxidases	4
1.2 Horseradish Peroxidase (HRP)	5
1.3 Lactoperoxidase (LPO)	9
1.4 Chloroperoxidase (CPO)	13
1.5 Principles of Spectroscopy	18
1.6 Thyroid Hormones	19
1.7 Hydrolysis of Iodine in Aqueous Solution	20
1.8 Antioxidant	21
1.8.1 Definition	21
1.8.2 Classification of antioxidants	22
1.8.3 Vitamin E : an antioxidant	24
1.9 References	30
2. KINETICS AND MECHANISM OF THE PEROXIDASE -CATALYZED IODINATION OF TYROSINE	45
2.1 Summary	45
2.2 Introduction	46
2.3 Experimental	48
2.4 Results	50
2.5 Discussion	58
2.6 Conclusions	63
2.7 References	82

3. KINETICS OF TROLOX C OXIDATION BY LACTOPEROXIDASE COMPOUND II 84

3.1 Summary 84
3.2 Introduction 85
3.3 Experimental 85
3.4 Results 87
3.5 Discussion 89
3.6 References 95

4. CATALASE ACTIVITY OF CHLOROPEROXIDASE AND ITS INTERACTION WITH PEROXIDASE ACTIVITY 96

4.1 Summary 96
4.2 Introduction 97
4.3 Experimental 99
4.4 Results 101
4.5 Discussion 105
4.6 References 123

5. PURIFICATION OF NITRIC OXIDE SYNTHASE (NOS) FROM PORCINE CEREBELLA 125

5.1 Introduction 125
5.2 Experimental 128
5.3 Results and Discussion 133
5.4 References 142

6. GENERAL DISCUSSION 144

6.1 Some preliminary work on two problems 144
6.1.1 Peroxidase-catalyzed oxidation of iodide in the presence of EDTA 146
6.1.1.a Introduction 146

6.1.1.b Some preliminary experiments 149
6.1.1.c Discussion 154
6.1.2 Kinetics and mechanism of the reaction of CPO with hypochlorous acid (HOCl) 158
6.1.2.a Some preliminary experiments 158
6.1.2.b Discussion 163
6.2 Suggestions for future work 167
6.3 Conclusions 168
6.4 References 191

APPENDIX I 195

APPENDIX II 196

APPENDIX III 198

APPENDIX IV 199

APPENDIX V 201

ABBREVIATION

AH_2, reducing substrate

AH·, free radical product

CPO, chloroperoxidase

CPO-I, chloroperoxidase compound I

CPO-II, chloroperoxidase compound II

CPO-I-H_2O_2, chloroperoxidase compound I-hydrogen peroxide complex

$[CPO]_0$, total chloroperoxidase concentration

DIT, diiodotyrosine

EDTA, ethylenediaminetetraacetic acid

EGTA, ethylene glycol-bis(β-aminoethyl ether) N,N,N',N'-tetraacetic acid

H_4B, tetrahydrobiopterin

HRP, horseradish peroxidase

HRP-I, horseradish peroxidase compound I

HRP-II, horseradish peroxidase compound II

HRP-O-I^-, horseradish peroxidase bound hypoiodite

LPO, Lactoperoxidase

LPO-I, lactoperoxidase compound I

LPO-O-I^-, lactoperoxidase bound hypoiodite

MIT, monoiodotyrosine

NADPH, nicotinamide adenine dinucleotide phosphate

pK_e, dissociation constant of an amino acid residue near heme of peroxidase

SDS-PAGE, sodium dodecyl sulfate-polyacrylamide gel electrophoresis

TMPD, N,N,N',N'-tetramethyl-*p*-phenylenediamine

TMPD·, free radical of TMPD

Tyr, tyrosine

$v_{(TMPD)}$, the product formation rate of TMPD demethylation

$v_{(O_2)}$, the initial formation rate of O_2 evolution

LIST OF TABLES

Number	Title	Page
2.1.	Dependence of the initial rates of I_2 and MIT formation on I^- concentrations for HRP and LPO iodination systems.	65
2.2.	Effect of tyrosine on the initial rate of I_2 formation for HRP and LPO systems.	66
2.3.	Stereoisomeric effect of D- and L-tyrosine on the initial rates of I_2 and MIT formation for LPO.	67

LIST OF FIGURES

Number	Title	Page
Figure 1.1.	Structure of ferriprotoporphyrin IX	27
Figure 1.2.	Tyrosine and the thyroid hormones	28
Figure 1.3.	α-Tocopherol (vitamin E)	29
Figure 2.1.	Optical spectra of L-tyrosine, monoiodotyrosine and diiodotyrosine	68
Figure 2.2.	Rapid scan spectra for the reaction of HRP with tyrosine	69
Figure 2.3.	Rapid scan spectra of the direct conversion of HRP-I to native HRP in the presence of equal amount of KI and tyrosine	70
Figure 2.4.	Formation and disappearance of I_3^- and I_2 and formation of MIT during the HRP-catalyzed iodination of tyrosine	71
Figure 2.5.	Time dependences of the concentrations of I_3^-, I^- and I_2 for the HRP-catalyzed iodination of tyrosine	73

Figure 2.6. Disappearance of I_2 for the HRP-catalyzed iodination of tyrosine 74

Figure 2.7. Relative O_2 production for the HRP-catalyzed iodination of tyrosine 75

Figure 2.8. Formation of I_2 for the HRP-catalyzed iodination of tyrosine 76

Figure 2.9. Formation of MIT for the HRP-catalyzed iodination of tyrosine 77

Figure 2.10. Absorbances at 353 nm and 290 nm for the LPO-catalyzed iodination of tyrosine 78

Figure 2.11. Plots of I_2 and MIT formation rates *versus* the [KI]/[tyr] 80

Figure 3.1. Rapid scan spectra of the reaction of LPO-II with Trolox C 92

Figure 3.2. Plot of k_{obs} *versus* Trolox C concentration for the oxidation of Trolox C by LPO-II 93

Figure 3.3. The rate-pH profile for the reaction of LPO-II

with Trolox C 94

Figure 4.1. Rapid scan spectra of the reaction of CPO with H_2O_2 113

Figure 4.2. Plot of k_{obs} *versus* H_2O_2 concentration for the reaction of CPO with H_2O_2 114

Figure 4.3. Plot of O_2 formation rate/$[CPO]_0$ *versus* $[H_2O_2]$ obtained by measuring the H_2O_2 disappearance at 240 nm 115

Figure 4.4. Plot of O_2 formation rate/$[CPO]_0$ *versus* $[H_2O_2]$ obtained by direct measurements of O_2 evolution 116

Figure 4.5. Double reciprocal plots of the initial rate of H_2O_2 -dependent TMPD demethylation by CPO at different [TMPD] 117

Figure 4.6. Plot of the intercepts from the double reciprocal plots in Fig. 4.5 *versus* the reciprocal of TMPD concentration 118

Figure 4.7. Double reciprocal plots of the initial rates of H_2O_2-dependent TMPD demethylation by CPO at different $[H_2O_2]$ 119

Figure 4.8. Plot of the intercepts from the double reciprocal plots in Fig. 4.7 *versus* the reciprocal of H_2O_2 concentration 120

Figure 4.9. Plot of the initial rate of O_2 evolution *versus* TMPD concentration 121

Figure 4.10. Plot of the reciprocal of the initial rate of O_2 evolution *versus* TMPD concentration 122

Figure 5.1. Reaction catalyzed by NO synthase 136

Figure 5.2. Concentration dependence of NO synthase activity on EGTA 137

Figure 5.3. Concentration dependence of NO synthase activity on hematin 138

Figure 5.4. Concentration dependence of NO synthase activity on calmodulin 139

Figure 5.5. SDS-PAGE analysis of purified NO synthase 140

Figure 5.6. Plot of the log of molecular weight of the protein standard *versus* the relative mobility from

SDS-PAGE 141

Figure 6.1. Initial formation rate of I_2 *versus* EDTA concentration in HRP-catalyzed iodide oxidation systems 172

Figure 6.2. Stopped-flow traces at 460 nm over 1.0 s with and without EDTA present in HRP-catalyzed iodide oxidation systems 173

Figure 6.3. Stopped-flow traces at 460 nm over 1.0 s with and without EDTA present in LPO-catalyzed iodide oxidation systems 174

Figure 6.4. Comparison of the initial formation rate of I_2 *versus* the pH values with and without EDTA present in HRP-catalyzed iodide oxidation systems 175

Figure 6.5. Relative O_2 evolution in HRP-catalyzed iodide Oxidation system with varied amount of EDTA 176

Figure 6.6. Comparison of the initial formation rate of I_2 *versus* the iodide concentration with and without EDTA present in non-enzymatic systems 177

Figure 6.7. Initial formation rate of I_2 *versus* EDTA concentration in non-enzymatic systems 178

Figure 6.8. I_3^- disappearance over 10 min in a reaction mixture of EDTA and I_3^- 179

Figure 6.9. Initial disappearance rate of I_3^- *versus* EDTA concentration in non-enzymatic systems 180

Figure 6.10. Rapid scan spectra over 91 ms for the reaction of 1.0 μM CPO and 6.0 μM HOCl 181

Figure 6.11. Rapid scan spectra over 830 ms for the reaction of 1.0 μM CPO and 6.0 μM HOCl 182

Figure 6.12. Rapid scan spectra over 9.1 s for the reaction of 0.16 μM CPO and 47.4 μM HOCl 183

Figure 6.13. Rapid scan spectra over 16.6 s for the reaction of 0.16 μM CPO and 47.4 μM HOCl 184

Figure 6.14. Rapid scan spectra over 16.6 s for the reaction of 0.16 μM CPO and 47.4 μM HOCl in the presence of 50 mM KCl 185

Figure 6.15. k_{obs} *versus* HOCl concentration for the reaction of HOCl and native CPO 186

Figure 6.16. Initial formation rate of compound I *versus* Cl^- concentration 187

Figure 6.17. Stopped-flow traces at 438 nm and 400 nm over 80 s for reaction of CPO and HOCl 188

Figure 6.18. Stopped-flow trace at 400 nm for reaction of CPO and HOCl with KCl present 189

Figure 6.19. Initial formation rate of compound II *versus* Cl^- concentration 190

CHAPTER ONE

INTRODUCTION

1.1 PEROXIDASES

1.1.1 Definition

Peroxidases are enzymes catalyzing the oxidation of a variety of organic and inorganic compounds by hydrogen peroxide or other peroxides of the ROOH type. As recommended by the Nomenclature Committee of the International Union of Biochemistry, peroxidases are classified as a sub-group of the oxidoreductases with EC number of 1.11.1.

Peroxidases play diverse physiological functions in nature. The fact that they can be used with a variety of synthetic substrates has stimulated a large number of investigations by organic chemists, biochemists and biophysicists for many years. It is probably true to say that among all enzymes few have attracted more attention than peroxidases. With various state-of-the-art techniques, more information is being continually gained about structure, function and their interrelationships. Our group has been concerned with kinetics and mechanisms. It is the purpose of this thesis to give a progress report on the function and mechanism of action of peroxidases. In this introductory chapter, background information is given which is relevant to the experimental studies reported later in the thesis.

Peroxidases are widely distributed throughout bacteria, fungi, molds, plants and animals and carry out a variety of biosynthetic and degradative functions (1). A peroxidase from the mold *Caldariomyces fumago*, chloroperoxidase, has been isolated and characterized (2-4). Cytochrome c

peroxidase is obtained from aerobically grown baker's yeast. A cytochrome c peroxidase has also been isolated from *Pseudomonas aeruginosa* (5-8). In many plants, the peroxidase content varies with its tissue location. Horseradish peroxidase, turnip peroxidase and Japanese radish peroxidase are examples of plant peroxidases (9). Horseradish roots and the sap of fig trees are the richest sources of plant peroxidases. Peroxidases from animal sources which have been studied extensively are thyroid peroxidase of the thyroid gland which is involved in the biosynthesis of the hormones thyroxine and triiodothyronine (10-12); myeloperoxidase of neutrophils which takes part in the phagocytic process (13); lactoperoxidase which has antibacterial activity in a number of mammalian exocrine gland secretions (14); prostaglandin H synthase (15) which catalyzes the initial two reactions in the biosynthesis of prostaglandins. A plausible hypothesis for the function of all peroxidases is that they were first used by primordial organisms in their defence mechanism against oxidative damage by toxic oxygen species and that once survival from oxidation was firmly established, more specialized functions evolved (13).

1.1.2 Active site of peroxidase

Enzymes are proteins. The tertiary structure of an enzyme usually contains a crevice. The crevice contains the active center of the enzyme. The substrate enters the crevice in order to react, and is held by groups in the crevice walls, which are suitably placed. The cleft penetrates far into the hydrophobic core; it has in fact been suggested that the remarkable catalytic power of enzymes is due to the hydrophobic environment into which the

reactants are brought. If a metal atom is present, it is usually found deep in the crevice, not far from the center of the molecule.

Generally, peroxidases consist of a heme group and glycoprotein. All the peroxidases purified so far from plants contain the prosthetic group hemin or ferriprotoporphyrin IX (Fig. 1.1). Peroxidases from animal sources present some exceptions. Usually they have prosthetic groups different from ferric protoporphyrin IX (9). The structure of the prosthetic group and its intimate interaction with the protein moiety result in a unique set of catalytic properties for each peroxidase. The heme prosthetic group contributes to the catalytic function of the enzyme in two ways: (i) the iron activates the heterolytic cleavage of peroxides and stores one oxidizing equivalent obtained from the oxidizing substrate, either a hydroperoxide or a peroxy acid, and (ii) the porphyrin regulates the oxidation-reduction potential and stores the other oxidizing equivalent. However, in terms of more detailed structure at the active site of peroxidase, much remains to be resolved (16). For example, the type of ligand at the sixth coordination position, and the nature of the halogenating intermediate, are still topics of controversy. The role of the carbohydrate in these enzymes is uncertain. However, horseradish peroxidase has long been known to be a very stable enzyme, even under conditions of elevated temperature, and this property could be due in part to the carbohydrate associated with the enzyme.

The picture given by X-ray crystallography is of the enzyme in the crystalline state, and the question arises whether the enzyme retains the same conformation in solution.

1.1.3 Reaction of peroxidase

The catalytic cycle of peroxidases normally is:

$$\text{Peroxidase} + H_2O_2 \longrightarrow \text{Compound I} + H_2O \qquad (1.1)$$

$$\text{Compound I} + AH_2 \longrightarrow \text{Compound II} + \cdot AH \qquad (1.2)$$

$$\text{Compound II} + AH_2 \longrightarrow \text{Peroxidase} + \cdot AH + H_2O \qquad (1.3)$$

where AH_2 represents the reducing substrate, commonly called the hydrogen donor. The structures of the intermediates (compounds I and II) are independent of the oxidizing and reducing substrates used to form them. The overall reaction is:

$$H_2O_2 + 2AH_2 \longrightarrow 2\cdot AH + 2H_2O \qquad (1.4)$$

and is known to be a modified form of "ping-pong" kinetics in which the reaction steps are not reversible, and the rate constant of the second reaction step (compound II formation) is larger than that of the third step (regeneration of the native enzyme) (17). The free radical product has several fates, depending upon its structure and the environment. It may dimerize, react with another substrate molecule, or attack another species causing cooxidation. It may also reduce dioxygen, if present, to superoxide or it may be scavenged by dioxygen to form a peroxyl radical.

Compound I is formed by the addition of a stoichiometric amount of hydrogen peroxide to the native enzyme. It appears to be a ferryl porphyrin π-

cation radical, wherein one of the oxidation equivalents is stored as the ferryl iron, $Fe^{IV}=O$, while the other equivalent is stored as a porphyrin-centered π-cation radical. Electron donating substrates reduce compound I to the native ferric enzyme in two steps *via* the formation of compound II, the second intermediate of the enzyme. Compound II contains one oxidizing equivalent above the native ferric enzyme. Thus it is a formal +4 state of the enzyme. Peroxidases contain two histidine residues which are proposed to be essential for activity. One of the histidine residues (proximal) is the axial ligand of the heme. The other histidine (distal) is located in the distal pocket. Residues in the distal pocket have been proposed to participate in peroxide cleavage to form compound I (18, 19).

The stability of the intermediates, compound I and II, and the intense environmentally sensitive Soret absorbance at about 400 nm have facilitated the large number of studies that have been carried out on peroxidases (1, 9, 16, 20, 21).

1.2 HORSERADISH PEROXIDASE

Horseradish peroxidase (HRP; donor H_2O_2 oxidoreductase, EC 1.11.1.7) is a heme-containing glycoprotein. There are three important isoenzymes of HRP: isoenzyme A (acidic); isoenzyme C (neutral or slightly basic), and a strongly basic isoenzyme E (22). Isoenzyme C which is the dominant isoenzyme of the horseradish root is used for the work presented here.

The amino acid sequence of HRP has been determined (23-29). HRP consists of 308 amino acid residues. The carbohydrate is located on the surface of the molecule with eight points of attachment to side chains of asparagine residues. There are four disulfide bridges and two Ca^{2+} ions are

bound per HRP molecule (30). The enzyme has less thermal stability when the Ca^{2+} is removed. One of the Ca^{2+} ions contributes to the structural stability in the region of the active site as determined by NMR, ESR and metal ion substitution experiments (31-33). The polypeptide chain has a molecular weight of 33,890 as calculated from its sequence. The hemin group weight 550.5 and with approximately 18% carbohydrate and two Ca^{2+} present, the molecular weight is about 42,100, excluding any bound water.

No crystal structure of HRP has yet been determined.

A ferric ion normally has a coordination number of six. The coordination number of the ferric ion in peroxidases is fundamental to an understanding of their chemical and physical properties. For HRP, four nitrogen atoms of the porphyrin ring are ligated to the ferric ion. The neutral imidazole of histidine residue 170 occupies the fifth coordination position. The prosthetic group of native HRP is identical to that of metmyoglobin and imidazole is the fifth ligand of the ferric ion in both species. Nevertheless, evidence has been mounting that the sixth coordination position of the ferric ion of HRP is vacant (34-36), unlike metmyoglobin, where the sixth position is occupied by a water molecule (37). Therefore, the striking difference between the two classes of native species is that the native peroxidases have five-coordinate ferric ion, the native ferric globins are six-coordinate.

The single heme group of HRP, identical to that in hemoglobin and myoglobin which display quite different biological functions, is non-covalently linked to the protein matrix through hydrophobic and electrostatic interactions among the propionic groups and the basic amino acids of the active site (38, 39). The dynamics of protoporphyrin IX in the heme pocket of HRP have been studied using fluorescence methods and compared with those of

hemoglobin and myoglobin (40, 41). The local motion of the protoporphyrin IX in the heme pocket of HRP is, in fact, similar to that found for hemoglobin and myoglobin.

The number of unpaired electrons present in a transition metal ion is a function of its oxidation state, coordination number and field strength of its ligands (21, 42). For native HRP, the experimental observation is that the ferric ion at room temperature has an intermediate spin state, a mixture of S = 3/2 and S = 5/2 (43-45).

Chemical and kinetic evidence for an essential histidine residue in the electron transfer from the aromatic donor to HRP compound I has been reported (46). Diethyl pyrocarbonate, a histidine-specific reagent, was used to modify HRP. The modified enzyme forms compound I with H_2O_2 but not compound II, suggesting that the electron transfer process is blocked. The modified HRP compound I cannot oxidize guaiacol, an aromatic electron donor. The most likely distal residue is histidine 42 which controls aromatic donor oxidation by regulating electron transport without affecting donor binding or compound I formation.

A resonance Raman spectroscopic study of bovine liver catalase compound II shows it has essentially the same behavior exhibited by HRP compound II (47). Thus, the structure and environment of the heme group of the compound II species of HRP and catalase are very similar. This indicates that the marked differences in their reactivities as oxidants are probably due to the manner in which the protein controls access of substrates to the heme group.

Two HRP-C isoenzyme genomic DNAs were cloned and sequenced (48). They code for 347 and 349 amino acid residues, respectively. The

cDNA sequence of a neutral HRP has been reported (49). The predicted amino acid sequence is nine amino acids shorter than the major isoenzyme belonging to the HRP-C group and the sequence shows 53.7% identity with this isoenzyme. Expression of each HRP isoenzyme-encoding gene in transgenic plants or microbial cells might be a fruitful approach to clarify the physiological function of these isoenzymes.

In order to define structure-function relationships for HRP relevant to the preparation of novel catalysts, site-specific mutagenesis studies of HRP have been performed recently by Ozaki and Ortiz de Montellano (50). In the absence of a crystal structure for HRP, they chose Phe-41 for initial mutagenesis based on the sequence alignments of HRP with cytochrome c peroxidase and lignin peroxidase, two peroxidases for which crystal structures are available. The results clearly identify Phe-41 as a major determinant of peroxygenase substrate binding in the HRP active site and suggest a model of the features of the active site that determine stereospecificity.

HRP is the most widely studied peroxidase since it is found in high concentration in horseradish roots and can therefore be readily isolated. A good preparation of HRP will give a purity number, commonly called the R. Z. (reinheitzahl), the ratio of absorbances at 403 nm and 280 nm, of 3.2 to 3.4. The R. Z. is a measure of hemin content using the aromatic amino acid content as reference, but is not a direct indication of enzymatic activity.

HRP is often used as a model of other peroxidases partly because of its stability and commercial availability. One of the other reasons is that all the discovered members of the peroxidase family form similar one- and two-electron oxidized intermediates, although the reaction mechanisms and the structures of the intermediate compounds of HRP are not yet fully understood.

1.3 LACTOPEROXIDASE

A peroxidase activity is found in exocrine secretions including milk, tears, and saliva, and perhaps in other secreted fluids. The enzymes responsible for this activity are synthesized in the glands that produce the secretions. A representative enzyme was first isolated from bovine milk and named lactoperoxidase (LPO; donor H_2O_2 oxidoreductase, EC 1.11.1.7). LPO had been considered important for the inhibition of lactic acid production by lactic bacteria (51). The original proposal of using LPO in food to the Food and Agriculture Organization (1957) was therefore based on the prevention of souring of milk, which is the most common form of spoilage. LPO, along with related peroxidases in tears and saliva, forms part of an antimicrobial defense system (52).

Bovine lactoperoxidase consists of a single peptide chain (53) of molecular mass 77,000 (54), a heme and about 10% carbohydrate (53, 55, 56). A calcium ion was found to be strongly bound to bovine LPO (57). The heme group of LPO has recently been identified to be a modified derivative of protoporphyrin IX, whose 8-methyl substituent is replaced by an 8-mercaptomethyl group and linked to apoprotein through the formation of a disulfide bond (58). The heme moiety of LPO is more difficult to remove from the enzyme than the heme moieties of most other hemoproteins.

The protein sequence of LPO from cow's milk has been recently determined (59). The primary structure of LPO displays a striking similarity with human leucocyte peroxidases (myeloperoxidase and eosinophil peroxidase) (60-65) as well as murine myeloperoxidase (66, 67). The single peptide chain of bovine LPO contains 612 amino acid residues, including 15 cysteine and 4 or 5 potential N-glycosylation sites. The occurrence of an odd

number of cysteine in bovine LPO supports the finding of a heme thiol released from this enzyme by a reducing agent (59).

No crystal structure of LPO has yet been available to indicate the pattern of disulfide bonding or the residues that make up the heme-binding site.

Extensive spectroscopic studies of LPO, including MCD (68), EPR (69, 70), NMR (71-75), and resonance Raman (RR) (76-78), have established that the enzyme contains a five-coordinate high-spin ferric heme in the resting state with histidine serving as the proximal ligand. Recently, resonance Raman studies have shown a close structural similarity of the heme active site of LPO to those of well-characterized cytochrome c peroxidase and myeloperoxidase, although a narrower heme pocket for LPO was observed (79). An extended X-ray absorption investigation of the structure of the active site of LPO has been recently reported (80). This study shows that the structure of the active site of LPO is similar to that of native lignin peroxidase (81) and different from that of horseradish peroxidase (82).

LPO exhibits similar optical spectra to other mammalian peroxidases such as thyroid peroxidase and intestinal peroxidase (83). However, the optical spectra of these mammalian peroxidases are different from those of typical plant or fungal peroxidases such as HRP (84) or lignin peroxidase (85).

LPO absorbs strongly (86, 87) at 412 to 413 nm at neutral pH, with a millimolar extinction coefficient of 112.3 to 114. The ratio of the heme absorbance at 412 nm to the absorbance of heme and aromatic amino acid residues at 280 nm is often used as an indication of the purity of LPO preparations, and values of 0.90 to 0.96 have been reported (88). However,

the oxidation of aromatic amino acid residues and the limited proteolysis could lower the 280 nm absorbance and give a mistaken impression of purity.

LPO, like other hemoprotein peroxidases, catalyzes the H_2O_2-dependent oxidations of iodide and many organic compounds including phenols, aromatic amines, and ene-diol compounds. LPO has barely detectable activity with Cl^- and Br^-. The reaction of H_2O_2 with the ferric LPO converts LPO to the compound I state, which can accept two electrons. The compound I state is not well characterized because it is short-lived. Even highly purified LPO preparations contain enough one-electron donors to reduce compound I to compound II. The endogenous one-electron donors have not been identified, but it has been proposed that they consist of tyrosine residues of LPO and any other proteins that may be present.

Following the reaction with a molecule of H_2O_2, LPO is able to catalyze the oxidation of endogenous thiocyanate to the antimicrobial hypothiocyanite ion in mammalian secretion systems (89). A novel view of the biological role of the LPO/H_2O_2/SCN^- system has been developed (90) and the chemistry of peroxidase-catalyzed SCN^- oxidation has been reviewed (91). In brief, the major observed product is the hypohalite ion analogue $OSCN^-$ (hypothiocyanite ion), which is in equilibrium with the hypohalous acid analogue HOSCN (hypothiocyanous acid). The pK_a of HOSCN is 5.3, and solutions at physiologic pH are HOSCN/$OSCN^-$ mixtures containing primarily $OSCN^-$. Nevertheless, HOSCN is the more reactive form of the oxidized SCN^- which inhibits the lactic acid formation by lactic bacteria. Therefore, it appears that the physiologic role of LPO is to use the H_2O_2 and SCN^- produced by host cells and microorganisms to produce HOSCN, which inhibits microbial metabolism and growth, particularly at low pH (92, 93). The

keeping quality of the milk collected at high ambient temperature (30 °C) was increased by supplementing the thiocyanate level to 0.58 mM and adjusting the peroxide level to 0.4 mM. Milk treated with LPO/H_2O_2/SCN^- system did not become sour and was stabilized for more than 8 hours, while the untreated milk spoiled after 4 hours (94).

The kinetics of reactions catalyzed by LPO and other peroxidases are of the "ping-pong" type as described for many other enzymes with two substrates, that is, H_2O_2 and an electron donor (95, 96). The mechanism of the oxidation of organic and inorganic substrates by hydrogen peroxide catalyzed by peroxidases involves an initial binding of the electron donor to the enzyme (9). Several studies have therefore been reported on the binding of oxidizable organic and inorganic substrates to the native enzymes. Among the oxidizable inorganic substrates, the interactions of iodide ion with HRP (97) and LPO (98) have been studied in order to understand the mechanism of the biosynthesis of the thyroid hormone catalyzed by thyroid peroxidase and lactoperoxidase. The prosthetic group of HRP is a protoheme IX, while it is an iron porphyrin thiol for LPO (58, 99). Iodide ion binds to HRP at almost equal distance from the heme peripheral 1- and 8-methyl groups at the distal side of the heme, and the interaction becomes stronger in acidic medium with protonation of the ionizable groups with the pK_a value of 4.0 of HRP (97). The interaction of iodide ion with LPO was studied by the use of ^1H NMR, ^{127}I NMR and optical difference spectrum techniques (98). It was suggested that iodide ion binds to LPO outside the heme crevice but at a position close enough to interact with the distal histidyl residue which possibly mediates electron transport in the iodide oxidation reaction. Beside iodide, thiocyanate is also an attractive inorganic substrate because the system of

$LPO/H_2O_2/SCN^-$ provides a potent nonspecific bacteriocidal activity (100, 101). The use of ^{15}N- and ^1H-NMR spectroscopy shows that thiocyanate ion binds to LPO at the distal side of heme at histidyl residue (pK_a of 6.1) (102). However, thiocyanate binds to HRP, away from the distal histidine, near 1- and 8-methyl heme groups with an amino acid group of pK_a of 4.0 (103, 104).

The importance of nitric oxide in biological systems was discovered recently (105-107). The interest in NO has therefore greatly increased (108). Polymorphonuclear neutrophils generate both nitric oxide and superoxide and these molecules can combine to form peroxynitrite. In order to know the roles of peroxidases in NO biology, the interaction of peroxidases and catalase with peroxynitrite has been therefore studied (109).

1.4 CHLOROPEROXIDASE

Chloroperoxidase (CPO; chloride:hydrogen peroxide oxidoreductase, EC 1.11.1.10) is a heme-containing monomeric glycoprotein with molecular weight of 42,000. The one isolated from the mold *Caldariomyces fumago* (110) is the main isoenzyme.

Chloroperoxidase has been the subject of several investigations because of its versatile catalytic properties typical of peroxidases, catalase, and oxygenases (111-115). In addition, CPO catalyzes the halogenation (except fluorination) of substrates in the presence of halide ions and hydrogen peroxide (110, 116, 117). The four distinctly different types of reactions catalyzed by CPO are as follows:

Halogenation: $$AH + H_2O_2 + X^- + H^+ \longrightarrow AX + 2H_2O \qquad (1.5)$$

where $X^- = Cl^-$, Br^- or I^-;

Dehydrogenation: $2BH + H_2O_2 \longrightarrow B\text{-}B + 2H_2O$ (1.6)

Decomposition of H_2O_2: $2H_2O_2 \longrightarrow O_2 + 2H_2O$ (1.7)
(Catalatic-like reaction)

Oxygen insertion: $R + H_2O_2 \longrightarrow RO + H_2O$ (1.8)

Although most peroxidases are able to utilize bromide and iodide anions as halogen source, only chloroperoxidase and myeloperoxidase (118) can catalyze the H_2O_2-dependent oxidation of chloride ion to incorporate it into organic substrates. CPO is also unusual among peroxidases in possessing strong catalase activity (115). Most recently, CPO has been found to be capable of some cytochrome P-450 type reactions such as the N-dealkylation of alkylamines (119, 120) and the epoxidation of alkenes (121, 122). Organic sulfides are also substrates of chloroperoxidase (123, 124) in oxygenation reactions that are typical of cytochrome P-450s and flavin-dependent monooxygenases (125-128).

Although CPO has been isolated in high yields from fermentation broths of the mold *C. fumago* and has been crystallized (110), only preliminary X-ray crystallographic data have been published (129). Various kinds of studies have been conducted to delineate the fine structural features of CPO that allow the enzyme to possess chemical and physical similarities to the peroxidases, catalase, and P-450 cytochromes.

When the optical spectra of various ferric and ferrous states of chloroperoxidase were characterized, many similarities between CPO and

cytochrome P-450s were discovered (130). It is particularly noteworthy that the carbon monoxide complex of ferrous chloroperoxidase exhibits an absorbance maximum near 450 nm, the feature which distinguishes and confers the name of the cytochrome P-450 class of hemoproteins (131, 132).

Extensive spectroscopic studies of CPO, including UV-visible absorption, magnetic circular dichroism (MCD), EPR and Mössbauer spectroscopy, have supported the conclusion that an endogeneous thiolate sulfur donor ligand is coordinated to the central heme iron of the enzyme (133-139). The most direct and conclusive evidence for the presence of a sulfur donor axial ligand in CPO has been provided by the EXAFS spectroscopy in which the Fe-S bond length has been determined (133, 134). A resonance Raman spectroscopic study has shown the detection of the Fe-S bond vibration of CPO (140). Thus, CPO has many spectroscopic properties similar to cytochrome P-450, the only other known thiolate-ligated heme protein (112, 141, 142).

The other axial ligand of the ferric CPO depends on its spin state. In the case of the high-spin (S = 5/2) species, the sixth ligand position of the enzyme is thought to be vacant (113). While the low-spin chloroperoxidase, produced from the native high-spin species by lowering the temperature below 200 K or increasing the pH above 7.0, is thought to have a histidine sixth ligand (143, 144).

Recently, the sequence of the chloroperoxidase-encoding gene from *C. fumago* has been reported (145). The complete primary sequence of CPO contains 300 amino acids having a molecular weight of 32,974. The CPO gene encodes three potential glycosylation sites. This study revealed the existence of three cysteine residues, only two of which had been detected as

a disulfide pair by an earlier chemical analysis of the enzyme (146). This has clarified the earlier puzzle about the identity and the origin of the axial thiolate ligand for CPO (147).

The roles of the proximal ligand in heme proteins have been recently studied (148). A replacement of the proximal histidine of human myoglobin with cysteine by site-directed mutagenesis results in a proximal cysteine mutant myoglobin which exhibits the altered axial ligation analogous to cytochrome P-450 and chloroperoxidase. The thiolate ligand enhances the heterolytic O-O bond cleavage of the oxidant.

The recent resonance Raman spectral studies have shown that CPO weakens the Fe-ligand linkage in the nitric oxide and carbon monoxide adducts (relative to imidazole-ligated heme proteins), but to a lesser extent than does cytochrome P-450 (149). The results of this study are entirely consistent with the current view that CPO possesses a peroxidase-like heme active site and a coordination linkage similar to cytochrome P-450s (144, 150).

The proton nuclear Overhauser effect study of the heme active site structure of CPO indicates structural similarity of the CPO heme pocket to the relatively better characterized peroxidases cytochrome c peroxidase (CCP) and HRP, rather than to the monooxygenase cytochrome P-450 (151). One piece of evidence is that, as in HRP and CCP, a distal histidine residue is also present in CPO-CN, which is in agreement with the previous chemical modification work of Blanke and Hager (152). Nevertheless, in terms of the hydrogen bonding with the ligated cyanide ion, the distal histidine in CPO-CN seems to differ from other peroxidases. The distal histidine N-H proton is hydrogen bonded to the ligated cyanide ion in HRP-CN (153) and CCP-CN

(154). However, there is no distal histidine in the case of cytochrome P-450 (155) as shown in its crystal structure. Another piece of evidence is that, as in HRP and CCP, the presence of an arginine residue in the heme pocket of CPO is reported (151), although the spatial disposition and heme distance differ from that in CCP and HRP. The β-CH_2 protons of arginine are 4.5 Å from the heme iron in CCP (156). The arginine in HRP is also placed at a similar distance from the heme (153). The arginine protons are calculated to be 6.6-6.8 Å from the iron atom in CPO (151). However, there is no arginine residue close to the heme periphery of cytochrome P-450. Thus, the active site of CPO-CN is quantitatively similar to other peroxidases, although there are subtle differences in terms of the stereochemistry of the two catalytically important distal histidine and arginine amino acid residues. Therefore, despite of the similarities between CPO and cytochrome P-450 in their physical properties such as the Fe^{III}-S bond length (133) and the Fe^{III}-S stretching frequencies (157), their reactivities are quite different: cytochrome P-450 serves as a monooxygenase but CPO works as a peroxidase.

The first evidence of the identification of the Fe^{IV}=O heme for a S^--coordinated heme enzyme was obtained recently from the resonance Raman and visible absorption spectra (158).

The mechanisms of chloroperoxidase-catalyzed chlorination reactions have been the subject of considerable interest. Concerning the identity of the enzymatically produced chlorinating species, data have been variously interpreted as supporting one of two possible forms of "active chlorine": free HOCl (159-161) and an OCl^- species coordinated to the heme iron (III) of chloroperoxidase (118, 162, 163). The exact mechanism of the chlorination reactions remains unknown.

1.5 SPECTROSCOPY

The current thrust of biochemistry and molecular biology is to understand life processes — replication, movement, communication, and control — at the atomic level. The techniques of physical chemistry that yield the most detailed information on the atomic level are the diffraction and spectroscopic methods. X-ray, neutron, and electron diffraction have the advantage of yielding a direct and often easily interpretable picture of matter, but these methods suffer from some limitations. The pictures frequently do not reveal as much molecular or atomic detail as one might wish. Moreover, the pictures are at best static snapshots of molecular events. The essential dynamics of enzymatic catalysis or transport, or whatever process is being studied, must be inferred from one or more of these snapshots. In addition, these pictures provide more details in the solid state rather than for the solution state that is more characteristic of living systems.

In contrast, spectroscopic techniques are applied readily to solutions, and can be used to follow dynamic processes. Many of them are sufficiently sensitive to detect movements on the order of tiny fractions of an angstrom or a small change in concentration of one component among many. The major limitation of spectroscopic techniques is that the information is in a less easily interpreted form: it consists of a list of the energy level differences of the system under study. Thus, to understand any system in much detail, both classes of techniques usually are necessary. The information from each complements the other.

1.6 THYROID HORMONES

There are two kinds of hormones secreted by the thyroid gland, thyroxine and L-3,5,3'-triiodothyronine (Fig. 1.2). One of the physiological functions of the thyroid hormones is known to be involved in mammalian body temperature regulation. The mechanism of this process is not fully understood. However, it is known that when these hormones are released, they cause an increased metabolic rate. This in turn results in an increased heat production, thus raising the body temperature.

Iodide is concentrated by thyroid tissue *in vivo*. The thyroid hormones are synthesized from two successive oxidative reactions, both of which are known to be catalyzed by thyroid peroxidase, TPO (164). In the first reaction, ~30 out of ~130 tyrosine residues present in the polypeptide backbone of thyroglobuline are either monoiodinated or diiodinated in a reaction involving I^- and H_2O_2. In a second reaction, ~8 of the iodinated tyrosines are coupled to form thyroxine, (L-3,5,3',5'-tetraiodothyronine), or L-3,5,3'-triiodothyronine. The mechanisms of these reactions have been the subject of many investigations (10, 164-167). The kinetics and the mechanism of the iodination of free tyrosine catalyzed by HRP and LPO will be discussed in detail in the following chapter.

The antimicrobial activity of peroxidases is due to their ability to catalyze the H_2O_2-dependent oxidation of halide ions or SCN^- to produce powerful oxidizing agents (168). Besides their roles in the synthesis of the thyroid hormones, peroxidase-catalyzed iodination reactions play important roles in the biological defense systems as well.

1.7 HYDROLYSIS OF IODINE IN AQUEOUS SOLUTION

In aqueous solution, the iodine system has been shown to be complex due to the number of oxidation states available to iodine (169). Many studies have been carried out to determine the most important iodine species present in aqueous solution under different conditions. An increased interest in kinetic and equilibrium studies of I_2 hydrolysis has now been brought about by the need for designing effective measurements to prevent the release of radioactive iodine species into the environment following a nuclear reactor accident (170). As a result, equilibrium constants have now been determined for most of the known equilibria in aqueous iodine solution, and kinetic parameters have been determined for many of them (169-173). Molecular iodine is known to be in equilibria with other species in aqueous solution as shown in the following equations:

$$I_2 + I^- \underset{k_{-9}}{\overset{k_9}{\rightleftharpoons}} I_3^- \qquad (1.9)$$

$$I_2 + H_2O \underset{k_{-10}}{\overset{k_{10}}{\rightleftharpoons}} HOI + I^- + H^+ \qquad (1.10)$$

where $k_9 = (6.2 \pm 0.8) \times 10^9\ M^{-1}s^{-1}$, $k_{-9} = (8.5 \pm 1.0) \times 10^6\ s^{-1}$ (171) and $k_{10} = 3.0\ s^{-1}$, $k_{-10} = 4.4 \times 10^{12}\ M^{-2}s^{-1}$ (172). The thermodynamics of the formation of I_3^- from I_2 and I^- have been extensively studied; reported values of K_9 are 768 M^{-1} (173), 721 M^{-1} (174), 698 M^{-1} (175) and 746 M^{-1} (176), within experimental error of 729 M^{-1} obtained from the kinetic data. The equilibrium constant of K_{10} is $5.4 \times 10^{-13}\ M^2$ at 25 ^{0}C (177).

From temperature-jump relaxation studies on the hydrolysis of iodine (169, 172, 178), a mechanism has been proposed in which the formation of HOI is controlled by the disproportionation of I_2OH^- (178). The proposed mechanism is shown as follows:

$$I_2 + H_2O \rightleftharpoons I_2OH^- + H^+ \qquad (1.11)$$

$$I_2 + OH^- \rightleftharpoons I_2OH^- \qquad (1.12)$$

$$I_2OH^- \rightleftharpoons HOI + I^- \qquad (1.13)$$

The existence of I_2OH^- as an intermediate was confirmed by the results of a Raman spectroscopic study of the disproportionation of hypoiodite in basic solutions (170).

1.8 ANTIOXIDANT

1.8.1 Definition

The spontaneous reaction of atmospheric oxygen with organic compounds leads to a number of degradative changes that reduce the lifetime of many products of interest to the chemical industry as well as causing the deterioration of lipids in foods. Antioxidants are present naturally in virtually all food commodities, providing them with a valuable degree of protection against oxidative attack.

The reaction between lipids and oxygen, which is an autoxidation reaction, is a free radical chain reaction. Like all chain reactions, the mechanism can be discussed in terms of initiation reactions during which free radicals are formed, propagation reactions during which free radicals are

converted into other radicals, and termination reactions which involve the combination of two radicals with the formation of stable products. According to a very general definition, antioxidants are substances capable of delaying, retarding or preventing oxidation processes.

1.8.2 Classification of antioxidants

Ingold (179) classified all antioxidants into two groups, namely primary or chain-breaking antioxidants, which can react with lipid radicals to convert them to more stable products, and secondary or preventive antioxidants which reduce the rate of chain initiation by a variety of mechanisms.

Primary (chain-breaking) antioxidants

A molecule will be able to act as a primary antioxidant if it is able to donate a hydrogen atom rapidly to a lipid radical and the radical derived from the antioxidant is more stable than the lipid radical, or is converted to other stable products. Phenol itself is inactive as an antioxidant but substitution of alkyl groups into its 2, 4 or 6 positions increases the electron density on the hydroxyl group by an inductive effect and thus increases the reactivity with lipid radicals. The radical formed by the reaction of a phenol with a lipid radical is stabilized by the delocalization of the unpaired electron around the aromatic ring as indicated by the valence bond isomers:

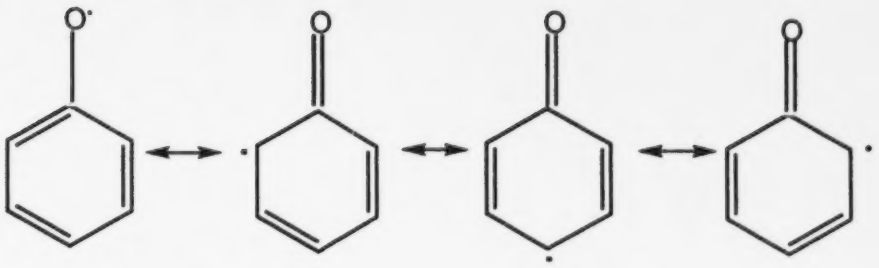

(1.14)

The stability of the phenoxyl radical reduces the rate of the propagation of the autoxidation chain reaction since propagation reactions caused by phenoxyl radical with oxygen are very slow compared with the propagation reactions of lipid radicals with oxygen. Endo *et al.* (180) have suggested that the antioxidant effects of chlorophyll in the dark occur by this mechanism.

The antioxidant action by donation of a hydrogen atom is unlikely to be limited to phenols.

Secondary antioxidants

Compounds which are able to retard the rate of autoxidation of lipids by processes other than that of interrupting the autoxidation chain by converting free radicals to more stable species are termed secondary antioxidants. These may operate by a variety of mechanisms including compounds that bind metal ions, scavenge oxygen, decompose hydroperoxide to non-radical species, absorb UV radiation or deactivate singlet oxygen. For example, ascorbic acid which functions by oxygen scavenging, an entirely different mechanism from that of phenolic antioxidants, is used as antioxidant to remove oxygen in solution.

Some secondary antioxidants usually only show their antioxidant activity if a second minor component is present in the sample. This minor

component is called a synergist. Synergists are substances enhancing the activity of antioxidants, without being antioxidants themselves. The synergistic effects of ascorbic acid and its derivatives with tocopherols have been demonstrated (181-191). Packer *et al.* (192) reported direct observations of the interaction of α-tocopherol and ascorbic acid and showed that they act synergistically. α-Tocopherol acts as the primary antioxidant and the resulting α-tocopheryl radical then reacts with ascorbic acid to regenerate α-tocopherol.

Some enzymes can be used as antioxidants as well. Various radicals can contribute to the lipid oxidation in biological systems. Superoxide radicals which may be produced by the enzyme xanthine oxidase and hydrogen peroxide (193) may be removed by the enzyme superoxide dismutase according to the following eq.:

$$2O_2^{\cdot-} + 2H^+ \xrightarrow[\text{dismutase}]{\text{superoxide}} H_2O_2 + O_2 \qquad (1.15)$$

The enzyme catalase may also play an important role in converting the hydrogen peroxide to water and oxygen:

$$2H_2O_2 \xrightarrow{\text{catalase}} 2H_2O + O_2 \qquad (1.16)$$

1.8.3 Vitamin E: an antioxidant

The view that the only components of the diet necessary for health, growth and reproduction were proteins, carbohydrates and certain minerals had to be changed when it was realized early this century that minute amounts of additional substances were also required. These 'accessory food

factors' were given the names 'vitamins' and divided into two classes: the fat-soluble class and the water-soluble class. Eventually, it was realized that both of these classes were mixtures of chemically unrelated compounds and the fat-soluble vitamins, found mainly in fatty foods, were later classified as A, D, E and K.

Because vitamin E is so widespread in foods and, like other fat-soluble vitamins, is stored in the body, deficiency states are rarely seen. A possible exception may be in premature infants with low fat stores. Although vitamin E is known to be necessary for normal fertility in rats, it has never been absolutely proven to be necessary for man. However, with a renewed interest in the adverse effects of lipid peroxidation, it is now frequently assumed to be essential.

Vitamin E is known to be a powerful antioxidant and prevents the peroxidation of unsaturated fatty acids. The products of peroxidation of unsaturated fatty acids can cause damage to cells if the oxidative process is not kept in check, and such damage appears to be exacerbated in animals given diets deficient in vitamin E. These observations have led to the postulation that vitamin E plays a vital role in the prevention of the oxidation of membrane fatty acids in living cells.

The activity of vitamin E is shared by a family of compounds known as tocopherols, the most active of which is α-tocopherol (Fig.1.3). α-Tocopherol is present in the lipid bilayers of biological membranes and may play a structure role there.

The richest sources of vitamin E are vegetable oils, cereal products and eggs. It is a generally held view that intake should be considered in relation to the polyunsaturated fatty acid content of the diet rather than in

absolute amounts.

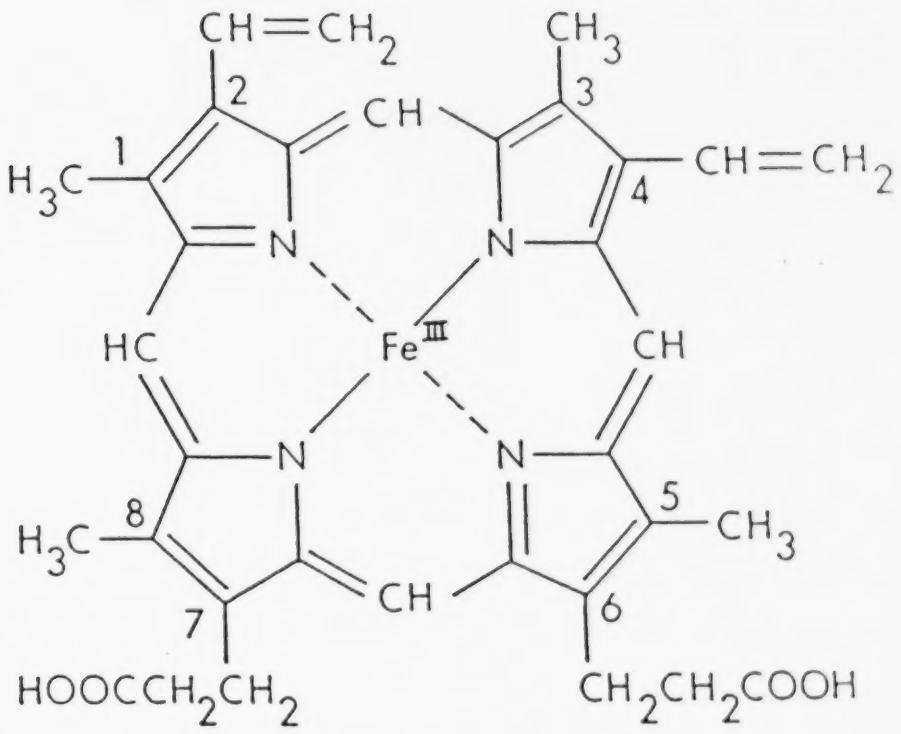

Figure 1.1. Structure of ferriprotoporphyrin IX: the prosthetic group of most peroxidases. The intense environmentally sensitive Soret absorbance at about 400 nm is due to the conjugated tetrapyrroles.

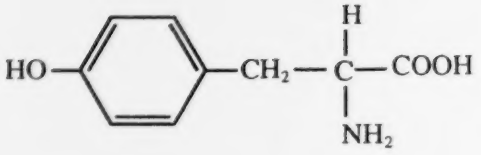

Tyrosine

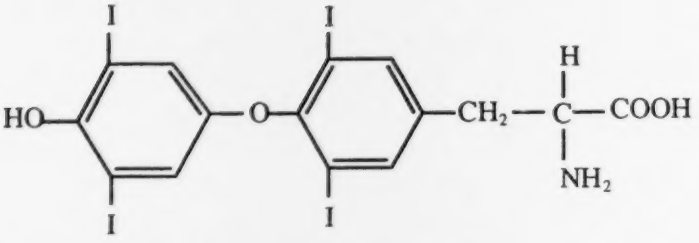

Thyroxine (L-3,5,3',5'-tetraiodothyronine)

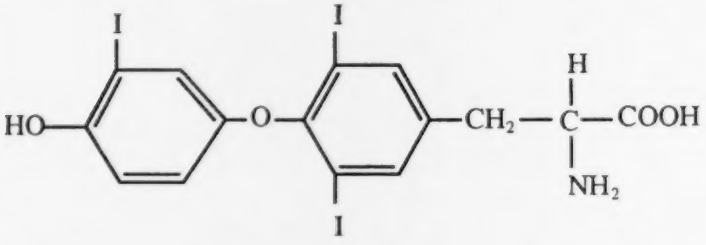

Triiodothyronine (L-3,5,3'-triiodothyronine)

Figure 1.2. Tyrosine and the thyroid hormones.

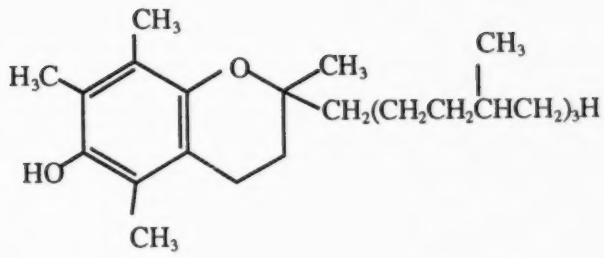

Figure 1.3. α-Tocopherol (vitamin E).

1.9 REFERENCES

1. Saunders, B. C., Holmes-Siedle, A. G., and Stark, B. P. (1964) *in* Peroxidase, Butterworths, London.
2. Hultquist, D. E., and Morrison, M. (1963) *J. Biol. Chem.* **238**, 2843-2846.
3. Morris, D. R., and Hager, L. P. (1966) *J. Biol. Chem.* **241**, 1763-1768.
4. Hager, L. P., Morris, D. R., Brown, F. S., and Eberwein, H. (1966) *J. Biol. Chem.* **241**, 1769-1777.
5. Ellfolk, N., and Soininen, R. (1970) *Acta Chem. Scand.* **24**, 2126-2136.
6. Ellfolk, N., and Soininen, R. (1971) *Acta Chem. Scand.* **25**, 1535-1540.
7. Soininen, R. (1972) *Acta Chem. Scand.* **26**, 2535-2537.
8. Soininen, R., Ellfolk, N., and Kalkkinen, N. (1973) *Acta Chem. Scand.* **27**, 1106-1107.
9. Dunford, H. B., and Stillman, J. S. (1976) *Coord. Chem. Rev.* **19**, 187-251.
10. Taurog, A. (1979) *Endocrinology*, **1**, 331-342.
11. Magnusson, R. P., Taurog, A., and Dorris, M. L. (1984) *J. Biol. Chem.* **259**, 13783-13790.
12. Ohtaki, S., Nakagawa, H., Nakamura, S., Nakamura, M., and Yamazaki, I. (1985) *J. Biol. Chem.* **260**, 441-448.
13. Klebanoff, S. J., and Clark, R. A. (1978) The Neutrophile: Function and Clinical Disorders, North-Holland, Amsterdam.
14. Mandel, I. D., and Ellison, S. A. (1985) *in* The Lactoperoxidase System, *Edited by* Pruitt, K. M., and Tenovuo, J. O., pp.1-14, Marcel Dekker Inc., New York.

15. Ohki, S., Ogino, N., Yamamoto, S., and Hayashi, O. (1979) *J. Biol. Chem.* **254**, 829-836.

16. Neidleman, S. L., and Geigert, J. (1986) *in* Biohalogenation, PP. 46-84 and 131-139, Ellis Harwood Ltd., Chichester.

17. Dunford, H. B. (1990) *in* Peroxidases: Chemistry and Biology *Edited by* Everse, J., and Grisham, M. B., Vol. I. pp. 1-24, CRC Press, Boca Raton.

18. Poulos, T. L., and Kraut, J. (1980) *J. Biol. Chem.* **255**, 8199-8205.

19. Finzel, B. C., Poulos, T. L., and Kraut, J. (1984) *J. Biol. Chem.* **259**, 13027-13036.

20. Dunford, H. B., Araiso, D. J., Richard, J., Rutter, R., Hager, L. P., Wever, R., Kast, W. M., Boelens, R., Ellfolk, N., and Ronnberg, K. (1982) *in* The Biological Chemistry of Iron (Dunford, H. B., Dolphin, D., Raymond, K. N., and Sieker, L., Eds.), pp.337-355 D. Reidel Publishing Company.

21. Dunford, H. B. (1982) *Adv. Inorg. Biochem.*. (Eichhorn, G. L., and Marzilli, L. G., Eds.) **Vol. 4**, pp. 41-68.

22. Yamazaki, I., and Nakajima, R. (1986) Physico-chemical comparison between horseradish peroxidases A and C, *in* Molecular and Physiological Aspects of Plant Peroxidases *Edited by* Greppin, H., Penel, C., and Gaspar, Th., pp. 71, Geneva.

23. Welinder, K. G., Smillie, L. B., and Schonbaum, G. R. (1972) *Can. J. Biochem.* **50**, 44-62.

24. Welinder, K. G., and Smillie, L. B. (1972) *Can. J. Biochem.* **50**, 63-90.

25. Welinder, K. G. (1976) *FEBS Lett.* **72**, 19-23.

26. Welinder, K. G. (1979) *Eur. J. Biochem.* **96**, 483-502.

27. Welinder, K. G. (1985) *Eur. J. Biochem.* **151**, 497-504.

28. Welinder, K. G., and Mazza, G. (1977) *Eur. J. Biochem.* **73**, 353-358.

29. Welinder, K. G., and Mazza, G. (1975) *Eur. J. Biochem.* **57**, 415-424.

30. Haschke, R. H., and Friedhoff, J. M. (1978) *Biochem. Biophys. Res. Commun.* **80**, 1039-1042.

31. Ogawa, S., Shiro, Y., and Morishima, I. (1979) *Biochem. Biophys. Res. Commun.* **90**, 674-678.

32. Shiro. Y., Kurono, M., and Morishima, I. (1986) *J. Biol. Chem.* **261**, 9382-9390.

33. Morishima, I., Kurono, M., and Shiro, Y. (1986) *J. Biol. Chem.* **261**, 9391-9399.

34. Lanir, A., and Schejter, A. (1975) *Biochem. Biophys. Res. Commun.* **62**, 199-203.

35. Vuk-Pavlovic, S., and Siderer, Y. (1977) *Biochem. Biophys. Res. Commun.* **79**, 885-889.

36. Spiro, T. G., Strong, J. D., and Stein, P. (1979) *J. Am. Chem. Soc.* **101**, 2648-2655.

37. Kobayashi, K., Tamura, M., Hayashi, K., Hori, H., and Morimoto, H. (1980) *J. Biol. Chem.* **255**, 2239-2242.

38. Yoeman, L. C., and Hager, L. P. (1980) *Biochim. Biophys. Res. Commun.* **97**, 1233-1240.

39. Yonetany, T., Yamamoto, H., Erman, J. E., Leigh, J. S., and Reed, G. H. (1972) *J. Biol. Chem.* **247**, 2447-2455.

40. Brunet, J., and Pulgar, M. (1993) *Biochim. Biophys. Acta* **1203**, 171-174.

41. Royer, C. A., and Alpert, B. (1987) *Chem. Phys. Lett.* **134**, 454-460.

42. Reed, C. A., Mashiko, T., Bentley, S. P., Kastner, M. E., Scheidt, W. R., Spartalian, K., and Lang, G. (1979) *J. Am. Che. Soc.* **101**, 2948-2958.

43. Maltempo, M. M., Ohlsson, P.-I., Paul, K.-G., Petersson, L., and Ehrenberg, A. (1979) *Biochemistry* **18**, 2935-2941.

44. LaMar, G. N., de Ropp, J. S., Smith, K. M., and Langry, K. C. (1980) *J. Biol. Chem.* **255**,6646-6652.

45. Morishima, I., Ogawa, S., and Yamada, H. (1980) *Biochemistry* **19**, 1569-1575.

46. Bhattacharyya, D. K., Bandyopadhyay, U., and Banerjee, R. K. (1993) *J Biol. Chem.* **268**, 22292-22298.

47. Chuang, W., Heldt, J., and *Van* Wart, H. (1989) *J. Biol. Chem.* **264**, 14209-14215.

48. Fujiyama, K., Takemura, H., Shinmyo, A., Okada, H., and Takano, M. (1990) *Gene* **89**, 163-169.

49. Bartonek-Roxa, E., Eriksson, H., and Mattiasson, B. (1991) *Biochim. Biophys. Acta* **1088**, 245-250.

50. Ozaki, S. I., and Ortiz de Montellano, P. R. (1994) *J. Am. Chem. Soc.* **116**, 4487-4488.

51. Reiter, B., Pickering, A., and Oram, J. D., (1964) in *Microbial Inhibitors in Food* (Molin, N., Ed.) Almqvist & Wiksel, Uppsala, pp. 297.

52. Reiter, B., and Perraudin, J. P. (1991) *in* Peroxidases in Chemistry and Biochemistry, Edited by Everse, J., Everse, K. E., and Grisham, M. B., **Vol. 1**, pp 143-180, CRC Press, Boca Raton.

53. Sievers, G. (1981) *FEBS Lett.* **127**, 253-256.

54. Carlstrom, A. (1969) *Acta Chem. Scand.* **23**, 203-213.

55. Rombauts, W. A., Schroeder, W. A., and Morrisson, M. (1967) *Biochemistry* **6**, 2965-2977.

56. Carlstrom, A. (1969) *Acta Chem. Scand.* **23**, 171-213.

57. Booth, K. S., Kimura, S., Lee, H. C., Ikeda-Saito, M., and Caughey, W. S. (1989) *Biochem. Biophys. Res. Commun.* **160**, 897-902.

58. Nichol, A. W., Angel, L. A., Moon, T., and Clezy, P. S. (1987) *Biochem. J.* **247**, 147-150.

59. Cals, M. M., Mailliart, P., Brignon, G., Anglade, P., and Dumas, B. R. (1991) *Eur. J. Biochem.* **198**, 733-739.

60. Morishita, K., Kubota, N., Asano, S., Kaziro, Y., and Nagata, S. (1987) *J. Biol.Chem.* **262**, 3844-3851.

61. Morishita, K., Tsuchiya, M., Asano, S., Kaziro, Y., and Nagata, S. (1987) *J. Biol.Chem.* **262**, 15208-15213.

62. Johnson, K. R., Nauseef, W. M., Care, A., Wheelock, M. J., Shane, S., Hudson, S., Koeffler, H. P., Selsted, M., Miller, C., and Rovera, G. (1987) *Nucleic Acids Res.* **15**, 2013-2028.

63. Johnson, K. R., Gemperlein, I., Hudson, S., Shane, S., and Rovera, G. (1989) *Nucleic Acids Res.* **17**, 7985-7986.

64. Ten, R. M., Pease, L. R., MoKean, D. J., Bell, M. P., and Gleich, G. J. (1989) *J. Exp. Med.* **169**, 1757-1769.

65. Sakamaki, K., Tomonaga, M., Tsukui, K., and Nagata, S. (1989) *J. Biol. Chem.* **264**, 16828-16836.

66. Venturelli, D., Bittenbender, S., and Rovera, G. (1989) *Nucleic Acids Res.* **17**, 7989-7988.

67. Venturelli, D., Shirsat, N., Gemperlein, I., Bittenbender, S., Hudson, S., and Rovera, G. (1989) *Nucleic Acids Res.* **17**, 5852.

68. Sievers, G., Gadsby, P. M. A., Peterson, J., and Thomson, A. J. (1983) *Biochim. Biophys. Acta* **742**, 659-668.

69. Sievers, G., Peterson, J., Gadsby, P. M. A., and Thomoson, A. J. (1984) *Biochim. Biophys. Acta* **785**, 7-13.

70. Lukat, G. S., Rodgers, K. R., and Goff, H. M. (1987) *Biochemistry* **26**, 6927-6932.

71. Behere, D. V., Gonzalez-Vergara, E., and Goff, H. M. (1985) *Biochem. Biophys. Res. Commun.* **131**, 607-613.

72. Behere, D. V., Gonzalez-Vergara, E., and Goff, H. M. (1985) *Biochim. Biophys. Acta* **832**, 319-325.

73. Goff, H. M., Gonzalez-Vergara, E., and Ales, D. C. (1985) *Biochem. Biophys. Res. Commun.* **133**, 794-799.

74. Shiro, Y., and Morishima, I. (1986) *Biochemistry* **25**, 5844-5849.

75. Thanabal, V., and La Mar, G. N. (1989) *Biochemistry* **28**, 7038-7044.

76. Kitagawa, T., Hashimoto, S., Teraoka, J., Nakamura, S., Yajima, H., and Hosoya, T. (1983) *Biochemistry* **22**, 2788-2792.

77. Manthey, J. A., Boldt, N. J., Bocian, D. F., and Chan, S. I. (1986) *J. Biol. Chem.* **261**, 6734-6741.

78. Hashimoto, S., Nakamima, R., Yamazaki, I., Kotani, T., Ohtaki, S., and Kitagawa, T. (1989) *FEBS Lett.* **248**, 205-209.

79. Hu, S., Treat, R. W., and Kincaid, J. R. (1993) *Biochemistry* **32**, 10125-10130.

80. Chang, C.-S., Sinclair, R., Khalid, S., Yamazaki, I., Nakamura, S., and Powers, L. (1993) *Biochemistry*, **32**, 2780-2786.

81. Sinclair, R., Yamazaki, I., Bumpus, J., Brock, B., Chang, C.-S., Albo, A., and Powers, L. (1992) *Biochemistry* **31**, 4892-4900.

82. Chance, B., Powers, L. Ching, Y., Poulos, T., Schonbaum, G. Yamazaki, I., and Paul, K. (1984) *Arch. Biochem. Biophys.* **235**, 596-611.

83. Ohtaki, S., Nakagawa, N., Nakamura, S., Nakamura, M., and Yamazaki, I. (1985) *J. Biol. Chem.* **260**, 441-448.

84. Yokota, K., and Yamazaki, I. (1977) *Biochemistry* **16**, 1913-1920.

85. Renganathan, V., and Gold, M. H. (1986) *Biochemistry* **25**, 1626-1631.

86. Morrison, M., Bayse, G., and Danner, D. J., (1970) *in* Biochemistry of the Phagocytic Process, *Edited by* Schultz, J., pp. 51, North-Holland, Amsterdam.

87. Paul, K.-G., and Ohlsson, P.-I., (1985) *in* The Lactoperoxidase System, Chemistry and Biological Significance *Edited by* Pruitt, K. M., and Tenovuo, J. O., pp.15, Marcel Dekker, New York.

88. Rombauts, W. A., Schroeder, W. A., and Morrison, M., (1967) *Biochemistry* **6**, 2965-2977.

89. Hamon, C. B., and Klebanoff, S. I. (1973) *J. Exp. Med.* **137**, 438-450.

90. Hanstrom, L., Johansson, A., and Carlsson, J., (1983) *Med. Biol.* **61**, 268-274.

91. Thomas, E. L., (1985) *in* The Lactoperoxidase System, Chemistry and Biological Significance *Edited by* Pruitt, K. M., and Tenovuo, J. O., Marcel Dekker, New York.

92. Thomas, E. L., Pera, K. A., Smith, K. W., and Chwang, A. K., (1983) *I nfect. Immun.*, **39**, 767-778.

93. Tenovuo, J. O. (1985) *in* The Lactoperoxidase System, Chemistry and Biological Significance *Edited by* Pruitt, K. M., and Tenovuo, J. O., pp. 101, Marcel Dekker, New York.

94. Harnulv, B. G., and Kandasamy, C., (1982) *Milchwissenschaft* **37**, 454-457.

95. Morrison, M., and Bayse, G. S., (1970) *Biochemistry* **9**, 2995-3000.

96. Bardsley, W. G., (1985) *in* The Lactoperoxidase System, Chemistry and Biological Significance, *Edited by* Pruitt, K. M., and Tenovuo, J. O., pp. 55, Marcel Dekker, New York.

97. Sakurada, J., Takahashi, S., and Hosoya, T. (1987) *J. Biol. Chem.* **262**, 4007-4010.

98. Sakurada, J., Takahashi, S., Shimizu, T., Hatano, M., Nakamura, S., and Hosoya, T. (1987) *Biochemistry* **26**, 6478-6483.

99. Modi, S., Saxena, A., Behere, D. V., and Mitra, S. (1990) *Biochim. Biophys. Acta* **1038**, 164-171.

100. Klebanoff, S. J., and Lleubke, R. G. (1965) *Proc. Soc. Exp. Biol. Med.* **118**, 483-489.

101. Slowey, R. R., Eidelman, S., and Klebanoff, S. J. (1968) *J. Bact.* **96**, 575-580.

102. Modi, S., Behere, D. V., and Mitra, S. (1989) *Biochemistry* **28**, 4689-4694.

103. Modi, S., Behere, D. V., and Mitra, S. (1989) *J. Biol. Chem.* **264**, 19677-19684.

104. Modi, S., Behere, D. V., and Mitra, S. (1991) *Biochim. Biophys. Acta* **1080**, 45-50.

105. Palmer, R. M. J., Ferrige, A. G., and Mancada, S. (1987) *Nature* **327**, 524-526.

106. Ignarro, L. J., Buga, G. M., Wood, K. S., Byrns, R. E., and Chaudhuri, G. (1987) *Proc. Natl. Acad. Sci. USA* **84**, 9265-9269.

107. Ignarro, L. J., Byrns, R. E., Buga, G. M., and Wood, K. S. (1987) *Circ. Res.* **61**, 866-879.

108. Koshland, D. E. Jr. (1992) *Science* **258**, 1861.

109. Floris, R., Piersma, S. R., Yang, G., Jones, P., and Wever, R. (1993) *Eur. J. Biochem.* **215**, 767-775.

110. Morris, D. R., and Hager, L. P. (1966) *J. Biol. Chem.* **241**, 1763-1768.

111. Hewson, W. D., and Hager, L. P. (1979) *in* The Porphyrins, Part B **Vol. 7**, pp. 295-332, Dolphin, D., Ed., Academic Press, New York.

112. Dawson, J. H., and Sono, M. (1987) *Chem. Rev.* **87**, 1255-1276.

113. Dawson, J. H. (1988) *Science* **240**, 433-439.

114. Araiso, T., Rutter, R., Palcic, M. M., Hager, L. P., and Dunford, H. B. (1981) *Can. J. Biochem.* **59**, 233-236.

115. Thomas, J. A., Morris, D. R., and Hager, L. P. (1970) *J. Biol. Chem.* **245**, 3129-3134.

116. Libby, R. D., Thomas, J. A., Kaiser, L. W., and Hager, L. P. (1982) *J. Biol. Chem.* **257**, 5030-5037.

117. Hager, L. P., Morris, D. R., Brown, F. S., and Eberwein, H. (1966) *J. Biol. Chem.* **241**, 1769-1777.

118. Harrison, J. E., and Schultz, J. (1976) *J. Biol. Chem.* **251**, 1371-1374.

119. Kedderis, G. L., and Hollenberg, P. F. (1983) *J. Biol. Chem.* **258**, 12413-12419.

120. Kedderis, G. L., Rickert, O. E., Pandey, R. N., and Hollenberg, P. F. (1986) *J. Biol. Chem.* **261**, 15910-15914.

121. McCarthy, M.-B., and White, R. E. (1983) *J. Biol. Chem.* **258**, 9153-9158.

122. Ortiz de Montellano, P. R., Choe, Y. S., DePillis, G., and Catalano, C. E. (1987) *J. Biol. Chem.* **262**, 11641-11646.

123. Kobayashi, S., Nakano, M., Goto, T., Kimura, T., and Schaap, A. P. (1986) *Biochem. Biophys. Res. Commun.* **135**, 166-171.

124. Doerge, D. (1986) *Arch. Biochem. Biophys.* **244**, 678-685.

125. Takata, T., Yamazaki, M., Fujimori, K., Kim, Y. H., Iyamagi, T., and Oae, S. (1983) *Bull. Chem. Soc. Jpn.* **56**, 2300-2310.

126. Fujimori, K., Matsuura, T., Mikami, A., Watanabe, Y., Oae, S., and Iyanagi, T. (1990) *J. Chem. Soc., Perkin Trans.* **I**, 1435-1440.

127. Cashman, J. R., Olsen, L. D., and Bornheim, L. M. (1990) *Chem. Res. Toxicol.* **3**, 344-349.

128. Cashman, J. R., and Olsen, L. D. (1990) *Mol. Pharmacol.* **38**, 573-585.

129. Rubin, B., Van Middlesworth, J., Thomas, K., and Hager, L. P. (1982) *J. Biol. Chem.* **257**, 7768-7769.

130. Hollenberg, P. F., and Hager, L. P. (1973) *J. Biol. Chem.* **248**, 2630-2633.

131. Griffin, B. W., Peterson, J. A., and Estabrook, R. W. (1979) *in* The Porphyrins, Part B. **Vol. 7**, pp. 333, Dolphin, D., Ed., Academic Press, New York.

132. Sligar, S. G., and Murray, R. I. (1986) *in* Cytochrome P-450: Structure, Mechanism, and Biochemistry, *Edited by* Ortiz de Montellano, P. R. pp. 429, Plenum Press, New York.

133. Cramer, S. P., Dawson, J. H., Hodgson, K. O., and Hager, L. P. (1978) *J. Am. Chem. Soc.* **100**, 7282-7290.

134. Dawson, J. H., Kau, L.-S., Penner-Hahn, J. E., Sono, M., Eble, K. S., Bruce, G. S., Hager, L. P., and Hodgson, K. O. (1986) *J. Am. Chem. Soc.* **108**, 8114-8116.

135. Hahn, J. E., Hodgson, K. O., Andersson, L. A., and Dawson, J. H. (1982) *J. Biol. Chem.* **257**, 10934-10941.

136. Caron, C., Mitschler, A., Riviere, G., Ricard, L., Schappacher, M., and Weiss, R. (1979) *J. Am. Chem. Soc.* **101**, 7401-7402.

137. Poulos, T. L. (1986) *in* Cytochrome P-450: Structure, Mechanism, and Biochemistry, *Edited by* Ortiz de Montellano, P. R. pp. 505, Plenum Press, New York.

138. Poulos, T. L., Finzel, B. C., and Howard, A. J. (1986) *Biochemistry*, **25**, 5314-5322 .

139. Mason, H. S., North, J. C., and Vanneste, M., (1965) *Fed. Proc. Fed. Am. Soc. Exp. Biol.* **24**, 1172-1180.

140. Bangcharoenpaurpong, O., Champion, P. M., Hall, K. S., and Hager, L. P. (1986) *Biochemistry* **25**, 2374-2378.

141. White, R. E., and Coon, M. J. (1980) *Annu. Rev. Biochem.* **49**, 315-356.

142. Poulos, T. L., Finzel, B. C., Gunsalus, I. C., Wagner, G. C., and Kraut, J. (1985) *J. Biol. Chem.* **260**, 16122-16130.

143. Champion, P. M., Munck, E., Debrunner, P. G., Hollenberg, P. F., and Hager, L. P. (1973) *Biochemistry* **12**, 426-435 .

144. Sono, M., Dawson, J. H., Hall, K., and Hager, L. P. (1986) *Biochemistry* **25**, 347-356.

145. Fang, G.-H., Kenigsberg, M. T., Axley, M., and Hager, L. P. (1986) *Nucleic Acids Res.* **14**, 8061-8071.

146. Chiang, R., Makino, R., Spomer, W. E., and Hager, L. P. (1975) *Biochemistry* **14**, 4166-4171.

147. Blanke, S. R., and Hager, L. P. (1988) *J. Biol. Chem.* **263**, 18739-18743.

148. Adachi, S., Nagano, S., Ishimori, K., Watanabe, Y., and Morishima, I. (1993) *Biochemistry* **32**, 241-252.

149. Hu, S., and Kincaid, J. R. (1993) *J. Biol. Chem.* **268**, 6189-6193.

150. Sono, M., Hager, L. P., and Dawson, J. H. (1991) *Biochim. Biophys. Acta* **1078**, 351-359.

151. Dugad, L. B., Wang, X., Wang, C.-C., Lukat, G. S., and Goff, H. M. (1992) *Biochemistry* **31**, 1651-1655.

152. Blanke, S. R., and Hager, L. P. (1990) *J. Biol. Chem.* **265**, 12454-12461.

153. Thanabal, V., de Ropp, J. S., and La Mar, G. N. (1988) *J. Am. Chem. Soc.* **110**, 3027-3035.

154. Satterlee, J. D., and Erman, J. E. (1991) *Biochemistry* **30**, 4398-4405.

155. Poulos, T. L., Finzel, B. C., and Howard, A. J. (1986) *Biochemistry* **25**, 5314-5322.

156. Finzel, B. C., Poulos, T. L., and Kraut, J. (1984) *J. Biol. Chem.* **259**, 13027-13036.

157. Champion, P. M., Stallard, B. R., Wagner, G. C., and Gunsalus, I. C. (1982) *J. Am. Chem. Soc.* **104**, 5469-5472.

158. Egawa, T., Miki, H., Ogara, T., Makino, R., Ishimura, Y., and Kitagawa, T. (1992) *FEBS Lett.* **305**, 206-208.

159. Neidleman, S. L., and Geigert, J. (1986) *in* Biohalogenation: Principles, Basic Roles, and Applications. Ellis Horwood, Chichester.

160. Ashley, P. L., and Griffin, B. W. (1981) *Arch. Biochem. Biophys.* **210**, 167-178.

161. Griffin, B. W., and Ashley, P. L. (1984) *Arch. Biochem. Biophys.* **233**, 188-196.

162. Lambeir, A.-M., and Dunford, H. B. (1983) *J. Biol. Chem.* **258**, 13558-13563.

163. Dunford, H. B., Lambeir, A.-M., Kashem, M. A., and Pickard, M. (1987) *Arch. Biochem. Biophys.* **252**, 292-302.

164. Morrison, M., and Schoubaum, G, R. (1976) *Annu. Rev. Biochem.* **45**, 861-888.

165. Nunez, J. (1980) *in* The Thyroid Gland (deVisscher, M. Ed.) pp. 39-59, Raven Press, Mew York.

166. Degroot, L. J., and Niepomniszcze, H. (1977) *Metabolism* **26**, 665-718.

167. Nunez, J., and Pommier, J. (1982) *Vitam. Horm.* **39**, 175-182.

168. Thomas, E. L. (1985) *in* The Lactoperoxidase System (Pruitt, K. M., and Tenovuo, J. O., Eds.) pp. 31-53, Marcel Dekker Inc., New York and Basel.

169. Palmer, D. A., and Lietzke, M. H. (1982) *Radiochimica Acta* **31**, 37-44.

170. Wren, J. C., Paquette, J., Sunder, S., and Ford, B. L. (1986) *Can. J. Chem.* **64**, 2284-2296.

171. Turner, D. H., Flynn, G. W., Sutin, N., and Beitz, J. V. (1972) *J. Am. Chem. Soc.* **94**, 1554-1559.

172. Eigen, M., and Kustin, K. (1962) *J. Am. Chem. Soc.* **84**, 1355-1361.

173. Davies, M., and Gwynne, E. (1952) *J. Am. Chem. Soc.* **74**, 2748-2752.

174. Ramette, R. W., and Sandford, R. W., Jr. (1965) *J. Am. Chem. Soc.* **87**, 5001-5005.

175. Palmer, D. A., Ramette, R. W., and Mesmer, R. E. (1984) *J. Solution Chem.* **13**, 673-683.

176. Wren, J. C., Paquette, J., Sunder, S., and Ford, B. L. (1986) *Can. J. Chem.* **64**, 2284-2296.

177. Allen, T. L., and Keefer, R. M. (1955) *J. Am. Chem. Soc.* **77**, 2957-2960.

178. Palmer, D. A., and vanEldik, R. (1986) *Inorg. Chem.* **25**, 928-931.

179. Ingold, K. U., (1968) *Adv. Chem. Ser.*, **75**, 296-305.

180. Endo, Y., Usuki, R. & Kareda, T. (1985) *J. Am. Oil Chem. Soc.*, **62** (9), 1387-1390.

181. Reinton, R. & Rogstad, A. (1981) *J. Food Sci.*, **46**, 970-1973.

182. Packer, J. E., Slater, T. F. & Willson, R. L. (1979) *Nature*, **278**, 737.

183. Masuyama, S. (1965) *J. Japan Oil Chem. Soc.*, **14** , 692-697.

184. Tappel, A. L., Brown, W. D., Zalkin, H. & Maier, V. P. (1961) *J. Am. Oil Chem. Soc.*, **38**, 5-9.

185. Pongracz, G. (1973) *Int. J. Vit. Nutr. Res.*, **43**, 517-525.

186. Cort, W. M. (1`974) *J. Am. Oil Chem. Soc.*, **51**, 321-325.

187. Cort, W. M. (1982) *Adv. Chem. Ser.*, **200**, 533.

188. Reinton, R. & Rogstad, A. (1981) *J. Food Sci.*, **46**, 970-971.

189. Barclay, L. R. C., Locke, S. J. & MacNeil, J. M. (1983) *Can. J. Chem.*, **61**, 1288-1290.

190. Kanematsu, H., Aoyama, M., Maruyama, T., Niiya, I., Tsukamoto, M., Tokairin, S. & Matsumoto, T. (1984) *J. Japan Oil Chem. Soc.*, **33** , 361-365.

191. Aoyama, M., Maruyama, T., Kanematsu, H., Niiya, I., Tsukamoto, M., Tokairin, S. & Matsumoto, T. (1985) *J. Japan Oil Chem. Soc.,* **34** , 48-52.

192. Packer, J. E., Slater, T. F. & Willson, R. L. (1979) *Nature (London),* **278**, 738.

193. Kellogg, E. W. III & Fridovich, I. (1975) *J. Biol. Chem.,* **250**, 8812-8815.

CHAPTER TWO

KINETICS AND MECHANISM OF THE PEROXIDASE-CATALYZED IODINATION OF TYROSINE

2.1 SUMMARY

The kinetics of iodination of tyrosine by hydrogen peroxide and iodide, catalyzed by both horseradish peroxidase (HRP) and lactoperoxidase (LPO) were studied. The initial rates of formation of both molecular I_2 and monoiodotyrosine (MIT) were measured with stopped flow techniques. The following reactions occur in both systems:

Enzymatic:

$$Fe^{III} + H_2O_2 \longrightarrow Fe^{V}=O + H_2O$$

$$Fe^{V}=O + I^- \longrightarrow Fe^{III}\text{-}O\text{-}I^-$$

$$Fe^{III}\text{-}O\text{-}I^- + H^+ \longrightarrow Fe^{III} + HOI$$

$$Fe^{III}\text{-}O\text{-}I^- + I^- + H^+ \longrightarrow Fe^{III} + I_2 + HO^-$$

Iodine Equilibria:

$$I_2 + I^- \rightleftharpoons I_3^-$$

$$I_2 + H_2O \rightleftharpoons HOI + I^- + H^+$$

A version of this chapter has been published. Sun, W., and Dunford, H. B. 1993 *Biochemistry* **32**: 1324-1331.

Non-Enzymatic Iodination. One or both of the following:

$$Tyr + HOI \longrightarrow MIT + H_2O$$

$$Tyr + I_2 \longrightarrow MIT + I^- + H^+$$

where Fe^{III} is native peroxidase, $Fe^{V} = O$ is compound I and Tyr is tyrosine. The big difference in the two systems is that the following reaction also occurs with LPO:

$$Fe^{III}\text{-}O\text{-}I^- + Tyr \longrightarrow MIT + Fe^{III} + HO^-$$

and is the dominant mechanism of iodination for the mammalian enzyme. The overall rate of formation of MIT is about 10 times faster for LPO compared to HRP under comparable conditions. A small decrease in rate occurs when D-tyrosine is substituted for L-tyrosine in the LPO reaction. Thus LPO has a tyrosine binding site near the heme. A kinetically-controlled maximum is observed in I_3^- concentration. Once equilibrium is established, I_2 is the dominant form of inorganic iodine in solution. However hypoiodous acid may be the inorganic iodination reagent.

2.2 INTRODUCTION

Because of the physiological significance of tyrosine iodination, several studies have been devoted to the peroxidase catalysis of this reaction. There are conflicting reports in the literature with respect to the iodination mechanism. The main conflict centers upon the identity of the iodinating species. Although it was suggested that I_2 is an obligatory intermediate (1)

there is evidence indicating that I_2 is not the active iodinating agent in thyroid peroxidase-catalyzed iodination (2). Other experimental results support the conclusion that iodination does not occur by way of free I_2, but rather via an iodinating species associated with the enzyme (3-5). It has been suggested that the iodinating species is enzyme-activated hypoiodous acid, HOI, based on a kinetic analysis of tyrosine iodination catalyzed by HRP at low pH (6). Magnusson *et al.* (7) claimed that free HOI is the active iodinating species in the LPO iodination system. A proposal has been made that both of I_2 and HOI may play roles as iodinating agents (8). The effect of iodide on the interconversion of oxidized enzyme species has been studied for lactoperoxidase and thyroid peroxidase (9). Huber *et al.* (10) concluded that a highly reactive iodinating intermediate is produced on lactoperoxidase, which diffuses from the enzyme before reacting.

The experiments described here were designed to study further the possible iodinating species in mixtures of hydrogen peroxide, iodide and tyrosine catalyzed by two different enzymes: the plant enzyme horseradish peroxidase (HRP, donor: H_2O_2 oxidoreductase, EC 1.11.1.7) and the mammalian enzyme lactoperoxidase (LPO, donor: H_2O_2 oxidoreductase, EC 1.11.1.7). The initial rates of formation of I_2 and MIT were measured at 460 nm (ε_{I_2} 7.46 x 10^2 $M^{-1}cm^{-1}$ (11)) and at 290 nm (ε_{MIT} 2.30 x 10^3 $M^{-1}cm^{-1}$, (Fig.2.1)), using the stopped-flow technique. Initial rates of I_2 formation were compared in the presence of tyrosine and in blank experiments without tyrosine present. It is shown that different mechanisms are required in order to describe the two different enzyme-catalyzed iodination reactions.

In the peroxidase-catalyzed iodination of tyrosine, the first step is the reaction of the native enzyme with H_2O_2 to form compound I, which contains

two more oxidizing equivalents than the native enzyme. This compound is able to oxidize an electron donor in a one-electron or two-electron transfer reaction. It has been shown that the oxidation of iodide by enzyme compound I is a two-electron transfer process. Iodide is oxidized to an oxidation state of +1 and compound I is reduced directly to the native enzyme (12). The direct oxidation of tyrosine is a one-electron transfer process in which compound I is reduced to compound II and a tyrosyl radical is generated (13). The oxidations of both iodide and tyrosine by HRP-I are strongly pH dependent. The HRP-I reaction with iodide is much faster in the pH 3-4 region than at alkaline pH (12) whereas the reaction of HRP-I with tyrosine reaches a maximum at pH 9.6 (13). In order to minimize the direct oxidation of tyrosine and maximize the oxidation of iodide we used a pH of 3.60 for the HRP system. For LPO, we used the same pH for optimal rate of iodination observed by Morrison and Bayse (14): pH 5.0.

2.3 EXPERIMENTAL

Horseradish peroxidase was purchased as an ammonium sulfate suspension from Boehringer-Mannheim. After dialysis against deionized water from the Milli-Q system, a purity number of 3.25-3.40 was determined from the ratio of absorbances at 403 and 280 nm. The concentration of the enzyme solution was measured spectrophotometrically at 403 nm where the molar absorptivity is $1.02 \times 10^5\ M^{-1}cm^{-1}$ (15). Lactoperoxidase with a purity number (A_{412}/A_{280}) of 0.85 was purchased from Sigma as a purified, lyophilized powder. Its concentration was determined using a molar absorptivity of $1.12 \times 10^5\ M^{-1}cm^{-1}$ at 412 nm (16).

The concentration of hydrogen peroxide, obtained from BDH

Chemicals, was determined after appropriate dilution using the horseradish peroxidase assay (17). L- and D-tyrosine, MIT and DIT were purchased from Sigma. Stock solutions of tyrosine, MIT and DIT (~2.8 mM) were prepared by dissolution in appropriate volumes of 0.1 M KOH, and then neutralizing the solutions by adding the same volumes of 0.1 M HNO_3. Reagent grade potassium iodide was purchased from Shawinigan Chemicals. All the chemicals were used without further purification. Solution concentrations were determined by weight and fresh stock solutions were prepared just before use.

Chemicals for the phosphate and citrate buffers were reagent grade and used without further purification. The ionic strength of the buffers was 0.01 M. Analytical reagent K_2SO_4, obtained from AnalaR, was used to keep the total ionic strength of reaction mixtures at 0.11 M.

All solutions were prepared using deionized water obtained from the Milli-Q system (Millipore).

Optical absorption measurements on a conventional time scale (>1 s) were made on a Cary 219 spectrophotometer. Stopped-flow and rapid scan experiments were performed on a Photal (formerly Union Giken) Model RA-601 Rapid Reaction Analyzer. O_2 production was determined with a Yellow Spring Instruments Model 53 Oxygen Monitor.

A pH-jump method was used for all stopped-flow experiments because the native HRP and LPO are not stable at low pH. We illustrate for measurement of rate constants involving HRP-I. One cuvette contained stable HRP-I (1:1 ratio of H_2O_2 and HRP) in phosphate buffer of ionic strength 0.01 M, pH 6.17, (total ionic strength 0.11 M); the other cuvette contained iodide (and tyrosine except for blank experiments) in citrate buffer,

pH 3.23, ionic strength 0.11 M. After mixing the two solutions, the final pH was 3.60. A Fisher Accumet Model 420 digital pH meter was used for pH measurements.

The absorbance scale of the single-beam Photal Rapid Reaction Analyzer was calibrated using the stopped flow mode at 353 nm. Different concentrations of I_3^- solutions were made by dissolving a small amount of crystalline I_2 with a relatively large amount of KI in pH 3.60 citrate buffer. The absolute absorbances, A, of these solutions were measured on a Cary 219 spectrophotometer at 353 nm. On the Photal instrument, pH 3.60 citrate buffer was used as a reference to adjust the baseline to a certain absorbance, A_b, and the relative absorbances, A_r, of the above I_3^- solutions were measured. Therefore ΔA, which is equal to A_r-A_b, could be obtained. A calibration curve was made by plotting ΔA against the absolute absorbance A for different concentrations of I_3^-.

All experiments were performed at 25.0 ± 0.1 °C.

2.4 RESULTS

Spectra of L-tyrosine, MIT and DIT

Fig. 2.1 shows the optical spectra of L-tyrosine, MIT and DIT at pH 3.60. An isosbestic point of MIT and DIT occurs at 292 nm. The biggest absorbance difference between MIT and tyrosine occurs at 290 nm where a molar absorptivity value of $2.30 \times 10^3\ M^{-1}cm^{-1}$ was obtained for MIT, while tyrosine shows almost no absorbance at this wavelength. Similar spectra were obtained at pH 4.97.

HRP Results

Rate of conversion of HRP-I to HRP in the presence of Iodide and/or tyrosine

Fig. 2.2 shows the rapid scan spectra for the reaction of HRP-I with tyrosine at pH 3.60. The partial conversion of HRP-I to HRP-II is observed, i.e., the start of a one-electron reduction of HRP-I.

In marked contrast Fig. 2.3 shows the rapid scan spectra during the conversion of HRP-I in the presence of both KI and tyrosine at pH 3.60. These spectra are very similar to those obtained when tyrosine is absent. Over a period of 80 ms, HRP-I is going directly to native HRP, i.e., only iodide is reacting with HRP-I and the iodide is converted to a +1 oxidation state.

Rate constants of the reaction of HRP-I with iodide were measured at 403 nm without and with tyrosine present at pH 3.60 as a function of iodide concentration. Linear plots of the pseudo-first order rate constants were obtained, and from the slopes the second order rate constants for the reaction of HRP-I with iodide could be obtained. The results are: (1.8 ± 0.2) $x10^6$ $M^{-1}s^{-1}$ without tyrosine present and $(1.9 \pm 0.2) \times 10^6$ $M^{-1}s^{-1}$ with tyrosine present, which are identical within experimental error. Hence, it was confirmed that tyrosine does not affect the reaction of HRP-I with iodide at pH 3.60.

Steady-state experiments

(1) The time dependences of I_3^-, I_2 and I^- concentrations in the iodination reaction from the stopped-flow experiments

Iodide has no absorption in the region 265-500 nm. Tyrosine has its maximum absorbance at 274 nm (Fig. 2.1). Triiodide ion has absorbance

maxima at 353 nm, 287.5 nm and 460 nm ($\varepsilon_{353} = 2.64 \times 10^4\ M^{-1}cm^{-1}$, $\varepsilon_{287.5} = 4.00 \times 10^4\ M^{-1}cm^{-1}$ and $\varepsilon_{460} = 9.75 \times 10^2\ M^{-1}cm^{-1}$ (11)). Iodine has its maximum absorbance at 460 nm ($\varepsilon_{460} = 7.46 \times 10^2\ M^{-1}cm^{-1}$(11)). The biggest absorbance difference between MIT and tyrosine is at 290 nm where $\varepsilon_{MIT} = 2.30 \times 10^3\ M^{-1}\ cm^{-1}$ while tyrosine does not have any absorption at this wavelength, as shown in Fig. 2.1. Fig. 2.4 shows stopped flow traces at 353 nm (a), 460 nm (b) and 290 nm (c) obtained from the reaction mixture containing 1.14 μM HRP, 1.02 mM H_2O_2, 324 μM KI and 324 μM tyrosine in pH 3.60 citrate buffer with ionic strength of 0.11 M. Hence, curve (a) is the time course for I_3^- at its maximum absorbance of 353 nm. By using the calibration curve which was obtained for the Photal instrument, the relative absorbances obtained from curve (a) could be converted to I_3^- concentrations. The results shown in Fig. 2.5a indicate that a kinetically-controlled maximum occurs in I_3^- concentration. The fast enzymatic oxidation of I^- to HOI is followed by reaction of HOI with I^- to generate I_2; the overall process is shown in eq 2.1. The I_2 in turn reacts with excess I^- to form I_3^- (eq 2.2).

$$H_2O_2 + 2I^- \xrightarrow{\text{Peroxidase}} I_2 + 2OH^- \qquad (2.1)$$

$$I_2 + I^- \underset{k_2}{\overset{k_1}{\rightleftharpoons}} I_3^- \qquad (2.2)$$

It follows that:

$$K_2 = \frac{[I_3^-]}{[I_2][I^-]} = \frac{k_1}{k_2} = 729\ M^{-1} \qquad (2.3)$$

$$[I^-]_{total} = [I^-] + 2[I_2] + 3[I_3^-] \qquad (2.4)$$

The thermodynamics of the formation of I_3^- has been extensively studied; reported values of K_2 are 768 M^{-1} (18), 721 M^{-1} (19), 698 M^{-1} (20) and 746 M^{-1} (21), within the experimental error in eq 2.3. Using the measured I_3^- concentrations and combining the equilibrium constant of eq 2.3 with the mass conservation in eq 2.4, the corresponding I^- and I_2 concentrations at different times were calculated. The results shown in Fig. 2.5b clearly show that once equilibrium is established, molecular I_2 is the dominant form of inorganic iodide in the solution. Therefore, in curve (b) of Fig. 2.4, the absorbance at 460 nm at times less than 400 ms is attributable to a mixture of I_2 and I_3^-. In order to determine an accurate initial rate of I_2 formation, the tangent from the starting point of curve (b) was taken because at that point only I_2 has been formed without any interference of I_3^- (Fig. 2.4). At times longer than 1.0 s, it was observed that the absorbance at 460 nm decreases which indicated that I_2 is being consumed. The time course at 290 nm in curve (c) of Fig. 2.4 shows that the absorbance increases after 1.0 s which is caused by MIT formation without any interference from I_3^-. By using the tangent from the starting point of this increase in absorbance in curve (c), the initial rate of MIT formation could be obtained accurately. Overall, from the results of Figs. 2.4 and 2.5b, we conclude that the iodination reaction coincides with depletion of the I_2 concentration.

Stopped-flow experiments were used to monitor the disappearance of

I_2 at 460 nm. Results over a 60 s span are shown in the absence (curve (a)) and presence (curve (b)) of tyrosine at pH 3.60 (as shown in Fig. 2.6). Curve (a) shows a small decrease of I_2 in the absence of tyrosine caused by the pseudo-catalatic (catalase-like) reaction of HRP (see later). Curve (b) shows the much larger decrease in I_2 in the presence of tyrosine.

(2) O_2 production from degradation of H_2O_2

Several investigators have reported that the so-called pseudo-catalatic degradation of H_2O_2 was detected in the lactoperoxidase iodination system (8, 22-24). The experiments described here were designed to study this phenomenon in the HRP iodination system. Under steady-state conditions with KI, H_2O_2 and HRP present, curve (a) of Fig. 2.7 shows that a large amount of O_2 was produced. In contrast, when tyrosine was present, the catalase-like reaction was markedly inhibited, as shown in curve (b). This indicated that H_2O_2 was utilized primarily for iodination in the presence of tyrosine, even though the degradation of excess H_2O_2 by hypoiodous acid, HOI, was still competing with the tyrosine iodination. The pseudo-catalatic reaction can be explained as follows:

$$Fe^{III} + H_2O_2 \longrightarrow Fe^{V}=O + H_2O \qquad (2.5)$$

$$Fe^{V}=O + H^+ + I^- \longrightarrow Fe^{III} + HOI \qquad (2.6)$$

$$HOI + H_2O_2 \longrightarrow O_2 + H_2O + H^+ + I^- \qquad (2.7)$$

$$2H_2O_2 \longrightarrow O_2 + 2H_2O \qquad (2.8)$$

where Fe^{III} represents native HRP and Fe^{V} = O HRP-I.

(3) Effect of I^- concentration on the initial rates of formation of I_2 and MIT

The steady-state conditions were changed by increasing the iodide concentration and hence the $[I^-]/[tyr]$ ratio. All experiments were carried out by keeping the concentrations of tyrosine, H_2O_2 and HRP constant. The $[I^-]/[tyr]$ ratio was varied over the range 1 : 1 to 6 : 1. Fig. 2.8 shows a representative time course at 460 nm for 750 ms and the initial rate of I_2 formation for an $[I^-]/[tyr]$ ratio of 1 : 1. Data for all $[I^-]/[tyr]$ ratios are collected in Table 2.1.

For the same experimental conditions, the time courses at 290 nm were measured. As the ratio of the $[I^-]/[tyr]$ increased from 1 : 1 to 4 : 1, the absorbance trace at 290 nm over 80 s was observed to change from a monophasic to a biphasic curve. Fig. 2.9 shows the curve for the $[I^-]/[tyr]$ ratio of 4 : 1 in the HRP system. The initial rate of MIT formation was obtained by constructing the tangent from the starting point of the first phase as shown. The second phase might be due to the mixture of the second product DIT and I_3^-. The initial rates of MIT formation were determined as the $[I^-]/[tyr]$ ratio increased. Data is shown in Table 2.1.

(4) The effect of tyrosine on I_2 formation

Experiments were performed to investigate I_2 formation in the presence and absence of tyrosine. The initial rates of I_2 formation are collected in Table 2.2. The rates of I_2 formation are almost the same with and without tyrosine present.

LPO Results

Steady-state experiments

(1) Effect of I^- concentration on the initial rates of formation of I_2 and MIT

The same steady-state conditions were used as for the HRP iodination system except that the pH was 4.97. The results are displayed in Fig. 2.10. Absorbance at 353 nm reflects the concentration of I_3^-. The 290 nm results show interference from I_3^- absorbance if I_3^- is present; in its absence they are an accurate measure of MIT concentration. There is an initial burst in I_3^- formation followed by its rapid disappearance as the equilibrium in eq. 2.2 is established. For a 4.5 : 1 ratio of [KI]/[tyr] or lower the absorbance of I_3^- falls effectively to zero and remains there, whereas MIT formation is occurring. This shows clearly that I_3^- is not the iodinating species. For higher ratios of [KI]/[tyr] the results in Fig. 2.10 show some reformation of I_3^- in later stages of the reaction. There is a lag phase in I_3^- reformation which is made shorter by higher ratios of [KI]/[tyr]. During the lag phase initial rates of MIT formation can be measured without interference from I_3^- absorbance. Hence, it is ensured that the measurement of the initial rate of MIT formation at 290 nm was accurate, i.e.: without any interference of the I_3^-, in the limited range of I^- concentration used in this study. We did not attempt to measure rates for [KI]/[tyr] greater than 5.5 : 1 where the reformation of I_3^- could not be distinguished from MIT formation. As is explained below the initial rates of MIT formation are a true measure of the LPO-catalyzed reaction and the reformation of I_3^- in the later stages is indicative of non-enzymatic iodination which occurs when all H_2O_2 is consumed.

The same method used to determine the initial rate of I_2 formation for

HRP was applied for LPO as well. The initial rates of I_2 formation were determined as the $[I^-]/[tyr]$ increased from 1 : 1 to 6 : 1. Data is collected in Table 2.1. Comparison plots of the rates of I_2 formation versus the $[I^-]/[tyr]$ ratio for the two systems are displayed in Fig. 2.11a. Under the same experimental conditions, the time courses at 290 nm were measured. The initial rates of MIT formation were determined as the $[I^-]/[tyr]$ ratio increased by the same method used for HRP. These data are also shown in Table 2.1. The overall rate of formation of MIT is about 10 times faster for LPO compared to HRP under comparable conditions. Comparison plots of the rates of MIT formation versus the $[I^-]/[tyr]$ ratio for the two systems are shown in Fig. 2.11b. Inhibition of MIT formation was observed in the LPO system as the $[I^-]/[tyr]$ ratio increased to 5.5 : 1.

(2) The effect of tyrosine on I_2 formation

Experiments in the presence and absence of tyrosine were also carried out for LPO. The initial rates of I_2 formation were measured as the $[I^-]$ changed from 324 μM to 1.94 mM. Data are collected in Table 2.2. The rates of I_2 formation are about five times faster without tyrosine present for LPO than when tyrosine was present. Thus when LPO is used, tyrosine is an effective competitor for the I_2 precursor. The HRP results, where the presence or absence of tyrosine had little or no effect on I_2 formation are in sharp contrast.

(3) Iodination of D-tyrosine

Measurements have been made under the same experimental conditions using D-tyrosine instead of L-tyrosine in the LPO-catalyzed

reaction. The results are shown in Table 2.3. It was observed that D-tyrosine is less reactive in MIT formation; this leads to more I_2 formation.

2.5 DISCUSSION

Although peroxidases are generally considered to catalyze oxidation in a similar manner and to be relatively nonspecific with regard to substrates, closer investigation shows striking differences. The present investigation shows that lactoperoxidase is more efficient than horseradish peroxidase in its ability to catalyze iodide oxidation, and much more efficient in its ability to catalyze iodination of tyrosine.

HRP mechanism

With respect to the HRP iodination system, the initial rate of I_2 formation was found to be unaffected by the presence of tyrosine (Table 2.2). This indicates that the species resulting from iodide oxidation, in which the iodine is in a +1 oxidation state, reacts much faster with excess I^- to form the I_2 than with the tyrosine to form MIT. Molecular iodine is known to be in equilibria with other species in aqueous solution as shown in eqs. 2.2 and 2.9:

$$I_2 + I^- \underset{k_2}{\overset{k_1}{\rightleftharpoons}} I_3^- \qquad (2.2)$$

$k_1 = (6.2 \pm 0.8) \times 10^9\ M^{-1}s^{-1}$, $k_2 = (8.5 \pm 1.0) \times 10^6\ s^{-1}$ (25).

$$I_2 + H_2O \underset{k_4}{\overset{k_3}{\rightleftharpoons}} HOI + I^- + H^+ \qquad (2.9)$$

The overall rate constant for the forward reaction, k_3, is 3.0 s^{-1}, k_4 is 4.4 x 10^{12} M^{-2} s^{-1} for the reverse reaction (26) and the equilibrium constant K_9 is 5.4 x 10^{-13} M^2 at 25.0 °C (27). From K_9 one can calculate the value of $[HOI][I^-]/[I_2]$ at any pH, and at pH 3.6 it is 2.2 x 10^{-9} M: strong supporting evidence for our contention that I_2 is the predominant species of iodine. It is shown clearly in Fig. 2.5b that I_3^- is not involved in the iodination reaction at all. Thus, the depletion of I_2, shown in Fig. 2.6, is due to iodination of tyrosine by either I_2 or HOI, which cannot be distinguished because of the equilibrium in eq 2.9. Therefore in the case of HRP, either I_2 or HOI is the iodinating reagent. The pseudo-catalatic degradation of H_2O_2 by iodide and HRP was observed by detection of O_2 evolution. The following overall mechanism is proposed for the reaction of I^-, H_2O_2 and tyrosine in oxygenated aqueous solution catalyzed by HRP.

HRP Reactions:

$$HRP + H_2O_2 \longrightarrow H\ \ RP\text{-}I\ +\ H_2O \qquad (2.10)$$

$$\left\{\begin{array}{l} HRP\text{-}I + I^- \longrightarrow HRP\text{-}O\text{-}I^- \\ HRP\text{-}O\text{-}I^- + H^+ \longrightarrow HRP + HOI \end{array}\right\} \qquad (2.11)$$

$$HRP\text{-}O\text{-}I^- + I^- + H^+ \longrightarrow HRP + I_2 + OH^- \qquad (2.12)$$

Iodine Equilibria:

$$I_2 + I^- \rightleftharpoons I_3^- \qquad (2.2)$$

$$I_2 + H_2O \rightleftharpoons HOI + I^- + H^+ \qquad (2.9)$$

Non-Enzymatic Iodination. One or both of the following:

$$Tyr + HOI \xrightarrow{k_{13}} MIT + H_2O \qquad (2.13)$$

$$Tyr + I_2 \xrightarrow{k_{14}} MIT + I^- + H^+ \qquad (2.14)$$

Oxygen Evolution:

$$HOI + H_2O_2 \longrightarrow O_2 + H_2O + I^- + H^+ \qquad (2.7)$$

HRP-O-I^- is the enzyme-bound hypoiodite which is not detected in any of our experiments and which must have a very short half-life. However it provides the only reasonable mechanism for HOI formation.

The maximum rate constants of eqs 2.13 and 2.14 can be obtained by assuming that only one of the reactions occurs for iodination. The HOI concentration at time of 1.0 s when MIT starts forming (Fig. 2.4c) can be calculated from eq 2.9 by the known concentrations of I_2 and I^- at that time (Fig. 2.5b). The calculated k_{13} is 9.3×10^5 $M^{-1}s^{-1}$ which is same as the result of 9×10^5 $M^{-1}s^{-1}$ obtained by Dunford and Ralston (6), and k_{14} is 1.18×10^4 $M^{-1}s^{-1}$. There is approximately two orders of magnitude difference between the two rate constants. Since there is an equilibrium between I_2 and HOI (eq 2.9), one cannot distinguish which of the non-enzymatic species, I_2 or HOI, is responsible for tyrosine iodination when HRP is the catalyst for their formation.

LPO mechanism

In the case of lactoperoxidase, the experimental results clearly show that the initial rate of I_2 formation is decreased by the presence of tyrosine

(Table 2.2). Also, the initial rate of MIT formation occurs in the absence of I_3^- formation (Fig. 2.10). If non-enzymatic iodination were occurring in this region, either through I_2 or HOI, then either of the following mechanisms of formation of I_3^- would occur:

$$\text{Tyr} + I_2 \longrightarrow \text{MIT} + H^+ + I^- \qquad (2.14)$$

$$\text{Tyr} + \text{HOI} \longrightarrow \text{MIT} + H_2O \qquad (2.13)$$

$$I_2 + H_2O \longrightarrow \text{HOI} + H^+ + I^- \qquad (2.9)$$

$$I^- + I_2 \rightleftharpoons I_3^- \qquad (2.2)$$

The combination of either eqs 2.14 and 2.2 or eqs 2.9, 2.13 and 2.2 leads to I_3^- formation, which is not occurring in the initial region, but only after H_2O_2 is exhausted. This indicates that the initial tyrosine iodination must take place through the LPO-bound hypoiodite complex, (LPO-O-I^-). The initial rate of MIT formation catalyzed by LPO is about 10 times faster than by HRP system (depending somewhat on the [KI]/[tyr] ratio) as shown in Fig. 2.11b. This provides further evidence that the LPO-bound hypoiodite complex serves as an iodinating species which is a much more efficient iodinating reagent than either I_2 or HOI. At the same time, it was observed that the rate of I_2 formation remains significant. Therefore, non-enzymatic iodination becomes important in later stages of the reaction and is the only mechanism of iodination when H_2O_2 is exhausted. The mechanism of catalysis for LPO is summarized in the following equations:

LPO Reactions:

$$LPO + H_2O_2 \longrightarrow LPO\text{-}I + H_2O \quad (2.15)$$

$$LPO\text{-}I + I^- \longrightarrow LPO\text{-}O\text{-}I^- \quad (2.16)$$

$$LPO\text{-}O\text{-}I^- + Tyr + H^+ \longrightarrow MIT + LPO + H_2O \quad (2.17)$$

$$LPO\text{-}O\text{-}I^- + H^+ \longrightarrow LPO + HOI \quad (2.18)$$

$$LPO\text{-}O\text{-}I^- + I^- + H^+ \longrightarrow LPO + I_2 + OH^- \quad (2.19)$$

Iodine Equilibria:

$$I_2 + I^- \rightleftharpoons I_3^- \quad (2.2)$$

$$I_2 + H_2O \rightleftharpoons HOI + I^- + H^+ \quad (2.9)$$

Non-Enzymatic Iodination. One or both of the following:

$$Tyr + HOI \longrightarrow MIT + H_2O \quad (2.13)$$

$$Tyr + I_2 \longrightarrow MIT + I^- + H^+ \quad (2.14)$$

Oxygen Evolution:

$$HOI + H_2O_2 \longrightarrow O_2 + H_2O + I^- + H^+ \quad (2.7)$$

Over a wide range the rate of I_2 formation is independent of the initial I^- concentration (Fig. 2.11a) whereas at sufficiently low I^- concentrations, it is dependent (data not shown). This phenomenon can be explained by four eqs 2.16, 2.18, 2.19 and 2.9. At low I^- concentrations, eq 2.16, 2.19 or 2.9 is the rate-determining step, therefore the rate of I_2 formation is dependent on I^- concentration. However, when I^- concentration is increased, the rates of eqs 2.16, 2.19 and 2.9 are increased, so that eq 2.18 becomes the rate-

determining step which is independent on the I^- concentration.

Our results on the iodination of D-tyrosine are in contrast to those of Morrison and Bayse (14) who claimed that D-tyrosine is more reactive. Our results indicate that the LPO-catalyzed tyrosine iodination reaction has some stereospecificity under our experimental conditions. Therefore, tyrosine is bound to LPO when the iodination reaction occurs. This is further evidence that the LPO-bound hypoiodite complex is responsible for the iodination of tyrosine. Nevertheless, the D-isomer still has significant reactivity which can be explained because of the large distance between the chiral carbon center and the iodination positions.

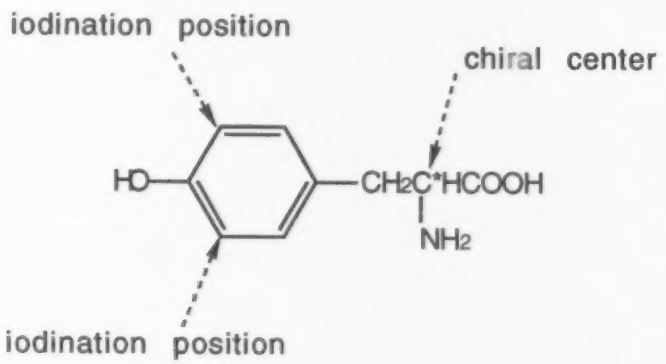

2.6 CONCLUSIONS

The data reported in the present study indicates that either I_2 or HOI is the iodinating species in the HRP iodination system. The role of HRP is to catalyze the formation of HOI which reacts with excess I^- to form I_2. Thus in the HRP system the actual iodination step is non-enzymatic. For the mammalian enzyme a LPO-bound hypoiodite complex, LPO-O-I^-, is an efficient iodinating species, and under physiological conditions is probably

the only iodinating reagent. Under our experimental conditions either I_2 or HOI also is important in later stages of the reaction. While it is impossible to make a choice, based exclusively on kinetic data, between HOI and I_2 as non-enzymatic iodinating reagents, there is a good physiological reason to favor HOI. Our data show that its rate constant for reaction with tyrosine is about 100 times larger than that for I_2. Therefore, about a 200-fold lower initial concentration of iodide would lead to the same rate of formation of MIT from HOI as one would obtain from I_2. This also fits a picture of the simplest evolutionary progression: from use of HOI free in solution to enzyme-bound hypoiodite as the iodinating reagent.

TABLE 2.1. Dependence of the initial rates of I_2 and MIT formation on I^- concentrations for HRP and LPO iodination systems. [HRP] or [LPO] 1.14 μM; [H_2O_2] 1.02 mM; [tyr] 324 μM.

[I^-] (mM)	I_2 formation rate ($M\,s^{-1}$)		MIT formation rate ($M\,s^{-1}$)	
	HRP ($x10^3$)	LPO	HRP ($x10^5$)	LPO ($x10^4$)
0.324	0.62	2.20	0.44	0.37
0.648	1.23	2.16	0.89	1.04
0.972	1.61	2.25	1.42	2.15
1.13				2.88
1.30	1.94	2.21	2.32	3.66
1.46				5.40
1.62	2.24	2.16	3.05	5.98
1.78		2.10		4.99
1.94	2.47	2.09	4.19	

TABLE 2.2. Effect of tyrosine on the initial rate of I_2 formation for HRP and LPO systems. Concentrations as in Table 2.1.

$[I^-]$ (mM)	I_2 formation rate ($x10^3$ M s^{-1})			
	HRP		LPO	
	with Tyr present	without Tyr present	with Tyr present	without Tyr present
0.324	0.62	0.72	2.20	10.3
0.648	1.23	1.33	2.16	9.69
0.972	1.61	1.60	2.25	10.2
1.30	1.94	1.78	2.21	9.57
1.62	2.24	2.04	2.16	9.76
1.78		2.26	2.10	9.24
1.94	2.47	2.44	2.09	8.92

TABLE 2.3. Stereoisomeric effect of D- and L-tyrosine on the initial rates of I_2 and MIT formation for LPO. [LPO] 1.14 μM; [H_2O_2] 1.02 mM; [L-tyr] or [D-tyr] 324 μM.

$[I^-]$ (mM)	I_2 formation rate ($x10^3$ M s^{-1})		MIT formation rate ($x10^4$ M s^{-1})	
	L-tyr	D-tyr	L-tyr	D-tyr
0.324	2.20	2.95	0.37	0.20
0.648	2.16	3.00	1.04	0.50
0.972	2.25	2.94	2.15	1.08
1.30	2.21	2.78	3.66	1.84
1.62	2.16	2.77	5.98	3.02
1.78	2.10	2.83	4.99	3.95

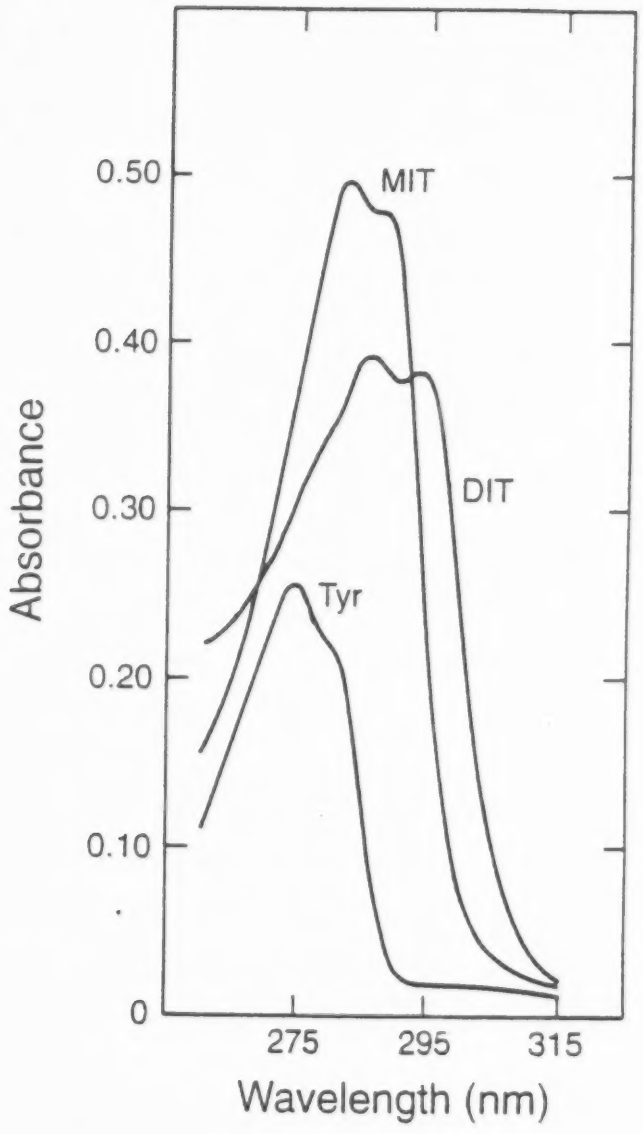

Figure 2.1. Optical spectra of 0.20 mM L-tyrosine, 0.20 mM monoiodotyrosine and 0.20 mM diiodotyrosine in citrate buffer of ionic strength 0.11 M, pH 3.60, at temperature 25 °C.

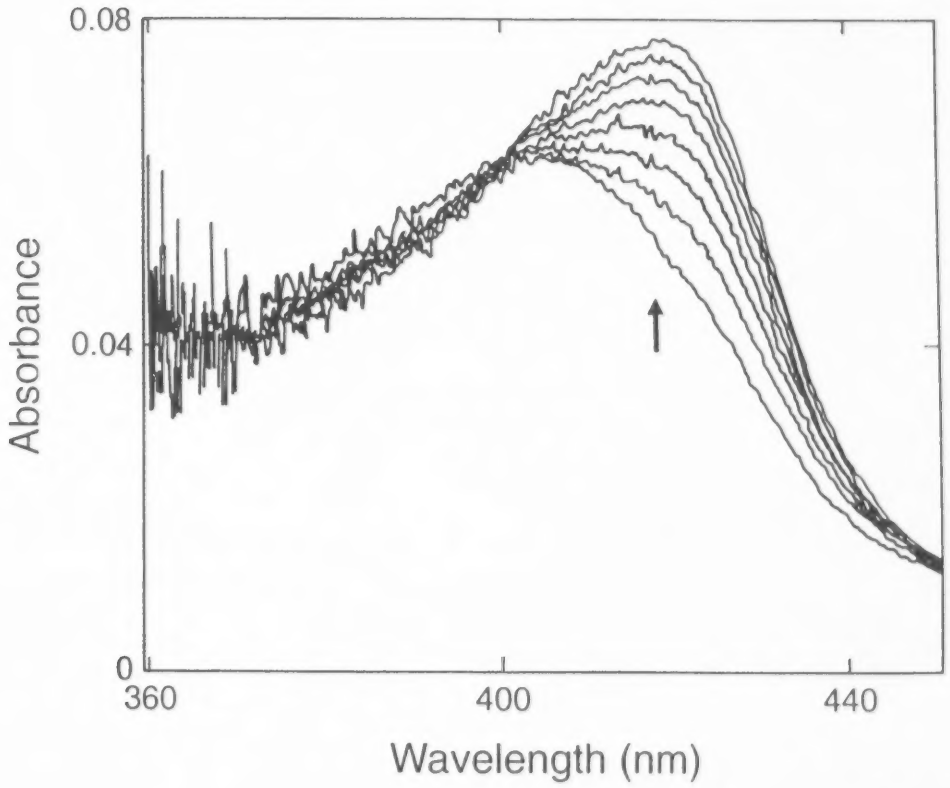

Figure 2.2. Rapid scan spectra over 8.3 s for the reaction of 1.14 μM HRP-I with 16.7 μM L-tyrosine at pH 3.60. One cuvette contained HRP-I in phosphate buffer, pH 6.17, total ionic strength 0.11 M; the other contained L-tyrosine in citrate buffer, pH 3.23, ionic strength 0.11 M. Final pH 3.60. The partial conversion of HRP-I to HRP-II is shown clearly. The arrow indicates the direction of absorbance change with increasing time.

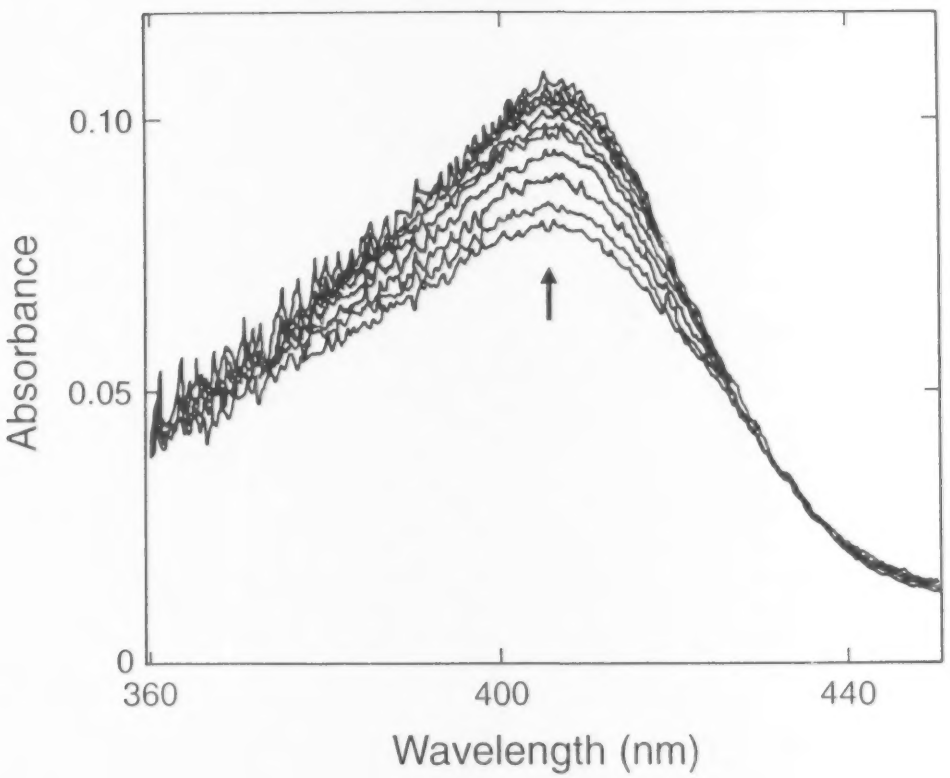

Figure 2.3. Rapid scan spectra over 80 ms during the direct conversion of 1.14 μM HRP-I to native HRP in the presence of both 17.2 μM KI and 17.2 μM L-tyrosine at pH 3.60. Other experimental conditions as in Fig. 2.2. The results indicate that the only reaction is the two-electron transfer from iodide to HRP-I.

Figure 2.4. Formation and disappearance of I_3^- and I_2 and formation of MIT during the HRP-catalyzed iodination of tyrosine:
(a) I_3^- measured at 353 nm;
(b) I_2 measured at 460 nm and
(c) MIT measured at 290 nm.
Initial concentrations are: [KI] = [tyrosine], 324 μM; [H_2O_2], 1.02 mM; [HRP], 1.14 μM. One cuvette contained H_2O_2 and L-tyrosine in citrate buffer, pH 3.50, ionic strength 0.11 M; the other contained KI and HRP in K_2SO_4 solution of ionic strength 0.11 M. Final pH 3.50.

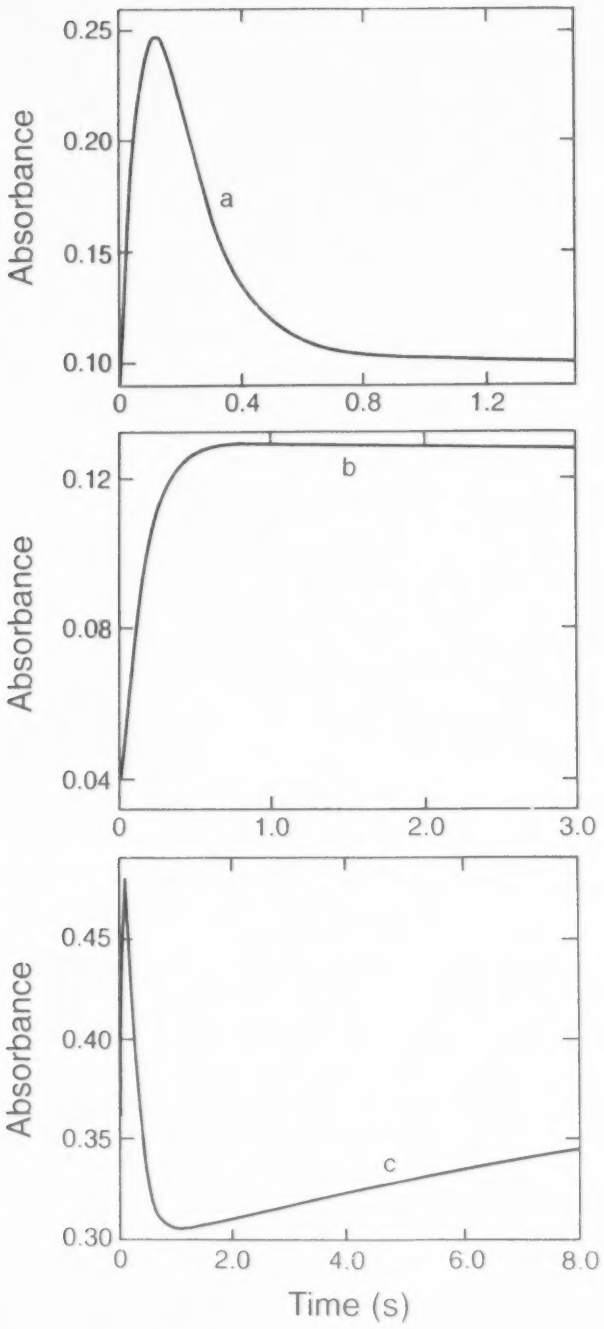
Absorbance
0.25
0.20
0.15
0.10
a
0
0.4
0.8
1.2
Absorbance
0.12
0.08
0.04
b
0
1.0
2.0
3.0
Absorbance
0.45
0.40
0.35
0.30
c
0
2.0
4.0
6.0
8.0
Time (s)

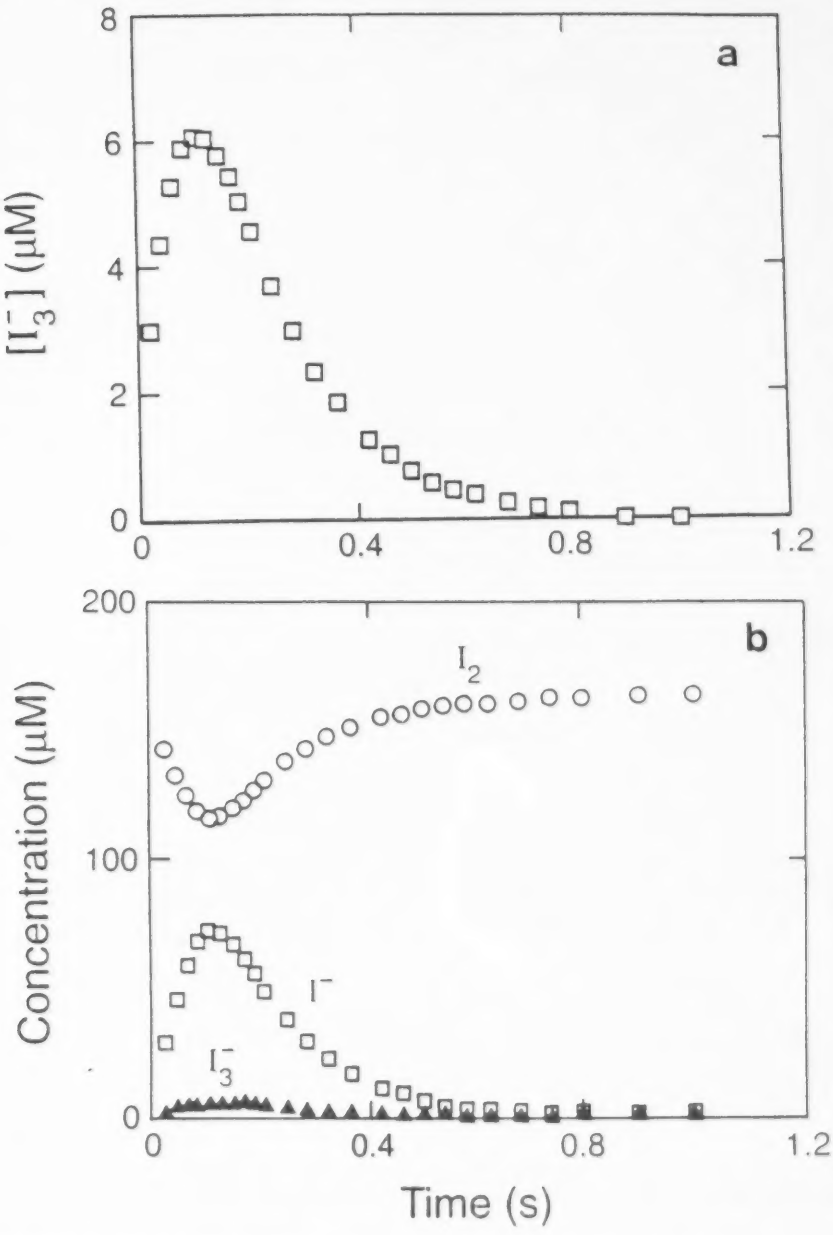

Figure 2.5. (a) I_3^- concentration over a period of 1.2 s in the reaction mixture of 1.14 μM HRP, 1.02 mM H_2O_2, 324 μM KI and 324 μM tyrosine at pH 3.60. (b) Comparison of time dependences of the concentrations of I_3^-, I^- and I_2. Conditions as in (a).

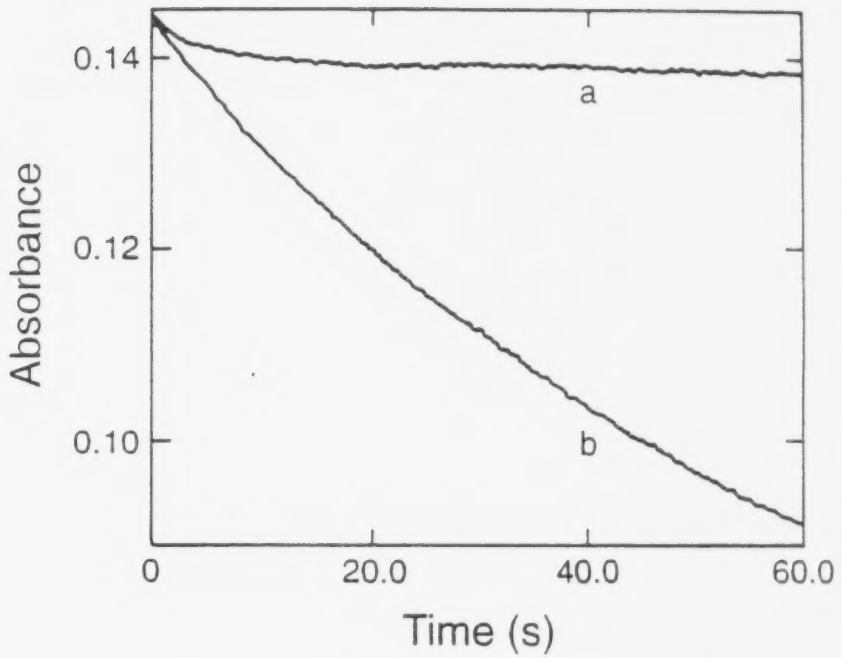

Figure 2.6. Disappearance of I_2 monitored over 60 s at 460 nm in a reaction mixture of HRP, H_2O_2 and KI in the absence (curve a) and presence (curve b) of L-tyrosine. Except for the longer time scale and the absence of tyrosine for curve (a), experimental conditions as in Fig. 2.4.

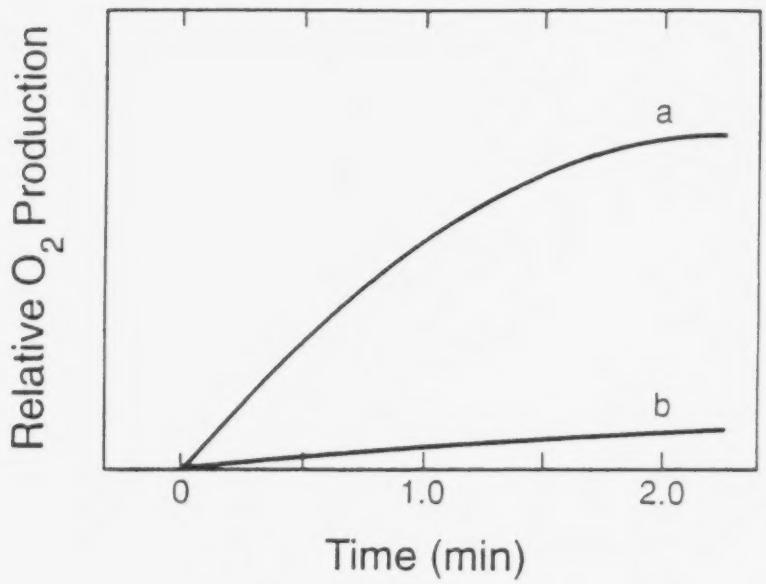

Figure 2.7. Relative O_2 production in a reaction mixture of 324 μM KI, 2.03 mM H_2O_2 and 2.27 μM HRP, curve (a); and same reaction mixture with 324 μM tyrosine added, curve (b). Citrate buffer pH 3.60.

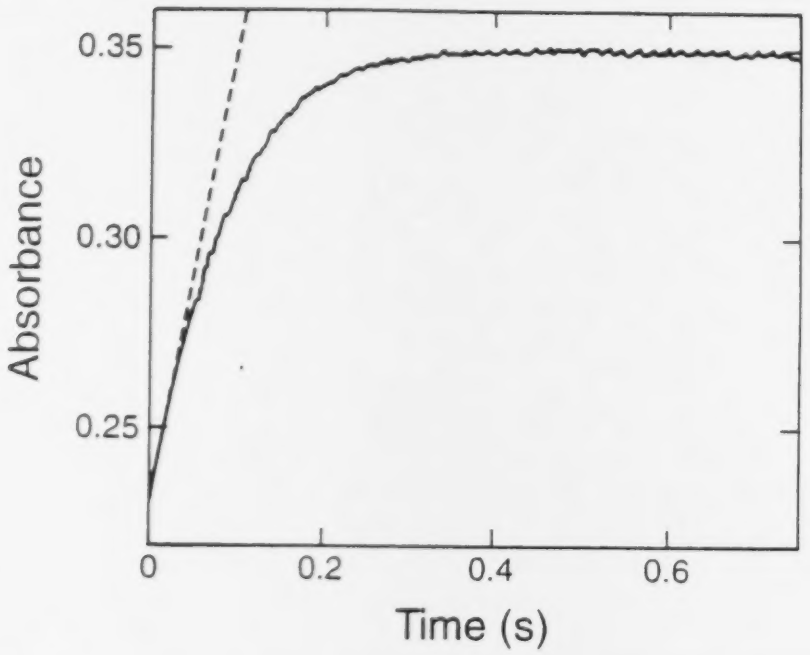

Figure 2.8. Formation of I_2 monitored at 460 nm in a reaction mixture of 324 μM KI, 324 μM tyrosine, 1.02 mM H_2O_2 and 1.14 μM HRP at pH 3.60. Initial rate determined from the tangent to the curve.

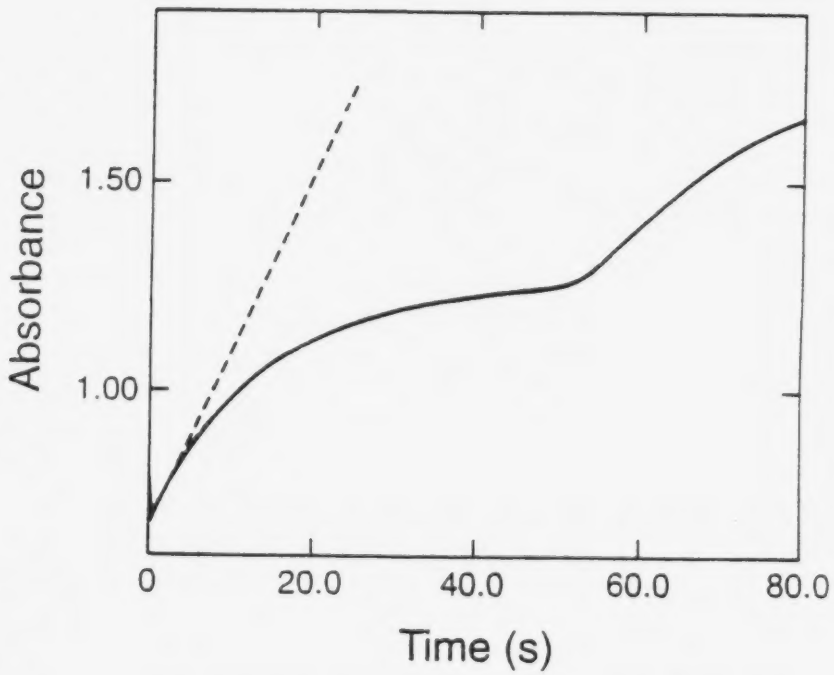

Figure 2.9. Formation of MIT (and subsequent reaction) monitored over 80 s at 290 nm in a reaction mixture of 1.14 μM HRP, 1.02 mM H_2O_2, 324 μM tyrosine and 1.29 mM KI (i.e. a [KI]/[tyr] ratio of 4.0) at pH 3.50. Initial rate determined from the tangent to the first phase.

Figure 2.10. Absorbances at 353 nm and 290 nm for the LPO-catalyzed iodination of tyrosine. The measurements at 353 nm (i) are proportional to the concentration of I_3^-. Measurements at 290 nm (ii) reflect the concentration of MIT, but are interfered with by the presence of I_3^- if it is present (initial portions of all traces (a-d) and the final portions of traces (b-d)). Initial concentrations are: [tyr], 324 μM; [H_2O_2], 1.02 mM; [LPO], 1.14 μM with varying concentration of KI: (a) [KI]/[tyr] 4.5; (b) [KI]/[tyr] 5.0; (c) [KI]/[tyr] 5.5 and (d) [KI]/[tyr] 6.0.

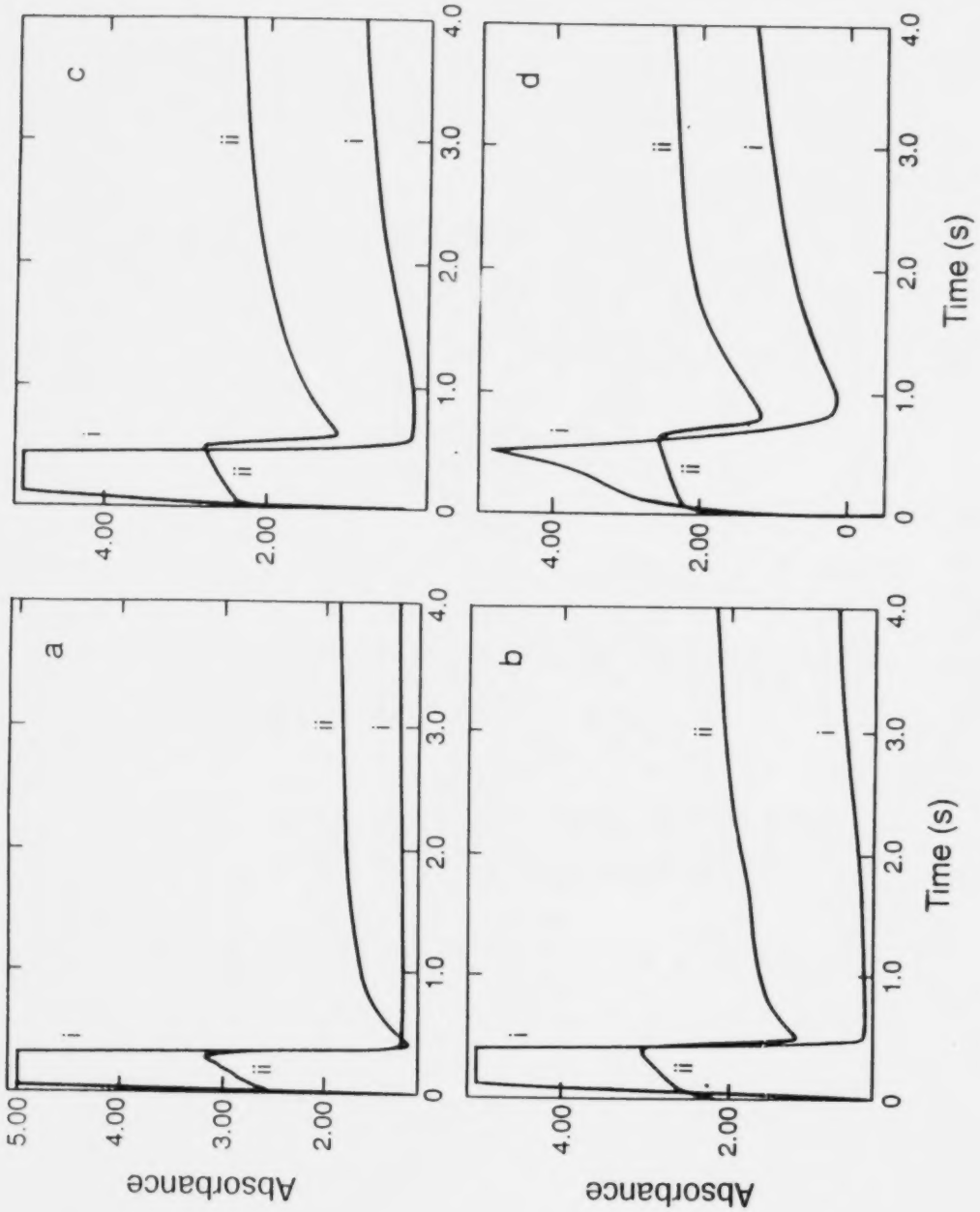
a
b
c
d
i
ii
Absorbance
Time (s)
5.00
4.00
3.00
2.00
0
1.0
2.0
3.0
4.0

Figure 2.11. (a) Plots of initial formation rates of I_2 versus the $[I^-]/[tyr]$ ratio in both the HRP and LPO iodination systems. The initial formation rates of I_2 were obtained as shown in Fig. 2.8. One cuvette contained H_2O_2 and KI in citrate buffer of ionic strength 0.11 M, pH 3.50 (for HRP) or pH 4.97 (for LPO); the other contained HRP or LPO and tyrosine in K_2SO_4 solution of ionic strength 0.11 M. (b) Plots of monoiodotyrosine formation rates which were obtained as shown in Fig. 2.9 *versus* the [KI]/[tyr] ratio. Experimental conditions as in (a).

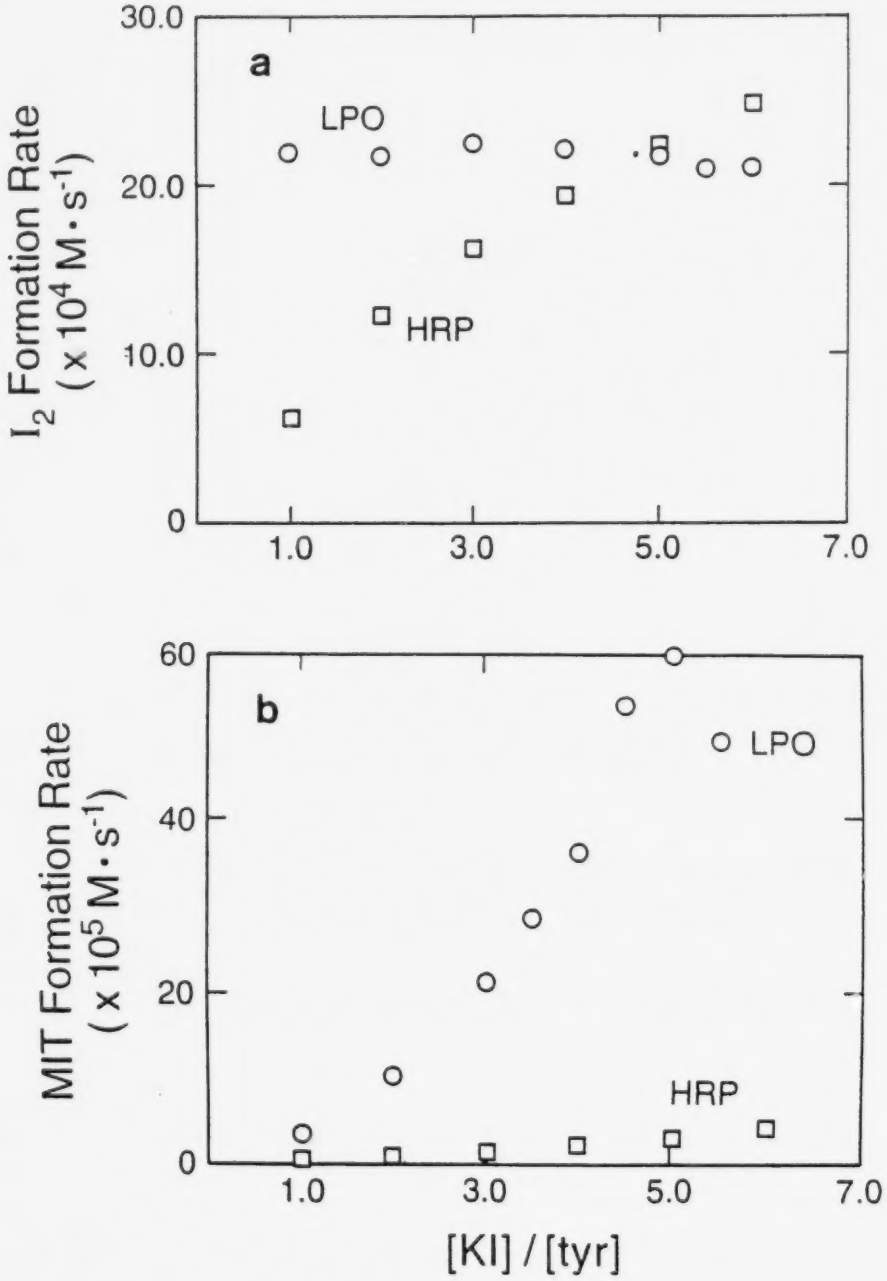
a
LPO
HRP
I_2 Formation Rate
(x 10^4 M • s^{-1})
30.0
20.0
10.0
0
1.0
3.0
5.0
7.0
b
LPO
HRP
MIT Formation Rate
(x 10^5 M • s^{-1})
60
40
20
0
1.0
3.0
5.0
7.0
[KI] / [tyr]

2.7 REFERENCES

1. Thomas, J. A., & Hager, L. P. (1969) *Biochem. Biophys. Res. Commun.* **35,** 444-450.
2. Taurog, A. (1970) *Arch. Biochem. Biophys.***139,** 212-220.
3. Bayse, G. S., & Morrison, M. (1971) *Arch. Biochem. Biophys.* **145,** 143-148.
4. Pommier, J., Sokoloff, L., & Nunez, J. (1973) *Eur. J. Biochem.* **38,** 497-506.
5. Davidson, B., Neary, J. T., Strout, H. V., Maloof, F., & Soodak, M. (1978) *Biochim. Biophys. Acta* **522,** 318-326.
6. Dunford, H. B., & Ralston, I. M. (1983) *Biochem. Biophys. Res. Commun.* **116,** 639-643.
7. Magnusson, R. P., Taurog, A., & Dorris M. L. (1984) *J. Biol. Chem.* **259,** 13783-13790.
8. Huwiler, M., Bürgi, U., & Kohler, H. (1985) *Eur. J. Biochem.* **147,** 469-476.
9. Kohler, H., Taurog, A., & Dunford, H.B. (1988) *Arch. Biochem. Biophys.* **264,** 438-449.
10. Huber, R. E., Edwards, L. A., & Carne, T. J. (1989) *J. Biol. Chem.* **264,** 1381-1386.
11. Awtrey, A. D., & Connick, R. E. (1951) *J. Am. Chem. Soc.* **73,** 1842-1843.
12. Roman, R., & Dunford, H. B. (1972) *Biochemistry* **11,** 2076-2082.
13. Ralston, I., & Dunford, H.B. (1978) *Can. J. Biochem.* **56,** 1115-1119.
14. Morrison, M., & Bayse, G. S. (1970) *Biochemistry* **9,** 2995-3000.

15. Ohlsson, P.-I., & Paul, K.-G. (1976) *Acta Chem. Scand.* **B30,** 373-375.

16. Paul, K.-G., & Ohlsson, P.-J. (1985) *in*The Lactoperoxidase System *Edited by* K. M. Pruitt & Y. O. Tenovuo. Dekker, New York. **27**, pp. 15-30.

17. Cotton, M. L., & Dunford, H. B. (1973) *Can. J. Chem.* **51,** 582-587.

18. Davies, M., & Gwynne, E. (1952) *J. Am. Chem. Soc.* **74,** 2748-2752.

19. Ramette, R. W., & Sandford, R. W., Jr. (1965) *J. Am. Chem. Soc.* **87,** 5001-5005.

20. Palmer, D. A., Ramette, R. W., & Mesmer, R. E. (1984) *J. Solution Chem.* **13,** 673-683.

21. Wren, J. C., Paquette, J., Sunder, S., & Ford, B. L. (1986) *Can. J. Chem.* **64,** 2284-2296.

22. Magnusson, R. P., & Taurog, A. (1983) *Biochem. Biophys. Res. Commun.* **112,** 475-481.

23. Magnusson, R. P., Taurog, A., & Dorris, M. L. (1984) *J. Biol. Chem.* **259,** 197-205.

24. Huwiler M., & Kohler H. (1984) *Eur. J. Biochem.* **141,** 69-74.

25. Turner, D. H., Flynn, G. W., Sutin, N., & Beitz, J. V. (1972) *J. Am. Chem. Soc.* **94,** 1554-1559.

26. Eigen, M., & Kustin, K. (1962) *J. Am. Chem. Soc.* **84,** 1355-1361.

27. Allen, T. L., & Keefer, R. M. (1955) *J. Am. Chem. Soc.* **77,** 2957-2960.

CHAPTER THREE

KINETICS OF TROLOX C OXIDATION BY LACTOPEROXIDASE COMPOUND II

3.1 SUMMARY

The lactoperoxidase (LPO) compound II catalyzed oxidation of Trolox C, a vitamin E water-soluble derivative, was studied by rapid scan spectral analysis and stopped-flow kinetic measurements. Our rapid scan spectral analysis clearly indicates that LPO compound II is reduced to native enzyme by Trolox C; hence the reaction is a one-electron redox process. The reaction was investigated at pH's ranging from 3.0 to 7.0. Trolox C is more reactive with LPO-II in acidic solutions. Kinetic and spectroscopic studies demonstrate that LPO has a binding site in the vicinity of the heme for Trolox C. Trolox C exhibits a quantitative 1:1 binding to native LPO in acidic solutions. The binding ability of Trolox C to native LPO decreases with increasing pH. The same trend is observed when the second order rate constants k_{app} for the reaction are plotted against pH. A mechanism of Trolox C oxidation by LPO-II has been proposed in which protonation of an amino acid residue on LPO-II with a pK_e of 2.3 is essential and ionization of the carboxylic acid group on Trolox C accelerates the reaction rate. The second-order rate constants were determined to be $(4.1 \pm 0.5) \times 10^6\ M^{-1}s^{-1}$ for protonated Trolox C oxidation and $(1.9 \pm 0.3) \times 10^7\ M^{-1}s^{-1}$ for deprotonated Trolox C.

A version of this chapter has been published. Sun, W., and Dunford, H. B. 1993 *Biochem. Biophys. Res. Commun.* **194**: 306-311.

3.2 INTRODUCTION

The biological activity of vitamin E (α-tocopherol) is generally believed to be due to its antioxidant action to inhibit lipid peroxidation in biological membranes by donating a hydrogen atom to the chain-propagating peroxyl radicals (ROO·) and giving rise to chromanoxyl radicals of the antioxidant (1):

$$ROO\cdot + Toc\text{-}OH \longrightarrow ROOH + Toc\text{-}O\cdot \qquad (3.1)$$

where Toc-OH is tocopherol and Toc-O· is the chromanoxyl radical. Trolox C:

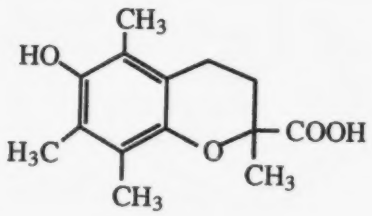

an antioxidant originally designed for food preservation (2), has a chromane structure similar to α-tocopherol but without the inert hydrophobic tail; it is both water and lipid soluble. The oxidation of Trolox C by lactoperoxidase has potential physiological relevance. It could help maintain the catalytic cycle and activity of animal peroxidases, leading to detoxification of hydrogen peroxide formed as a product of inflammation processes. A water-soluble derivative of vitamin E may have more therapeutic value than vitamin E itself (3).

3.3 EXPERIMENTAL

Lactoperoxidase (LPO) (EC 1.11.1.7, donor-H_2O_2 oxidoreductase) was purchased from Sigma. The R.Z. (A_{412}/A_{280}) of the samples was 0.70-0.85. The enzyme concentration was determined by using a molar absorptivity of $1.12 \times 10^5\ M^{-1}cm^{-1}$ at 412 nm (4). LPO-II(λ_{max} 430 nm) stable for 8 min was

prepared after mixing 2.0 μM LPO with 4.0 μM H_2O_2 in pH 7.3 and ionic strength 0.11 M phosphate buffer.

Hydrogen peroxide was obtained as a 30% solution from Fisher. The concentration of diluted H_2O_2 stock solution was determined by the peroxidase assay (5). Trolox C was obtained from Aldrich. The solution of Trolox C was freshly prepared just before each experiment. Trolox C was found to be stable in buffers in the pH range from 3.0 to 7.0, monitored at its maximum absorbance at 288 nm. All buffer solutions had an ionic strength 0.11 M, adjusted by adding K_2SO_4 as an inert salt. All solutions were prepared using the deionized water from a Milli-Q water purification system.

Kinetic measurements were performed on a Photal (formerly Union Giken) stopped-flow spectrophotometer Model RA-601. The 1-cm observation cell was thermostated at 25^{0}C for all measurements. A pH-jump method was used for all experiments because of the instability of LPO-II in acidic solutions. For stopped-flow experiments, one drive syringe was filled with LPO-II in 0.01 M phosphate buffer at pH 7.3. Inert salt (K_2SO_4) was used to maintain the ionic strength at 0.11 M. The other syringe was filled with Trolox C in 0.05 M citrate buffers at pH values ranging from 2.8 to 7.0. The ionic strength was also kept at 0.11 M by adding the inert salt. The pH after mixing the solutions in the two syringes were in the range from 3.0 to 7.0. At least a 10-fold excess of Trolox C was used to maintain pseudo-first-order conditions. The reaction was monitored by the disappearance of LPO-II at its maximum absorbance of 430 nm. Between six to eight traces were collected for each substrate concentration. The standard deviation was below 5%. Measurements of relative absorbance at regular time intervals from the

recorded exponential traces followed by a nonlinear least-square analysis gave the observed pseudo-first-order rate constants.

The pK_a value of the carboxylic acid group of Trolox C was determined by titration with concentrated NaOH using a Fisher Scientific Accumet pH Meter. The ionic strength of the solution was kept at 0.11 M by adding inert salt (K_2SO_4) to the dilute Trolox C solution. The effect of the small volume of NaOH could be ignored.

Trolox C binding to native LPO experiments were performed on a Cary 210 spectrophotometer. Both the reference and sample cuvettes contained LPO (6.47 μM). Trolox C was added only to the sample cuvette, and difference spectra in the range of 370-490 nm were determined in several low pH citrate buffer solutions, ionic strength 0.11 M. The dissociation constants (K_D) were calculated from the plot of $1/\Delta A$ *versus* 1/[Trolox C] where ΔA is the difference in absorbance at maximum absorption of the native enzyme. The number of binding sites near the heme was calculated from ΔA using a Hill plot (6).

3.4 RESULTS

Determination of pK_a of Trolox C.

The pK_a value of the carboxylic acid group of Trolox C was determined to be 4.03 in the solution of the ionic strength 0.11 M.

Oxidation of Trolox C by LPO-II.

The spectral changes observed during the reaction indicate that LPO-II is reduced directly to native state as shown in Fig. 3.1. The isosbestic point

appearing at 421 nm is proof of an LPO-II to native LPO conversion with no detectable intermediates:

$$\text{LPO-II} + \text{Trolox C} \longrightarrow \text{LPO} + \text{Trolox C}\cdot \qquad (3.2)$$

Kinetic Measurements.

With Trolox C in excess of LPO-II, pseudo-first-order kinetics were observed. One example is shown in the inset of Fig. 3.2. The corresponding differential rate expression is eq. 3.3:

$$-d[\text{LPO-II}]/dt = k_{obs}[\text{LPO-II}] \qquad (3.3)$$

where k_{obs} is the observed pseudo-first-order rate constant. The apparent second-order rate constant, k_{app}, is related to k_{obs} by eq. 3.4:

$$k_{obs} = k_{app}[\text{Trolox C}] \qquad (3.4)$$

Values of k_{app} were then obtained from the slopes of plots of k_{obs} versus [Trolox C], as shown by an example in Fig. 3.2. The small intercept is zero within the experimental error. A plot of k_{app} *versus* pH is shown in Fig. 3.3 for the oxidation of Trolox C by LPO-II.

Trolox C Binding to Native LPO.

Native LPO binds Trolox C in acidic solutions which results in a decrease in absorbance at the Soret maximum. Results of Hill plots (data not shown) indicate 1:1 binding within 10% error, and the binding increases with decreasing pH. The dissociation constants (mM) are 0.56 ± 0.04, 4.0 ± 0.3

and 12.1 ± 0.5 at pH's 2.93, 3.18 and 3.38. At pH higher than 3.38, the binding is weak and the difference spectra could not provide accurate data.

3.5 DISCUSSION

Our rapid scan spectral analysis of the changes in the enzyme oxidation states clearly indicates that the oxidation of Trolox C catalyzed by LPO-II is a one-electron redox process. The oxidation of Trolox C is similar to that of vitamin E and the reaction results in phenoxyl radical formation (7-10). The spectral changes observed upon binding of Trolox C to native LPO suggest that the binding site of Trolox C is near the heme. The extent of binding of Trolox C to native LPO as a function of pH indicates that an amino acid residue with a small pK_a value in the vicinity of the heme is part of the binding site for Trolox C. It has been reported from this group that LPO-II has an amino acid residue of pK_a 2.3 near the heme (7). The simplest mechanism which will account for the experimental data is one in which the protonated LPO-II with a pK_e of 2.3 reacting with both the protonated and deprotonated Trolox C as follows:

$$\begin{array}{l} \text{LPO-II} \\ \quad \uparrow\downarrow K_e \\ \text{HLPO-II}^+ \end{array} + \left\{ \begin{array}{ll} \text{HS}^+ \rightleftharpoons \text{H}^+ + \text{S} & \text{(with } K_a\text{)} \\ \text{HS}^+ \xrightarrow{k_1} \text{product} & \\ \text{S} \xrightarrow{k_2} \text{product} & \end{array} \right. \qquad (3.5)$$

The k_{app}-$[H^+]$ relationship corresponding to eq. 3.5 is:

$$k_{app} = \frac{k_1}{(1+K_a/[H^+])(1+K_e/[H^+])} + \frac{k_2}{(1+[H^+]/K_a)(1+K_e/[H^+])} \qquad (3.6)$$

Using nonlinear least-square analysis, the experimental k_{app}-pH data points shown in Fig. 3.3 were fitted to eq. 3.6 by using fixed values of $pK_a = 4.03$ and $pK_e = 2.3$ (11). The best-fit kinetic parameters are $k_1 = (4.1 \pm 0.5) \times 10^6$ $M^{-1}s^{-1}$ and $k_2 = (1.9 \pm 0.3) \times 10^7$ $M^{-1} s^{-1}$. The curve computed on the basis of the best-fit parameters is also shown in Fig. 3.3.

In conclusion the oxidation of Trolox C by LPO-II takes place first by binding to a site near the heme. The tighter binding of Trolox C at lower pH facilitates the reaction. The binding process is followed by hydrogen atom transfer from the phenolic hydroxyl group of Trolox C to LPO-II. A simple although speculative explanation of our results is that the carboxylate group of Trolox C binds to the acidic form of the LPO-II group with pK_e of 2.3.

Lipid peroxidation of iron-loaded liposomes has been found to increase with decreasing pH (12). The myeloperoxidase-H_2O_2-Cl^- system, a key part of the phagocytic process, displays maximum activity at about pH 5 (13, 14). Furthermore a decrease to pH 4 occurs in the vacuole upon phagocytosis (15). Our k_{app}-pH profile shows that Trolox C is more reactive at lower pH, which correlates with the trend in lipid peroxidation. Trolox C is reported to be the most efficient antioxidant in a series of analogues with a similar chromane structure to α-tocopherol (2).

This work can be compared to the oxidation of *p*-cresol by LPO-II, in which the second-order rate constants were studied over the pH range 2.1-11.2 by the same technique (11). The second-order rate constant for *p*-cresol oxidation by LPO-II is greater than the rate constant for Trolox C oxidation over the pH range 3.0-7.0. The difference in the pH-rate profiles for these two substrates may be a result of different binding sites. Contrary to the Trolox C results, protonation of an amino acid residue with pK_e 2.3 results in a

decreasing rate of reaction of LPO-II with *p*-cresol. The bigger chromane ring of Trolox C compared to the single benzene ring of *p*-cresol may result in some steric hindrance for Trolox C to attain the same position relative to the heme active site as *p*-cresol.

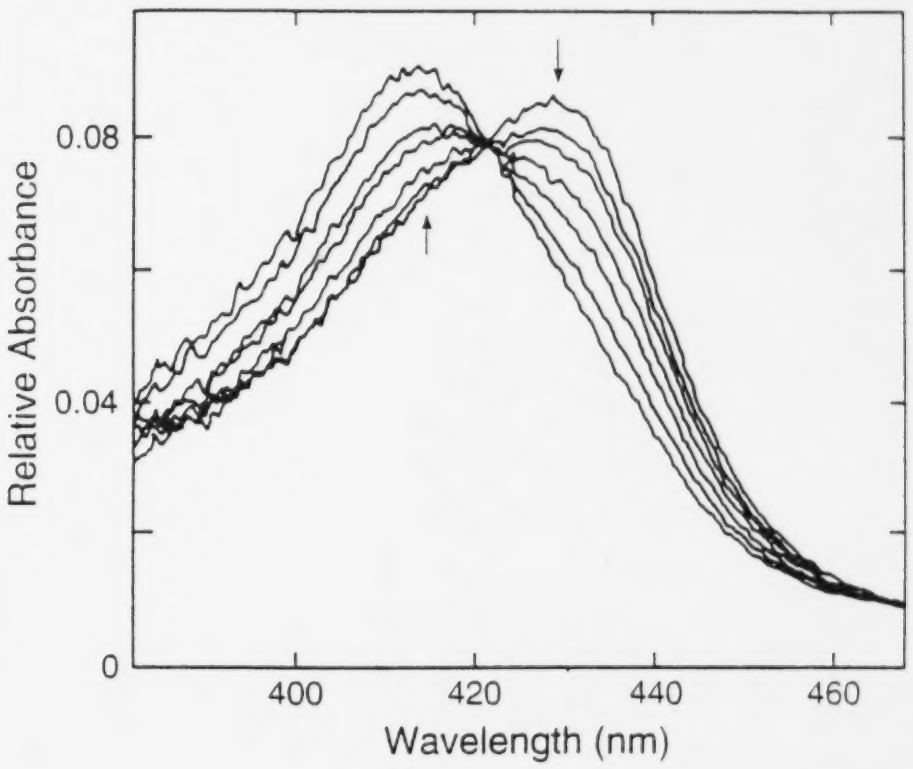

Figure 3.1. Rapid scan spectrophotometric measurements of the reaction of LPO-II with Trolox C over 166 ms. One drive syringe contained LPO-II by mixing 1.0 μM LPO with 2.0 μM H_2O_2 in phosphate buffer, pH 7.30, total ionic strength 0.11 M; the other contained 30 μM Trolox C in citrate buffer, pH 4.14, ionic strength 0.11 M. Final pH 4.33. The partial conversion of LPO-II to LPO is shown clearly. The arrow indicates the direction of absorbance change with increasing time.

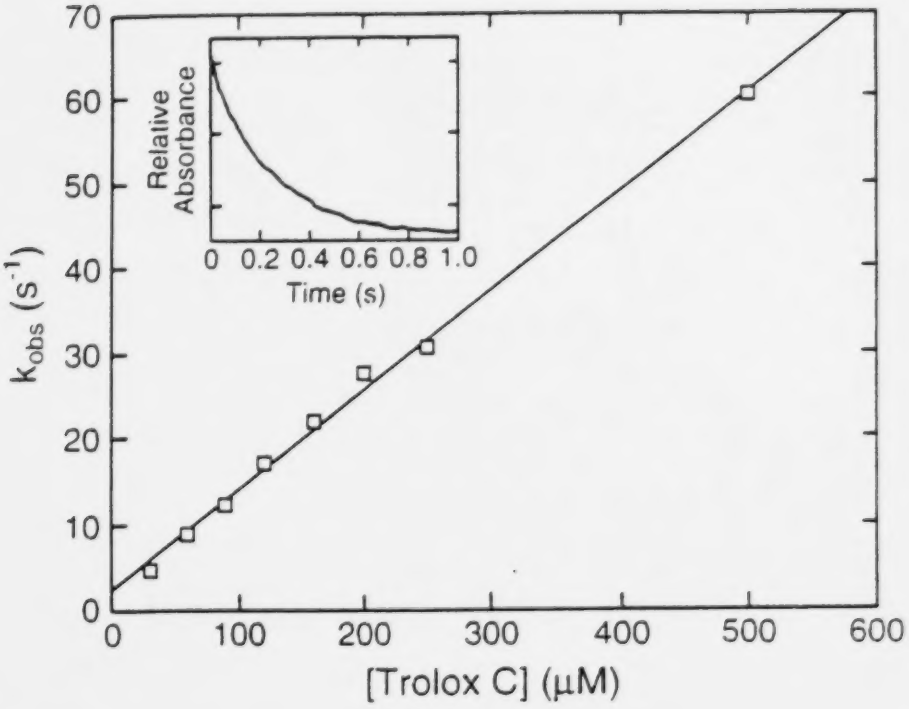

Figure 3.2. Plot of k_{obs} versus Trolox C concentration for the oxidation of Trolox C by lactoperoxidase compound II. The reactions were carried out in buffer solutions of final pH 4.33, ionic strength 0.11 M. Experimental conditions as in Fig. 3.1. The inset shows an example of a first order exponential trace (30 μM Trolox C) from which k_{obs} was obtained.

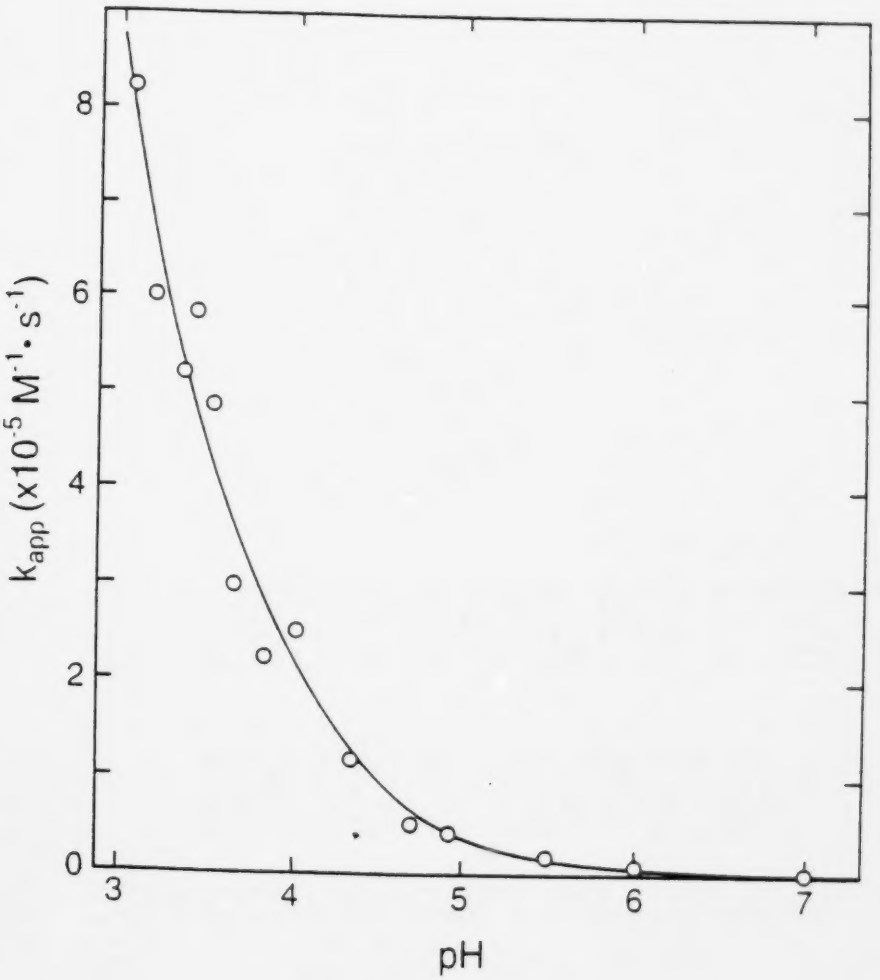

Figure 3.3. The rate-pH profile for the reaction of LPO-II with Trolox C at 25 °C and ionic strength 0.11 M. The experimental points and the computer fitted curve are shown.

3.6 REFERENCES

1. Serbinova, E., Kagan, V., Han, D. and Packer, L. (1991) *Free Rad. Biol. Med.* **10**, 263-275.
2. Scott, J. W., Cort, W. M. and Harley, H., Parrish, D. R. and Saucy, G. (1974) *J. Amer. Oil Chem. Soc.* **51**, 200-203.
3. Doba, T., Burton, G. W. and Ingold, K. U. (1985) *Biochim. Biophys. Acta* **835**, 298-303.
4. Paul, K.-G. and Ohlsson, P.-J. (1985) *In* The Lactoperoxidase System. *Edited by* K. M. Pruitt and Y. O. Tenovuo. Marcel Dekker, New York. pp. 15-30.
5. Cotton, M. L., and Dunford, H. B.(1973) *Can J. Chem.* **51**, 582-587.
6. Hill, A. V. (1913) *Biochem. J.* **7**, 471-480.
7. Bisby, R. H., Ahmed, S. and Cundall, R. B. (1984) *Biochem. Biophys. Res. Commun.* **119**, 245-251.
8. Davies, M. J., Forni, L. G. and Willson, R. L. (1988) *Biochem. J.* **255**, 513-522.
9. Thomas, M. J. and Bielski, B. H. J. (1989) *J. Am. Chem. Soc.* **111**, 3315-3319.
10. Nakamura, M. (1990) *Free Rad. Biol. Med.* **9** (Suppl.1), 18.
11. Maguire, R. J. and Dunford, H. B. (1973) *Can. J. Chem.* **51**, 1721-1723.
12. Link, G., Pinson, A., Kahane, I. and Hershko, C. (1989) *J. Lab. Clin. Med.* **114**, 243-249.
13. Klebanoff, S. J. (1968) *J. Bacteriol.* **95**, 2131-2138.
14. McRipley, R. J. and Sbarra, A. J. (1967) *J. Bacteriol.* **94**, 1425-1430.
15. Jensen, M. S. and Bainton, D. F. (1973) *J. Cell Biol.* **56**, 379-388.

CHAPTER FOUR

CATALASE ACTIVITY OF CHLOROPEROXIDASE AND ITS INTERACTION WITH PEROXIDASE ACTIVITY

4.1 SUMMARY

The catalatic activity of chloroperoxidase (CPO) is demonstrated to exhibit saturation kinetics under steady state conditions, which is not observed with catalase under comparable conditions. Results were obtained on reaction mixtures of CPO and H_2O_2 at pH 6.2, using both rapid spectral scan and single wavelength measurements, and both transient state and steady state reaction conditions. The observed rectangular hyperbolae can be fit quantitatively by two methods which are in agreement, measurement of rates of disappearance of H_2O_2 and of appearance of O_2, to

$$\frac{v}{[CPO]_0} = \frac{B_1[H_2O_2]}{B_2 + [H_2O_2]}$$

A version of this chapter has been submitted for publication. Sun, W., Kadima, T. A., Pickard, M. A., and Dunford, H. B. (1994) *Biochem. Cell Biol.*. Colorimetric assay results on TMPD are those of Dr. Tenshuk Kadima (M.Sc. thesis, University of Alberta, 1989, under the direction of Dr. M. Pickard, Department of Microbiology). They are included in this chapter because the interaction of peroxidatic activity (with TMPD) and catalatic activity (H_2O_2) has not previously been examined.

where v is rate of O_2 evolution and $[CPO]_0$ is total enzyme concentration. The mean values of the parameters are $B_1 = (9 \pm 1) \times 10^2\ s^{-1}$ and $B_2 = (3.3 \pm 0.4) \times 10^{-3}$ M. The results indicate formation of a complex of compound I and H_2O_2 which dissociates to native CPO, O_2 and H_2O with a rate constant of $(9 \pm 1) \times 10^2\ s^{-1}$.

The determination of the peroxidatic activity of CPO is performed using the demethylation of N,N,N',N'-tetramethyl-*p*-phenylenediamine (TMPD) under steady state conditions. Attempts to determine Michaelis-Menten constants for the substrates TMPD and H_2O_2 gave rise to apparently anomalous data. Our data show that the modified ping-pong mechanism established for horseradish peroxidase is applicable to the peroxidatic reaction catalyzed by chloroperoxidase.

Both of the peroxidatic and catalatic reactions occur in the reaction system containing H_2O_2, a reducing substrate, and CPO. A combined reaction mechanism, which fits our experimental results very well, is proposed for CPO catalyzed-reactions in which the modified ping-pong mechanism works for the peroxidatic reactions and the complex formation of CPO-I-H_2O_2 occurs for the catalatic reaction.

4.2 INTRODUCTION

Chloroperoxidase (chloride:hydrogen peroxide oxidoreductase, EC 1.11.1.10), CPO, is a heme enzyme which exhibits versatile properties. CPO name derives from its catalytic ability of utilizing H_2O_2 to oxidize chloride ion. CPO is efficient as a catalase and a chlorination catalyst as well as a peroxidase (1). It has a thiolate ligand in the fifth coordination position of the heme iron (2). Because of the catalase type of activity, it is difficult to obtain

pure CPO-I (3, 4). Although the catalatic activity of CPO has been reported earlier (4, 5), for the first time we demonstrate here that its catalatic activity is controlled by the dissociation of a complex of CPO-I and H_2O_2, a mechanism which is not observed with catalase under comparable conditions (6). As a peroxidase, CPO has been shown to catalyze the N-dealkylation of arylamines (7). We have developed a colorimetric assay for CPO using N,N,N',N'-tetramethyl-*p*-phenylenediamine (TMPD) as the reducing chromogenic substrate (8).

Horseradish peroxidase (HRP), the most extensively studied peroxidase, has a mechanism as follows:

$$HRP + H_2O_2 \xrightarrow{k_1} HRP\text{-}I + H_2O \qquad (4.1)$$

$$HRP\text{-}I + AH_2 \xrightarrow{k_2} HRP\text{-}II + AH\bullet \qquad (4.2)$$

$$HRP\text{-}II + AH_2 \xrightarrow{k_3} HRP + AH\bullet + H_2O \qquad (4.3)$$

where HRP-I and HRP-II are compounds I and II of horseradish peroxidase, AH_2 is a reducing substrate and AH· is a free radical product. HRP conforms to a modified form of ping-pong kinetics (9, 10), and not to the classical ping-pong kinetic scheme (11). The classical ping-pong mechanism is a reversible, ordered, two-substrate:two-product mechanism. The peroxidase ping-pong scheme is a non-reversible reaction mechanism, in which compound I is usually reduced faster than compound II, and the conversion of the latter to the native enzyme is often the rate-limiting step. The rate constant k_2 is about 10 times greater than k_3 for most substrates of HRP (10).

Our data show that the modified ping-pong mechanism for horseradish peroxidase is applicable for the peroxidatic reaction catalyzed by chloroperoxidase and that the complex CPO-I-H_2O_2 has a finite lifetime. The latter complex is not detectable under comparable conditions in the reactions of catalase.

4.1 EXPERIMENTAL

CPO from *Caldariomyces fumago* was isolated and purified by established procedures (12). The concentration of the enzyme was determined from the absorbance at 400 nm using a molar absorptivity of 9.12 x 10^4 $M^{-1}cm^{-1}$ (13). The R.Z. value (A_{400}/A_{280}) of the enzyme used in our experiments was 1.26-1.30.

H_2O_2 was obtained as a 30% solution from BDH Chemicals (Toronto, Canada). The concentration of the diluted H_2O_2 stock solution was determined by the peroxidase assay (14). Chemicals for the phosphate buffer (pH 6.2) were reagent grade and used without further purification. The ionic strength of the buffer was 0.03 M. Analytical reagent K_2SO_4, obtained from BDH Chemicals (Toronto, Canada), was used to keep the total ionic strength of the reaction mixtures at 0.11 M. N,N,N',N'-tetramethyl-*p*-phenylenediamine (TMPD) was from Sigma (St. Louis, USA). The concentration of TMPD solution is determined by weight. All solutions were prepared using deionized water from a Milli-Q water purification system (Millipore Corp., Bedford, MA).

Kinetic measurements were performed on a Photal (formerly Union Giken, Atago Bussan Co., Tokyo, Japan) stopped-flow spectrophotometer Model RA-601. The 1-cm observation cell was thermostated at 25°C for all measurements. For both rapid scan and stopped-flow experiments, one drive

syringe was filled with H_2O_2 in pH 6.2, ionic strength 0.11 M phosphate buffer. The other syringe was filled with CPO in the same phosphate buffer. The pH after mixing the solutions in the two syringes was therefore controlled at pH 6.2. Final ionic strength was 0.11 M.

For measuring the rate constants of CPO-I formation as well as its reverse reaction yielding initial reactants, at least a 10-fold excess of H_2O_2 was used to maintain pseudo-first-order conditions. CPO concentration was kept at 1.0 μM in all measurements. The enzyme behavior was monitored using the rate of decrease in absorbance at 400 nm. A nonlinear least-square analysis of the exponential traces at 400 nm gave the observed pseudo-first-order rate constants.

The catalatic activity of CPO was studied under steady-state conditions in which CPO concentration was 10 nM and more than 5×10^4 times the H_2O_2 concentration was used compared to that of CPO. The disappearance of H_2O_2 was monitored at 240 nm by stopped-flow measurements and the oxygen evolution was determined with a Yellow Spring Instruments (YSI Incorp., Yellow Springs, OH) Model 53 Oxygen Monitor. The O_2 concentration dissolved in phosphate buffer was found to be 260 μM at 25°C as measured in this lab by a method previously described (15). The initial rates of both the H_2O_2 disappearance and the O_2 evolution were obtained by taking tangents to the recorded traces. The molar absorptivity of H_2O_2 at 240 nm is 43.6 M^{-1} cm^{-1} (16). Every determination is the average of at least three measurements.

The colorimetric assay for CPO was carried out essentially as described (8). Reaction mixture contained 1.2 nM CPO, 20 mM TMPD, 1 mM H_2O_2 and 0.1 M KCl phosphate buffer, pH 6.0. Reactions were carried out at

25°C for 5 min and the resulting colour read at 563 nm. Substrate-limited reactions were used to determine the molar absorptivity of the reaction product, which was 1.17×10^4 $M^{-1}cm^{-1}$. Stock solutions of TMPD (200 mM) were prepared freshly from the dihydrochloride salt and kept cold at pH 3.0 between use to limit the pH- and temperature-dependent autooxidation of TMPD. Heat inactivated CPO (10 min, 70°C), or the reaction mixture without CPO was used to correct for autooxidation of TMPD.

The effect of the peroxidatic activity on the catalatic activity of CPO was studied under steady-state conditions of 13.5 nM CPO and 3.0 mM H_2O_2 in the presence of varied concentrations of TMPD. The initial rates of the O_2 evolution were obtained by taking tangents to the recorded traces. Every determination is the average of at least three measurements.

All experiments were performed at 25°C.

4.4 RESULTS

Transient-State Measurements of Compound I Formation

Fig. 4.1 shows the rapid scan spectra of the reaction of 20.0 μM H_2O_2 with 2.0 μM CPO over 166 ms at pH 6.2, ionic strength 0.11 M. The absorbance decrease at 400 nm is caused by the conversion of native CPO to CPO-I by its reaction with H_2O_2 which can be described as follows:

$$\mathrm{CPO} + \mathrm{H_2O_2} \underset{k_{-4}}{\overset{k_4}{\rightleftharpoons}} \mathrm{CPO\text{-}I} + \mathrm{H_2O} \qquad (4.4)$$

With H_2O_2 in excess of CPO, pseudo-first-order kinetics was observed at 400 nm, which shows that the reactions in eq. 4.4 can be isolated from subsequent reactions by using transient state kinetics. One example is shown

in the inset of Fig. 4.2. The corresponding differential rate expression is eq. 4.5:

$$- d[CPO] / dt = k_{obs} [CPO] \quad (4.5)$$

where k_{obs} is the observed pseudo-first-order rate constant. The apparent second-order rate constant, k_4 is related to k_{obs} by eq. 4.6 (see Appendix I):

$$k_{obs} = k_4 [H_2O_2] + k_{-4} \quad (4.6)$$

Values of k_4 and k_{-4} were then obtained from the slope and the intercept of the plot of k_{obs} versus $[H_2O_2]$, as shown in Fig. 4.2. Therefore, $k_4 = (2.3 \pm 0.1) \times 10^6\ M^{-1}\ s^{-1}$ and $k_{-4} = (4 \pm 2)\ s^{-1}$. The reverse reaction of compound I and water reforming native enzyme and H_2O_2 is so small that it does not influence subsequent reactions.

Steady-State Experiments to Measure the Catalatic Activity

The overall reaction in the steady state system is represented by eq. 4.7:

$$2H_2O_2 \xrightarrow{CPO} O_2 + 2H_2O \quad (4.7)$$

Therefore,

$$-d[H_2O_2] / dt = 2\, d[O_2] / dt = 2v_{(O_2)} \quad (4.8)$$

where $v_{(O2)}$ is the initial rate of oxygen formation. The initial rates of H_2O_2 disappearance and oxygen evolution were measured as a function of H_2O_2 concentration. The plot of $v_{(O_2)}/[CPO]_0$ obtained from monitoring H_2O_2

disappearance *versus* $[H_2O_2]$ is shown in Fig.4. 3. The inset of Fig.4. 3 shows one example of the stopped-flow trace of H_2O_2 disappearance at 240 nm. Using a weighted nonlinear least square program, the experimental data were fitted to rectangular hyperbolae of the form:

$$\frac{v_{(O2)}}{[CPO]_0} = \frac{B_1[H_2O_2]}{B_2 + [H_2O_2]} \qquad (4.9)$$

The smooth curve with zero intercept resulted in $B_1 = (1.07 \pm 0.02) \times 10^3\ s^{-1}$ and $B_2 = (3.6 \pm 0.2) \times 10^{-3}$ M.

Direct measurement of oxygen evolution yielded another set of experimental data. The plot of $v_{(O2)}/[CPO]_0$ from this method *versus* $[H_2O_2]$ is shown in Fig. 4.4. One example of oxygen evolution measurements is displayed in the inset of Fig. 4.4. The smooth curve with zero intercept in Fig. 4.4 shows the fit to eq. 4.9 which gives $B_1 = (8.0 \pm 0.2) \times 10^2\ s^{-1}$, $B_2 = (2.9 \pm 0.2) \times 10^{-3}$ M. Therefore the mean values from two different methods are $B_1 = (9 \pm 1) \times 10^2\ s^{-1}$ and $B_2 = (3.3 \pm 0.4) \times 10^{-3}$ M.

Colorimetric Assay to Measure the Peroxidatic Activity

In accordance with the conventional analysis of two-substrate reactions (11), the reciprocal of the reaction velocities of TMPD demethylation were first plotted against the reciprocal of the H_2O_2 concentrations, each plot at a fixed concentration of TMPD. A family of parallel lines were obtained (Fig. 4.5), which shifted downward with increasing TMPD concentration. The slope of these straight lines is $(5.0 \pm 0.1) \times 10^{-7}$ M·s. Some of the double reciprocal plots curve upwards for large concentrations of H_2O_2 (close to the ordinate, Fig. 4.5). The larger the TMPD concentration, the closer the upward

curvature to the ordinate, until with a sufficiently large concentration of TMPD, the upward curvature disappears.

The ordinate intercepts of the graphs in Fig. 4.5 were then plotted against the reciprocal of the TMPD concentrations. The resultant graph passed through the origin within the experimental error (Fig. 4.6) with a slope of $(3.4 \pm 0.1) \times 10^{-5}$ M·s: thus, the K_m for TMPD was infinite.

Similarly, in an attempt to obtain the K_m for H_2O_2, the reciprocal of the reaction velocities of TMPD demethylation obtained at different H_2O_2 concentrations were plotted against the reciprocal of the TMPD concentrations (Fig. 4.7). The slope of these straight lines is $(2.8 \pm 0.1) \times 10^{-5}$ M·s. As with TMPD, the replot of the intercepts passed through the origin, and therefore the K_m value for H_2O_2 was also infinite (Fig. 4.8). The slope of the straight line is $(9.1 \pm 0.1) \times 10^{-7}$ M·s.

The results were consistent on repetition and indicated that the K_m of CPO could not be determined for either substrate.

Interaction of Catalatic Activity and Peroxidatic Activity

The catalatic activity of CPO was measured at 13.5 nM CPO, 3.0 mM H_2O_2 in the presence of varied TMPD concentration from 0 to 25 μM TMPD. When the concentration of TMPD is increased beyond 25 μM, it was found that the amount of evolved O_2 is so small that it cannot be measured accurately. Therefore, in order to measure accurately the catalatic activity of CPO, the TMPD concentration was kept in the range from 0 to 25 μM. With increasing TMPD concentration, the catalatic activity decreases markedly as shown in Fig. 4.9. This indicates clearly that TMPD competes with H_2O_2 for reaction with CPO-I. Thus there is a competition between the peroxidatic and

catalatic reactions. Fig. 4.10 shows the plot of $1/v_{(O_2)}$ `obtained from Fig. 4.9 *versus* [TMPD], where $v_{(O_2)}$ is the initial rate of O_2 evolution.

4.5 DISCUSSION

From the transient state kinetic results obtained by following spectral changes of the enzyme, a plot of k_{obs} as a function of the hydrogen peroxide concentration (Fig. 4.2) gives a straight line from which the rate constant for compound I formation is obtained. The intercept, although very small, is finite, indicating that compound I formation is slightly reversible. The effect of this reversibility upon the subsequent catalatic activity is negligible (see below). The steady state results on the catalatic activity show a saturation effect in the millimolar range of hydrogen peroxide concentration (Figs. 4.3 and 4.4), which can be fitted very well to the equation for rectangular hyperbolae. The mechanism of the CPO catalatic activity can, therefore, be described as follows:

$$\text{CPO} + H_2O_2 \xrightarrow{k_4} \text{CPO-I} + H_2O \qquad (4.4)$$

$$\text{CPO-I} + H_2O_2 \underset{k_{-5}}{\overset{k_5}{\rightleftharpoons}} \text{CPO-I-}H_2O_2 \qquad (4.10)$$

$$\text{CPO-I-}H_2O_2 \xrightarrow{k_6} \text{CPO} + O_2 + H_2O \qquad (4.11)$$

As a result, eq. 4.12 can be derived from eqs. 4.4, 4.10 and 4.11 (see Appendix II):

$$v_{(O_2)} = d[O_2]/dt = \frac{k_4k_5k_6[H_2O_2]^2[CPO]_0}{(k_5k_6 + k_4k_5 + k_4k_6)[H_2O_2] + k_4k_5[H_2O_2]^2} \qquad (4.12)$$

If we assume that k_{-5} is much smaller than k_6 (discussed in detail later) then eq. 4.12 can be put into the form:

$$\frac{v(O_2)}{[CPO]_0} = \frac{k_6[H_2O_2]}{(k_4 + k_5)k_6 / k_4k_5 + [H_2O_2]} \qquad (4.13)$$

Therefore, by comparison of eqs. 4.9 and 4.13

$$B_1 = k_6 \qquad (4.14)$$

and

$$B_2 = (k_4 + k_5)k_6 / k_4k_5 \qquad (4.15)$$

Using eqs. 4.14 and 4.15, we calculated the values of k_5 and k_6 using the known k_4 value of $2.3 \times 10^6\ M^{-1}s^{-1}$. From the stopped-flow experiments monitoring the rate of disappearance of hydrogen peroxide at 240 nm, k_5 is calculated to be $(3.4 \pm 0.1) \times 10^5\ M^{-1}s^{-1}$ and k_6 is $(1.07 \pm 0.02) \times 10^3\ s^{-1}$; and from the oxygen evolution experiments k_5 is $(3.1 \pm 0.2) \times 10^5\ M^{-1}s^{-1}$ and k_6 is $(8.0 \pm 0.2) \times 10^2\ s^{-1}$. These results from different types of experiments agree within experimental error.

Our results show that the dissociation of the CPO-I-H_2O_2 complex is the rate-determining step in the overall reaction to generate oxygen from hydrogen peroxide.

In comparison, there are inconclusive reports regarding saturation effects in catalase at high $[H_2O_2]$ (17-21). The study of Ogura (18) shows that the initial velocity of O_2 evolution is proportional to $[H_2O_2]$ at low $[H_2O_2]$ from the initial rate measurements; his "saturation" curves are observed for $[H_2O_2]$

up to 5 M! The reports of the catalase reaction are primarily concerned with measurements over long periods of time at very high [H_2O_2]. Jones and Suggett (19) showed that there is a time-dependent inactivation effect and suggest that compound II formation, which is not part of the catalatic mechanism, becomes important at high [H_2O_2]. The apparent saturation effects and time dependent effects of catalase at high [H_2O_2] can be attributed to causes other than formation of a ternary complex. The results of Ogura confirm our point that there is no saturation exhibited in the catalase reaction with H_2O_2 for initial velocity measurements and for reasonable values of [H_2O_2] (in the millimolar range). It is important to distinguish initial rate measurements from measurements over a long period of time. It is customary in enzyme kinetics to make measurements of the initial velocity of the reaction. This has the advantage of removing complications such as inactivation of the enzyme during the assay. Therefore, our measurements of the initial rates of O_2 evolution and H_2O_2 disappearance are not affected by either the possible inactivation of enzyme by high [H_2O_2] or the inactive compound II formation. Our results indicate that the catalatic reaction of CPO is different from that of catalase in which the saturation effect is not observed under comparable conditions (6,22).

The first Soret spectrum of pure CPO-I was obtained by the reaction of native enzyme with peracetic acid (4). The spectra shown in Fig. 4.1 indicate that pure compound I cannot be obtained using hydrogen peroxide because of the catalatic reaction. The spectra taken in a reaction mixture of native enzyme and hydrogen peroxide are always due to the mixture of compound I with native enzyme. This mixture also contains a finite amount of the compound I-H_2O_2 complex given by (see Appendix III):

$$\frac{[CPO\text{–}I\text{–}H_2O_2]}{[CPO]_0} = \frac{[H_2O_2]}{B_2 + [H_2O_2]} \qquad (4.16)$$

Under our experimental conditions, the concentrations of H_2O_2 are in the range of 0.5 to 27 mM. Therefore, the percentage of CPO-I-H_2O_2 over the total enzyme concentration in the reaction mixture is calculated to be in the range of 13 to 89% using eq. 4.16.

The spectrum of the CPO-I-H_2O_2 complex may be virtually identical to that of uncomplexed CPO-I. There is supporting evidence: there are two types of lignin peroxidase compounds III. One is simply called LiP III and the other LiP III*. LiP III* is a complex of LiP III and H_2O_2, yet the two species have virtually indistinguishable spectra (23). Our results in Fig. 4.1 obtained using H_2O_2, compared to those using peracetic acid where catalatic activity is minimized (4), support the assumption that the binding of hydrogen peroxide to CPO-I would not affect its Soret spectrum.

The hypothesis that $k_{-5} = 0$ is the simplest, but not necessarily the best, assumption which enables one to fit all of the experimental data with the minimum number of parameters. An alternative is to assume that compound I and H_2O_2 react at the diffusion-controlled limit to form the CPO-I-H_2O_2 complex, which enables one to calculate a value for the rate of the reverse reaction (Appendix IV).

From the kinetic study of our colorimetric assay, we conclude that Michaelis-Menten constant cannot be determined for the peroxide-dependent demethylation of TMPD by CPO. This suggests that the modified ping-pong reaction mechanism (10) is applicable for the peroxidatic reactions of CPO, in which the reaction steps are not reversible, and the rate constant of the

second reaction step (k_7, compound II formation) is larger than that of the third step (k_8, regeneration of the native enzyme). Therefore, this study on CPO kinetics represents experimental data in support of the modified ping-pong kinetic mechanism of peroxidases.

The catalatic activity of CPO is demonstrated to be affected by its peroxidatic activity as shown in Fig. 4.9. The reducing substrate competes with H_2O_2 for CPO-I for the peroxidatic reactions. In a reaction system of CPO, H_2O_2 and a reducing substrate, both the peroxidatic and catalatic reactions occur. Combining the peroxidatic reactions with the catalase type of reactions, the following scheme is proposed for CPO reaction system:

$$\text{CPO} + H_2O_2 \xrightarrow{k_4} \text{CPO-I} + H_2O \qquad (4.4)$$

$$\text{CPO-I} + H_2O_2 \xrightarrow{k_5} \text{CPO-I-}H_2O_2 \qquad (4.10)$$

$$\text{CPO-I-}H_2O_2 \xrightarrow{k_6} \text{CPO} + O_2 + H_2O \qquad (4.11)$$

$$\text{CPO-I} + \text{TMPD} \xrightarrow{k_7} \text{CPO-II} + \text{TMPD}\cdot \qquad (4.17)$$

$$\text{CPO-II} + \text{TMPD} \xrightarrow{k_8} \text{CPO} + \text{TMPD}\cdot \qquad (4.18)$$

Based on this combined mechanism, the peroxidatic activity and the catalatic activity can be represented by eqs. 4.19 and 4.20 respectively (see Appendix V):

$$\frac{2[CPO]_0}{v_{(TMPD)}} = \frac{1}{k_4}\frac{1}{[H_2O_2]} + \left(\frac{1}{k_7} + \frac{1}{k_8} + \frac{k_5}{k_4k_7}\right)\frac{1}{[TMPD]} + \frac{k_5}{k_6k_7}\frac{[H_2O_2]}{[TMPD]} \quad (4.19)$$

where $v_{(TMPD)}$ is the reaction velocity of TMPD demethylation; and

$$\frac{[CPO]_0}{v_{(O2)}} = \left(\frac{1}{k_4} + \frac{1}{k_5} + \frac{k_7}{k_5k_8}\right)\frac{1}{[H_2O_2]} + \frac{1}{k_6} + \frac{k_7}{k_4k_5}\frac{[TMPD]}{[H_2O_2]^2} \quad (4.20)$$

where $v_{(O2)}$ is the initial rate of O_2 evolution. We have determined that k_4 is $(2.3 \pm 0.1) \times 10^6\ M^{-1}s^{-1}$, k_5 is $(3.3 \pm 0.2) \times 10^5\ M^{-1}s^{-1}$ and k_6 is $(9 \pm 1) \times 10^2\ s^{-1}$. Assuming $k_7 > k_8$, eqs. 4.19 and 4.20 can be simplified to be:

$$\frac{2[CPO]_0}{v_{(TMPD)}} = \frac{1}{k_4}\frac{1}{[H_2O_2]} + \frac{1}{k_8}\frac{1}{[TMPD]} + \frac{k_5}{k_6k_7}\frac{[H_2O_2]}{[TMPD]} \quad (4.21)$$

and

$$\frac{[CPO]_0}{v_{(O2)}} = \frac{k_7}{k_5k_8}\frac{1}{[H_2O_2]} + \frac{1}{k_6} + \frac{k_7}{k_4k_5}\frac{[TMPD]}{[H_2O_2]^2} \quad (4.22)$$

Therefore, eq. 4.22 indicates that, when we keep the enzyme and H_2O_2 concentrations constant, the plot of the reciprocal of the initial rate of O_2 evolution *versus* [TMPD] would yield a straight line which is the result shown in Fig. 4.10.

The combined reaction mechanism also demonstrates that the peroxidatic activity of CPO is affected by its catalatic activity shown by the last

term in eq. 4.21. However, the results we obtained from the colorimetric assay display that, under most of our experimental conditions (i.e.: [TMPD] is in excess of [H_2O_2]), the last term is so small compared to the other two terms in the equation that it can be ignored. Therefore, only the modified ping-pong mechanism for the peroxidatic reactions occurs and there is no upward curvature in the double reciprocal plot. However, the catalatic activity affects the peroxidatic reactions when [H_2O_2] is large enough compared to [TMPD]: the catalatic activity inhibits the peroxidatic activity as shown in Fig. 4.5. Overall, for our experimental conditions of colorimetric assay, the peroxidatic reactions occur preferentially. Thus the catalatic activity of CPO can be ignored except for very large concentrations of H_2O_2. For nearly all experimental conditions of colorimetric assay, the last term in eq. 4.21 can be ignored, and the modified ping-pong mechanism is valid for the peroxidatic reactions of CPO. The rate constants of k_4 and k_8 can be obtained from the slopes of Figs. 4.5 to 4.8. The values for k_4 are: $(1.0 \pm 0.1) \times 10^6$ $M^{-1}s^{-1}$ (Fig. 4.5) and $(9.5 \pm 0.1) \times 10^5$ $M^{-1}s^{-1}$ (Fig.4. 8); and for k_8: $(1.5 \pm 0.1) \times 10^4$ $M^{-1}s^{-1}$ (Fig. 4.6) and $(1.8 \pm 0.1) \times 10^4$ $M^{-1}s^{-1}$ (Fig. 4.7). The average value for k_4 is $(9.8 \pm 0.3) \times 10^5$ $M^{-1}s^{-1}$ and for k_8 $(1.7 \pm 0.2) \times 10^4$ $M^{-1}s^{-1}$. The value of k_4 determined using this steady-state method can be compared to the value of $(2.3 \pm 0.1) \times 10^6$ $M^{-1}s^{-1}$ which we determined directly by the transient-state measurement of compound I formation from native enzyme and H_2O_2.

There have been a number of reports on peroxidase kinetics in which Michaelis-Menten constants have been determined. In some instances, the constants were derived from primary plots, where only one substrate was varied (24-26), and kinetic values were derived, presumably dependent on the cosubstrate concentration. In other cases, kinetic parameters have been

derived from the slopes and intercepts of secondary plots (7, 25). Kedderis and Hollenberg (7), in their kinetic studies on CPO-catalyzed N-demethylations, reported kinetic constants for the demethylation reaction obtained from the intercepts of secondary plots. These authors found that the values of kinetic constants derived by this method were in good agreement with the apparent kinetic constants for the demethylation reaction determined using a single fixed concentration of the second substrate (25). Our results presented here delineate that the modified ping-pong mechanism works for the peroxidatic reactions catalyzed by CPO. Nevertheless, the catalatic activity of CPO affects the peroxidatic reaction when $[H_2O_2]$ is high enough compared to the reducing substrate. The kinetic measurements performed by the above investigators are based on the only peroxidatic activity for CPO; they ignored the effect of the catalatic activity. So, the discrepancy between those kinetic studies and the present study may be caused by the catalatic activity under different experimental conditions.

In summary, the catalase-like (catalatic) activity of chloroperoxidase exhibits saturation behavior. All of the kinetic results can be fit quantitatively by a mechanism in which a complex of compound I and H_2O_2 is formed. By use of transient state kinetics the rate of formation of compound I from native enzyme and H_2O_2 is determined accurately. From steady state experiments the rate of reaction of the CPO-I-H_2O_2 complex to form O_2 is also quantitated. Colorimetric kinetic studies of the peroxidatic activity of CPO demonstrate that the modified ping-pong mechanism for horseradish peroxidase is applicable for the peroxidatic reactions catalyzed by CPO. And the interaction of catalatic activity with peroxidatic activity is due to the competition of H_2O_2 and reducing substrate for CPO-I.

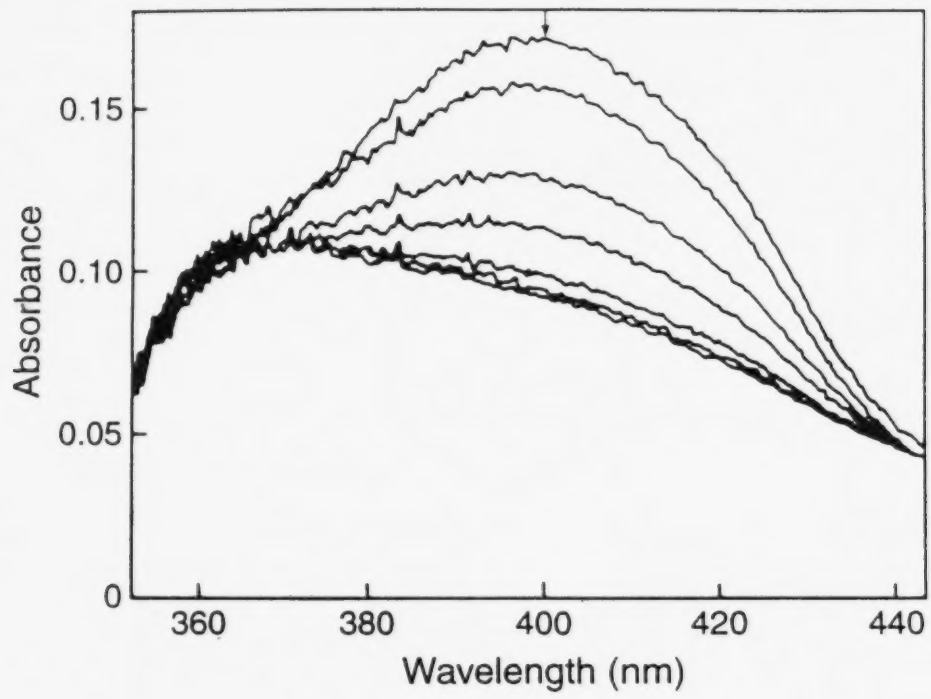

Figure 4.1. Rapid scan spectral measurements of the reaction of 2.0 μM CPO with 20.0 μM H_2O_2 up to 166 ms. One drive syringe contained H_2O_2 in phosphate buffer, pH 6.2, ionic strength 0.11 M; the other contained CPO in the same phosphate buffer. The partial conversion of native CPO to CPO-I is shown clearly. The arrow indicates the direction of absorbance change with increasing time.

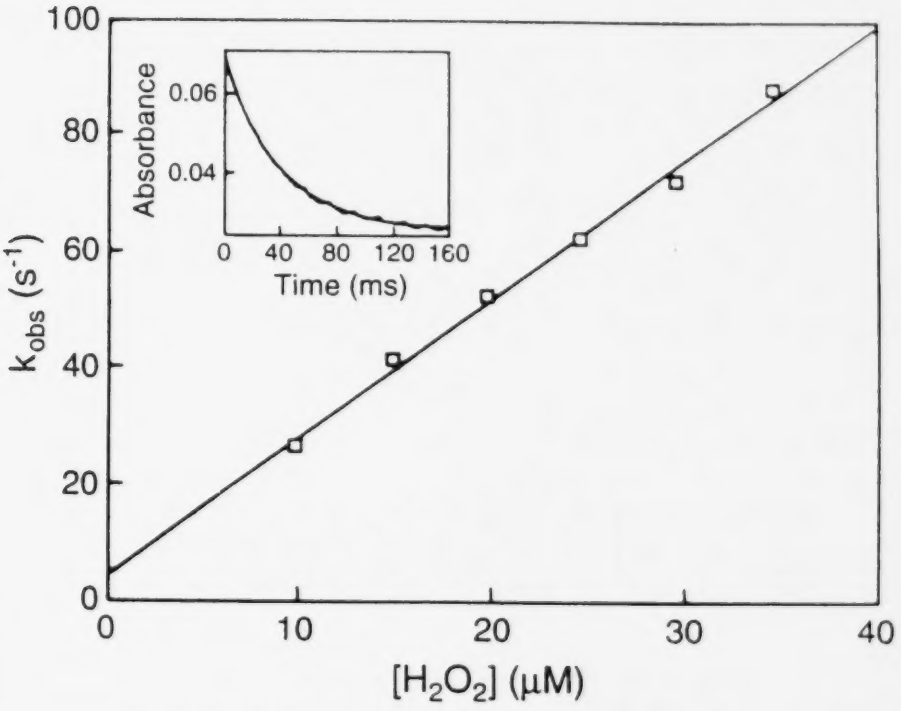

Figure 4.2. Plot of k_{obs} *versus* H_2O_2 concentration for the reaction of CPO with H_2O_2. The reactions were carried out in phosphate buffer solutions pH 6.2, ionic strength 0.11 M. The final CPO concentration was kept 1.0 μM. The inset shows an example of a first order exponential trace (10 μM H_2O_2) from which k_{obs} was obtained.

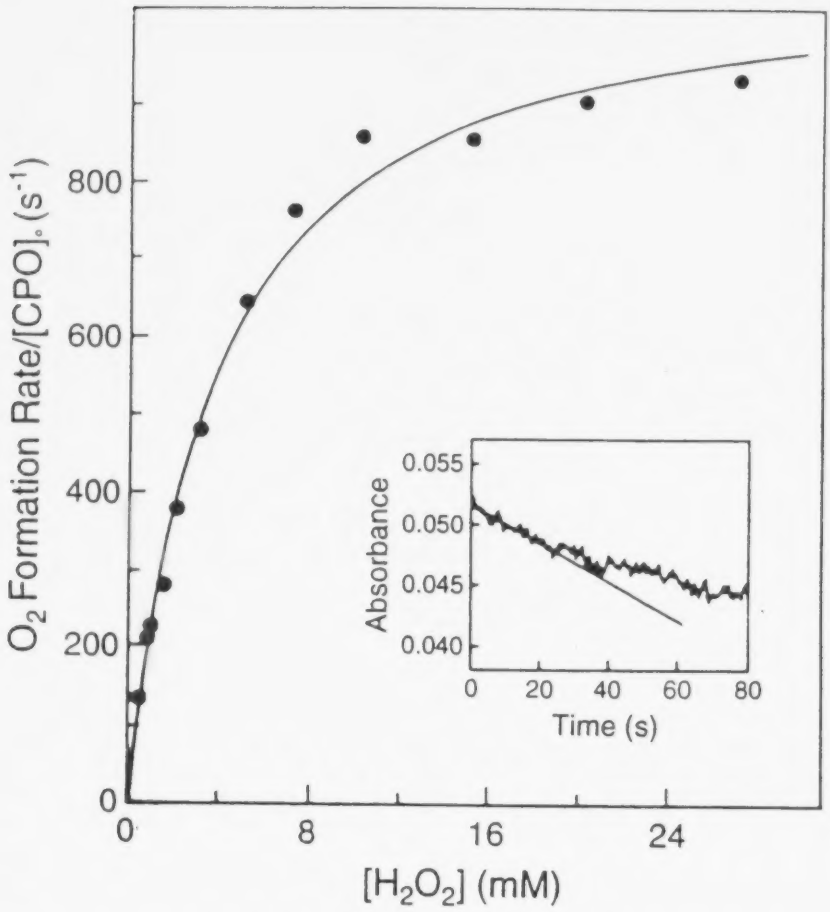

Figure 4.3. Plot of O_2 formation rate/$[CPO]_0$ *versus* $[H_2O_2]$ obtained by measuring the H_2O_2 disappearance at 240 nm. The reactions were carried out in phosphate buffer solutions pH 6.2, ionic strength 0.11 M. The final CPO concentration was 10 nM. H_2O_2 concentrations were: 0.5, 0.8, 1.0, 1.5, 2.0, 3.0, 5.0, 7.0, 10.0, 15.0, 20.0, 26.9 mM. The inset shows an example of the stopped-flow trace of the disappearance of H_2O_2 when its concentration is 1.0 mM.

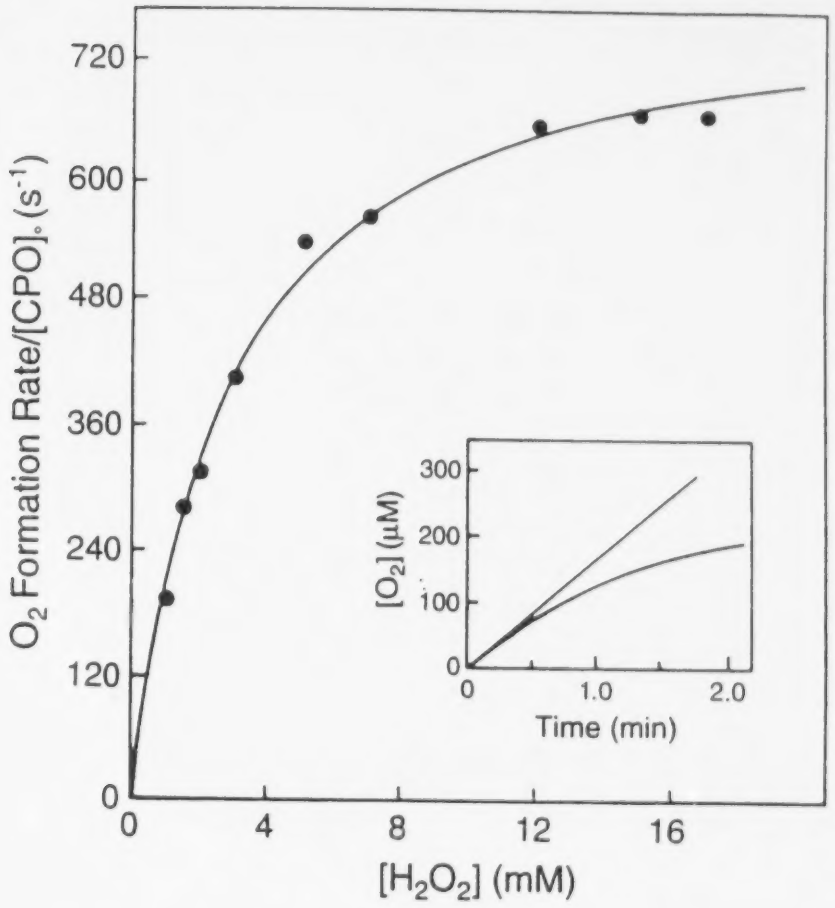

Figure 4.4. Plot of O_2 formation rate/$[CPO]_0$ *versus* $[H_2O_2]$ obtained by direct measurements of O_2 evolution. The reactions were carried out in phosphate buffer solutions pH 6.2, ionic strength 0.11 M. The final CPO concentration was 10 nM. H_2O_2 concentrations were: 1.0, 1.5, 2.0, 3.0, 5.0, 7.0, 12.0, 15.0, 17.0 mM. The inset shows an example of O_2 evolution when H_2O_2 concentration is 1.5 mM.

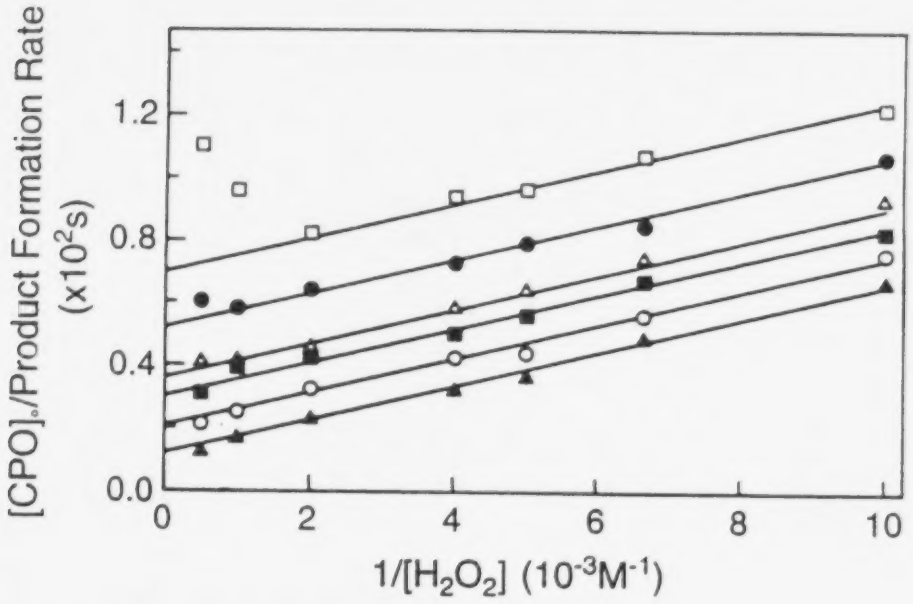

Figure 4.5. Double reciprocal plots of the initial rate of H_2O_2-dependent TMPD demethylation by CPO. Reactions were carried out at room temperature for 5 min, using 1.2 nM CPO in 0.1 M phosphate buffer, pH 6.0. Points displayed are averages of four determinations. TMPD concentrations : 5 mM (□); 6.7 mM (●); 10 mM (Δ); 12.5 mM (■); 20 mM (○); and 40 mM (▲).

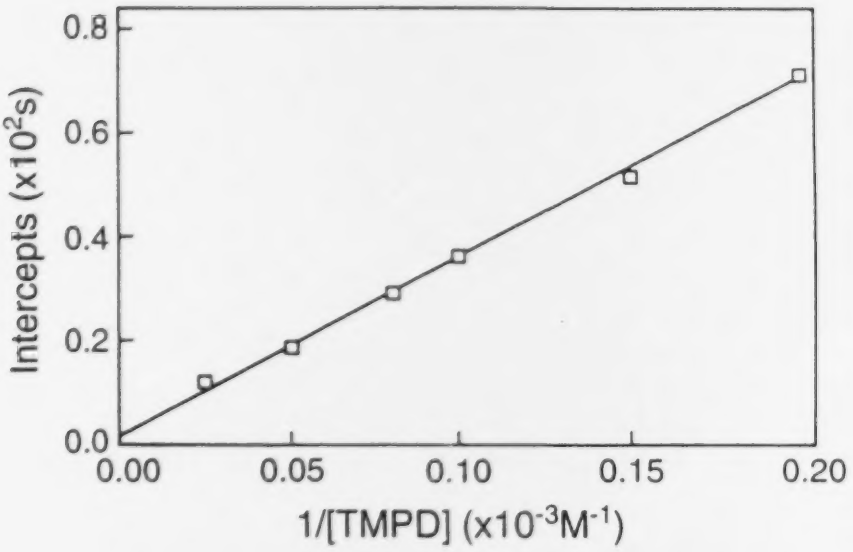

Figure 4.6. Plot of the intercepts from the double reciprocal plots in Fig. 4.5 against the reciprocal of TMPD concentration.

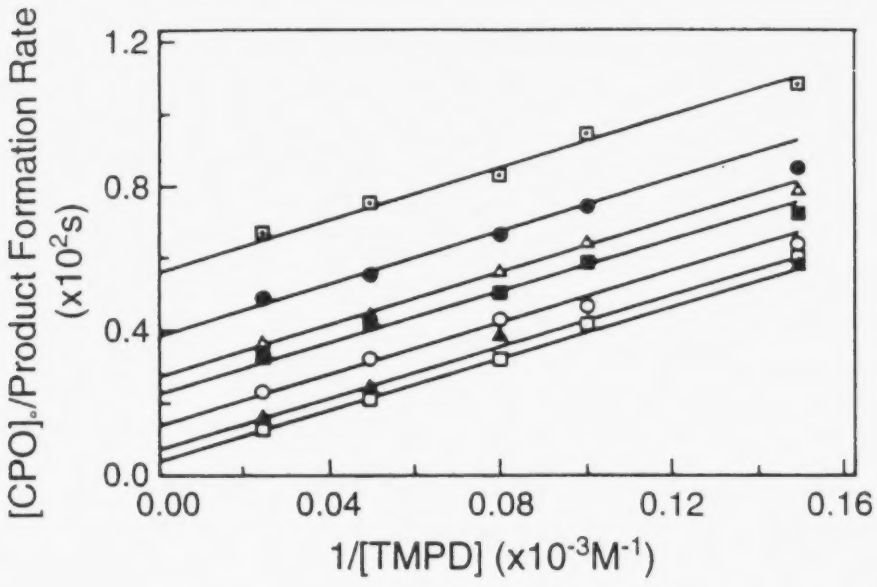

Figure 4.7. Double reciprocal plots of the initial rate of H_2O_2-dependent TMPD demethylation by CPO. Reaction conditions are as described for Fig. 4.5. Points displayed are averages of four determinations. H_2O_2 concentrations: 0.10 mM (⊡); 0.15 mM (●); 0.20 mM (Δ); 0.25 mM (■); 0.5 mM (○); 1 mM (▲); and 2 mM (□).

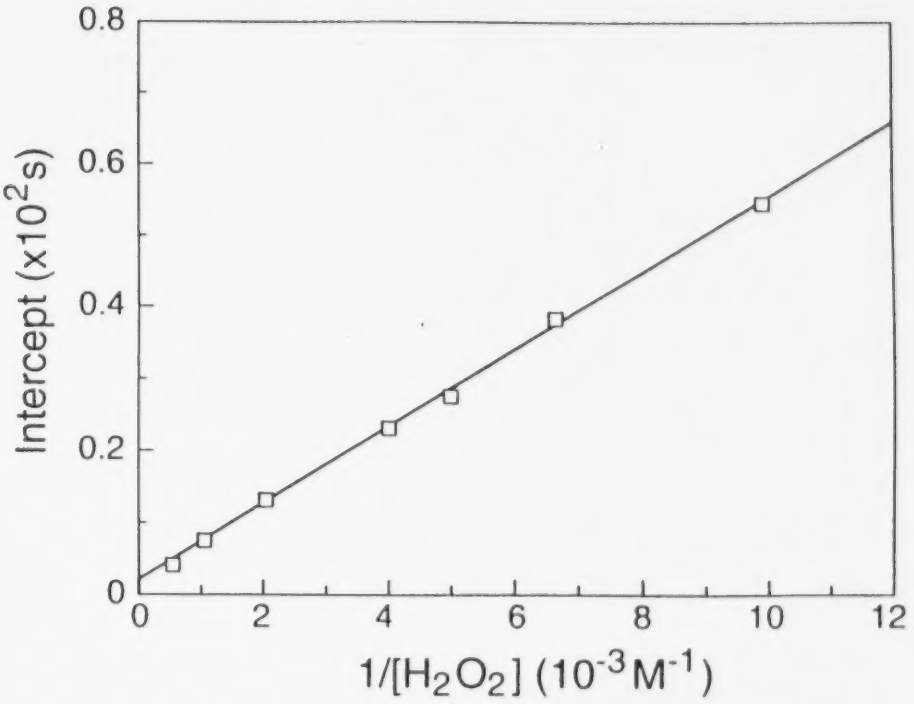

Figure 4.8. Plot of the intercepts from the double reciprocal plots in Fig. 4.7 against the reciprocal of H_2O_2 concentration.

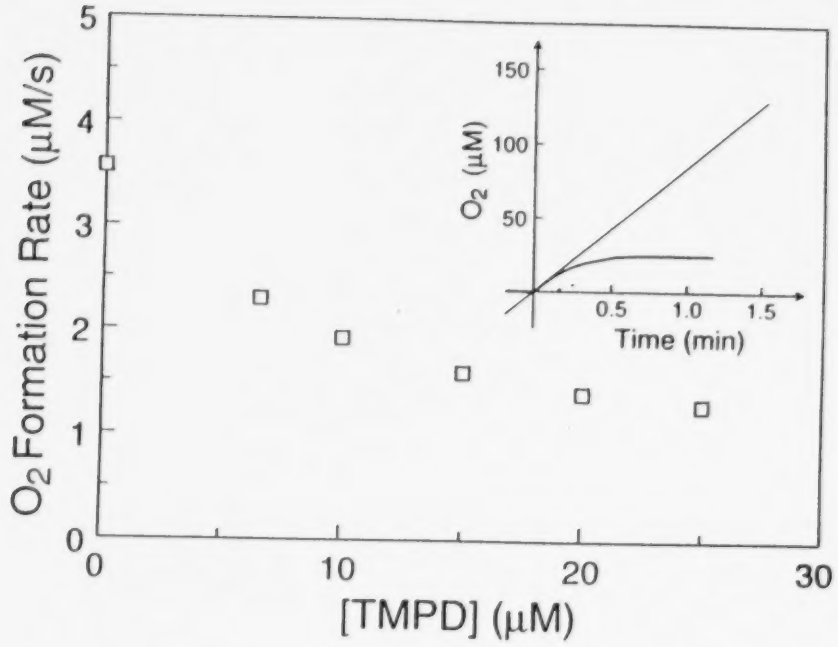

Figure 4.9. Plot of the initial rate of O_2 evolution *versus* TMPD concentration in a reaction mixture of 13.5 nM CPO, 3.0 mM H_2O_2 with varied concentrations of TMPD present, in phosphate buffer of pH 6.2, ionic strength 0.11 M. The inset shows an example of O_2 evolution when TMPD concentration is 25 μM.

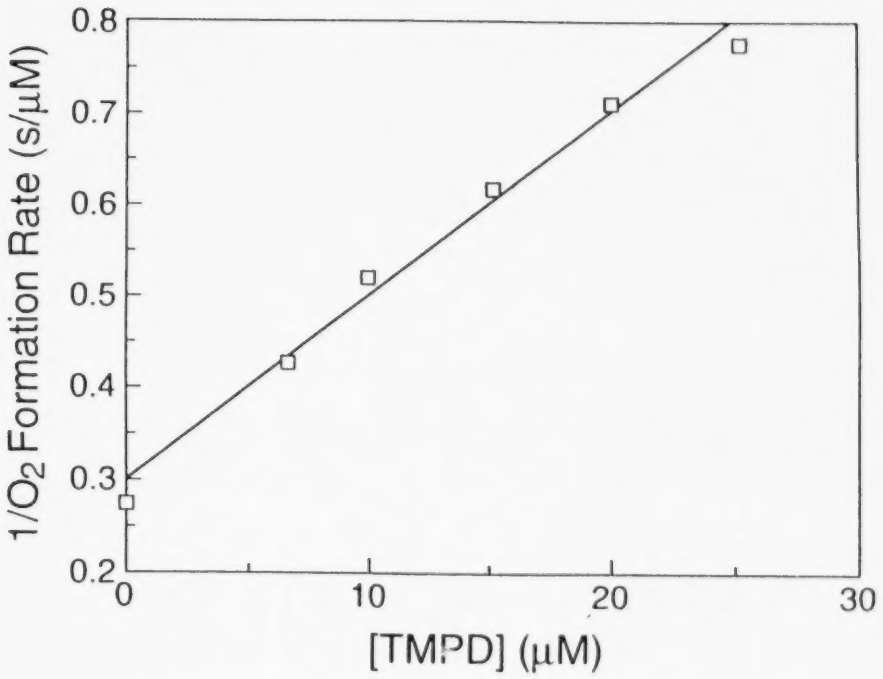

Figure 4.10. Plot of the reciprocal of the initial rate of O_2 evolution *versus* [TMPD]. Reaction conditions are as decribed for Fig. 4.9.

4.6 REFERENCES

1. Thomas, J. A., Morris, D. R., and Hager, L. P. (1970) *J. Biol. Chem.* **245**, 3135-3142.
2. Sono, M., Dawson, J. H., Hall, K., and Hager, L. P. (1986) *Biochemistry* **25**, 347-356.
3. Palcic, M. M., Rutter, R., Araiso, T., Hager, L. P., and Dunford, H. B. (1980) *Biochem. Biophys. Res. Commun.* **94**, 1123-1127.
4. Araiso, T., Rutter, R., Palcic, M. M., Hager, L. P., and Dunford, H. B. (1981) *Can. J. Biochem.* **59**, 233-236.
5. Thomas, J. A., Morris, D. R., and Hager, L. P.(1970) *J. Biol. Chem.* **245**, 3129-3134.
6. Frew, J., and Jones, P. (1984) *In* Advances in inorganic and bioinorganic mechanisms. *Edited by* A. G. Sykes. Academic Press, New York. pp. 175-212.
7. Kedderis, G. L., and Hollenberg, P. F. (1983) *J. Biol. Chem.* **258**, 12413-12419.
8. Kadima, T. A., and Pickard, M. A. (1990) *Can. J. Microbiol.* **36**, 302-304.
9. Dunford, H. B., and Stillman, J. S. (1976) *Coord. Chem. Rev.* **19**, 187-251.
10. Dunford, H. B. (1990) *In* Peroxidases: chemistry and biology. *Edited by* J.Everse and M. B. Grisham. CRC Press, Boca Raton. pp. 1-24.
11. Segel, I. H. (1975) Enzyme kinetics: behavior and analysis of rapid equilibrium and steady-state enzyme systems. John Wiley and Sons, New York. pp. 606-625.

12. Carmichael, R. D., Jones, A., and Pickard, M. A. (1986) *Appl. Environmental Microbiol.* **51**, 276-280.

13. Hollenberg, P. F., Hager, L. P., Blumberg, W. E., and Peisach, J. (1980) *J. Biol. Chem.* **255**, 4801-4807.

14. Cotton, M. L., and Dunford, H. B. (1973) *Can. J. Chem.* **51**, 582-587.

15. Hsuanyu, Y., and Dunford, H. B. (1989) *Biochem. Cell Biol.* **68**, 965-972.

16. Beers Jr., R. F., and Sizer, I. W. (1952) *J. Biol. Chem.* **195**, 133-140.

17. George, P. (1949) *Biochem. J.* **44**, 197-20521.

18. Ogura, Y. (1955) *Arch. Biochem. Biophys.* **57**, 288-300.

19. Jones, P., and Suggett, A. (1968) *Biochem. J.* **110**, 617-620.

20. Seah, T. C. M., and Kaplan, J. G. (1973) *J. Biol. Chem.* **248**, 2889-2893.

21. Abe, K., Makino, N., and Anan, F. K. (1979) *J. Biochem.* **85**, 473-479.

22. Chance, B., Greenstein, D. S., and Roughton, F. J. W. (1952) *Arch. Biochem. Biophys.* **37**, 301-321.

23. Wariishi, H., Marquez, L., Dunford, H. B., and Gold, M. H. (1990) *J. Biol. Chem.* **265**, 11137-11142.

24. Hollenberg, P. F., Rand-Meir, T., and Hager, L. P. (1974) *J. Biol. Chem.* **249**, 5816-5825.

25. Kedderis, G. L., Koop, D. R., and Hollenberg, P. F. (1980) *J. Biol. Chem.* **255**, 10174-10182.

26. Hong, Y., Li, C.-H., Burgess, J. R., Chang, M., Salem, A, Srikumar, K., and Reddy, C. C. (1989) J. Biol. Chem. **264**, 13793-13800.

CHAPTER FIVE

PURIFICATION OF NITRIC OXIDE SYNTHASE FROM PORCINE CEREBELLA

5.1 INTRODUCTION

Nitric oxide (NO) is a poisonous gas found in smog, acid rain, and cigarette smoke. The discovery in 1987/88 that vascular endothelial cells are able to synthesize nitric oxide from L-arginine as a transcellular signal (1-4) was initially received by most biologists with considerable scepticism. However, NO — a small, relatively unstable, potentially toxic, diatomic free radical — has become in the past few years one of the more studied and fascinating entities in biological chemistry. It plays a role, often as a biological messenger, in an astonishing range of physiological processes in humans and other animals. Its expanding range of functions already includes neurotransmission, blood clotting, blood pressure control, and a role in the immune system's ability to kill tumor cells and intracellular parasites (5-7).

The enzyme responsible for the synthesis of NO from L-arginine in mammalian tissues is known as nitric oxide synthase (EC 1.14.13.39) (6). Nitric oxide synthase (NOS) catalyzes the five-electron oxidation of L-arginine to citrulline and nitric oxide at the expense of molecular oxygen and NADPH (Fig. 5.1). As shown in Fig. 5.1, NO synthesis from arginine is a reaction which involves two separate mono-oxygenation steps (8-11).

The enzyme was first purified in 1990 (12) from rat cerebella. The NOS characterized to date falls into two general categories. The NOS involved in signalling is found to be constitutively expressed and has been

purified from rat cerebella (13, 14) and porcine brain (15-17). This NOS requires both Ca^{2+} and calmodulin. The NOS from murine macrophages is inducible and shows no requirement for Ca^{2+} and calmodulin (18). Both forms of NOS utilize NADPH (18).

Both forms of NOS are dimeric enzymes containing two identical subunits. The molecular weight of the monomer is 140 ± 10 KDa. All forms of the enzyme studied thus far contain four prosthetic groups: flavin-adenine dinucleotide (FAD); flavin mononucleotide (FMN); tetrahydrobiopterin (H_4B); and a heme complex, iron protoporphyrin IX (heme). Each subunit contains one molecule of each of the flavin nucleotides and heme (16, 19, 20). The active enzyme *in vivo* is thought to contain one molecule of H_4B per subunit although the amount of H_4B contained in each subunit varies from 0.1 to 1 molecule when isolated. Although all four of these cofactors are widely found in nature and help to catalyze a large number of oxidative and reductive reactions, NOS is the only enzyme known to use all four. Molecular cloning of several forms of NOS suggests how the enzyme's amino acid sequence might relate to its function. Each subunit is about equally divided into a reductase and an oxygenase domain. The link between the two domains is a sequence that forms the binding site for calmodulin. The amino acid sequence of the reductase domain, which contains the binding sites for NADPH, FAD, and FMN, is strikingly similar to sequences present in the mammalian cytochrome P-450 reductase (21). This similarity suggests that reducing equivalents from NADPH may be shuttled into the active site *via* the flavins, which store electrons derived from NADPH and transfer them to a catalytic center located within the oxygenase domain. The oxygenase domains, which are highly

conserved among the NOS isoforms, are presumed to contain binding sites for heme, H_4B, and L-arginine.

The heme complex likely plays a central role in catalyzing NO synthesis. The similarity of the heme environment in NOS to that in the cytochrome P-450s suggests that this site is likely to bind and activate molecular oxygen, which then reacts with L-arginine to produce NO and L-citrulline (22).

The role of H_4B in NOS is not clear. Mayer and Werner at the Free University of Berlin were the first to show that variable amounts of the cofactor are tightly bound to isolated NOS, making NOS the first protein known to contain stably bound H_4B. The role of H_4B in the NOS reaction involves stabilization of the enzyme and redox chemistry wherein a 1:1 stoichiometry between bound pterin and NOS subunit results in maximum activity (23).

The relationship of the quaternary structure of the cytokine-induced nitric oxide synthase from macrophages to its catalytic activity was recently investigated (24). This study shows that, in contrast to dimeric NOS, purified subunits do not synthesize NO. Dimeric NOS and NOS subunits are equivalent in catalyzing electron transfer from NADPH to cytochrome c at rates that are faster than the maximal rate of NO synthesis by dimeric NOS. Reconstitution of subunits requires their incubation with L-arginine, tetrahydrobiopterin, and stoichiometric amounts of heme. The dimeric NOS reconstituted from its subunits has the spectral and catalytic properties of native dimeric NOS. In brief, NOS subunits are NADPH-dependent reductases that acquire the capacity to synthesize NO only through their dimerization and binding of heme and tetrahydrobiopterin.

5.2 PURIFICATION OF NITRIC OXIDE SYNTHASE FROM PORCINE CEREBELLA

5.2.1 Materials

2',5'-ADP-Sepharose, calmodulin-agarose and Sepharose 4B were purchased from Sigma. Chemicals: β-NADPH (β-nicotinamide adenine dinucleotide phosphate, reduced form), EGTA (ethylene-bis-[β-aminoethylether]-N,N,N',N'-tetraacetic acid), calmodulin (phosphodiesterase 3',5'-cyclic nucleotide activator), pepstatin A and PMSF (phenylmethylsulfonyl fluoride), and PEG4000 (polyethylene glycol) were purchased from Sigma. L-arginine was obtained from General Intermediates of Canada. 2-Mercaptoethanol was obtained from Aldrich. Triethanolamine, calcium chloride and sodium chloride were obtained from Fisher. EDTA was obtained from BDH Chemicals.

Citrulline assay materials: the cation exchange resin AG 50W-X8 Resin was obtained from Bio-Rad Laboratories. ^{14}C-Arginine was purchased from Amersham. L-Valine, L-citrulline were obtained from Sigma. Scintillant was purchased from Fisher.

SDS-PAGE materials: TEMED (N,N,N',N'-tetramethylethylene diamine) is an electrophoresis reagent from Sigma. Acrylamide was obtained from Bio-Rad Laboratories. Ammonium persulfate was purchased from Bethesda Research Laboratories. Molecular weight markers were obtained from Sigma.

All other reagents were of analytical grade.

Buffers used for enzyme isolation were as follows:

Buffer A, 50 mM triethanolamine-HCl buffer, pH 7.5, 0.5 mM EDTA, 12.5 mM 2-mercaptoethanol, 0.5 mM L-arginine, 1 μM pepstatin A, 0.1 mM PMSF.

Buffer B, 10 mM triethanolamine-HCl buffer, pH 7.5, 0.1 mM EDTA, 12.5 mM 2-mercaptoethanol, 0.5 mM L-arginine, 1 μM pepstatin A, 0.1 mM PMSF.

Buffer C, 50 mM triethanolamine-HCl buffer, pH 7.5, 1 mM $CaCl_2$, 12.5 mM 2-mercaptoethanol, 0.5 mM L-arginine, 1 μM pepstatin A, 0.1 mM PMSF.

5.2.2 Enzyme preparation

The purification of NO synthase from porcine cerebella was carried out following a combination of published procedures (14-17) with some details added and some modifications as described below.

Porcine cerebella were obtained from Oullet Packer Ltd., a meat-packing plant in Edmonton, Alberta. Connective fat tissues and arachnoidea were removed from the cerebella and the cerebella were then frozen on dry ice within 20 minutes of slaughter. This step is crucial for later purification due to the fact that the high content of fat material dramatically interferes with the separation of cytosol from cell tissues. Subsequent centrifugation involving very high speed and long time was then required. Cerebella which were stored at -70 °C for three weeks were found to give lower NO synthase activity than fresh cerebella based on the NO synthase activity measurements of the cytosols. For isolation, about 1 kg of porcine cerebella (frozen for only two days) were thawed and blended in a Waring Blender for 1.5 minutes in ice-cold buffer A at 3-4 mL of buffer per g of tissue. All subsequent procedures were conducted at 4°C. The mixture was then homogenized with a IKA-Werk, Ultra Turrac T25 homogenizer equipped with a UT-dispersing tool at medium speed for 3.5 minutes. The homogenate was passed through

four layers of cheesecloth to further remove fat material. Instead of ultracentrifugation used by other investigators, the homogenate was then centrifuged at 30,100 x g (14,000 RPM) in a Beckman JA-14 rotor at 4 °C for 60 minutes. A clear supernatant was obtained to which ammonium sulfate was added to a concentration of 176 g/L (30% saturation) following the procedure of Mayer *et al.* (15, 16). The mixture was incubated with continuous gentle stirring for 2 hours. The solution was centrifuged at 30,100 x g for 40 minutes and the supernatant was decanted. The remaining pellets were dissolved in buffer B and the resulting solution was then centrifuged for 30 minutes at 30,100 x g. For subsequent column chromatography, the large volume of supernatant was concentrated to about 20 mL by polyethylene glycol 4000. This concentration step required approximately 8 hours. The concentrated protein extract was mixed with 25 mL of buffer B preequilibrated 2',5'-ADP-Sepharose, as used by all other investigators (14-17). The slurry was gently stirred for 2 hours and then centrifuged at 3,110 x g (4,500 RPM) in a Beckman JA-14 rotor for 20 minutes after which the supernatant was removed. This was required because of the presence of high contents of non-binding proteins in the slurry. The ADP-binding proteins remained in the gel as pellets. The pelleted gel was suspended in 20 mL of buffer B and poured into a chromatography column (30 cm x 2 cm). The gel was washed with 25 mL of buffer B, followed by 200 mL of buffer B containing 0.5 M NaCl. The absorbance at 280 nm (A_{280}) is used to monitor the protein content in the eluate; and the elution was stopped when A_{280} dropped below 0.08. Finally, another 60 mL of buffer B was used to wash the column. NO synthase was eluted with 50 mL of buffer B containing 10 mM NADPH as done previously (14-17). The NADPH eluted solution was dialyzed against 3 L of buffer C for

three 2-hour periods (for elimination of EDTA which interferes with NO synthase binding to the following affinity column) following the procedure of Schmidt *et al.* (14). The dialyzed pool from 2',5'-ADP-Sepharose was incubated for 1 hour with 18 mL of calmodulin-agarose gel and noncoupled sepharose 4B, (1 : 8 vol/vol which yields 8.6 nmol of calmodulin per mL of packed gel), which had been pre-equilibrated with buffer C. The slurry was transferred to a chromatography column (30 cm x 1.2 cm) and was washed with 1.5 L of buffer C, followed by 1.5 L of buffer C containing 0.3 M NaCl. NO synthase was then eluted with buffer C containing 1 M NaCl and 6 mM EGTA. The eluate was immediately concentrated by use of an Amicon Centriprep- 30 concentrator to a final volume of 4 mL. The enzyme was stored at - 70 °C after addition of 20 % (vol/vol) glycerol.

5.2.3 Activity and protein assays

NO synthase activity can be assayed by a range of methods, based on the formation of either citrulline or (indirectly) NO itself. Formation of ^{3}H- or ^{14}C-labelled citrulline from labelled L-arginine is perhaps the most widely used method, using a simple ion-exchange separation of substrate and product (12, 25).

The following procedure was followed for the ^{14}C analysis. Weigh out a certain amount of AG 50W-X8 Resin (0.33 g per measurement) and add to 2 M NaOH, swirl and allow to settle. Decant the NaOH and wash three times with deionized water. After the final wash, add a measured amount of deionized water to the resin (1.0 mL of water x the number of samples). A final pH of ~7.0 is required after these steps. 50 mM phosphate buffer, pH 7.2, was used for the assay. The reaction mixture contains 10 mM L-arginine,

1 mM L-citrulline, 50 mM L-valine, 4 mM H_4B, 10 mg/mL PMSF, 0.24 mM Ca^{2+} and 1.24 mM Mg^{2+}. Pipette 100 µL of the above mixture directly into the bottom of a 2.0 mL Eppendorf tube. Add 5 µL each of different concentrations of cofactors into the tube for measurement of concentration dependant effects on the enzyme activity. Place the tubes in a water bath at 37 °C. Pre-incubate for at least 5 minutes but not longer than 10 minutes. Add 20 µL of enzyme extract (3.85 µg) to the tube. Vortex briefly at a low setting before replacing the tube in the 37 °C water bath. Incubate the solution for a total of 12 minutes. At 12 minutes, add 1 mL of activated Dowex resin slurry (swirl before pipetting) to the tube to stop the reaction. Add 300 µL of water to the tube and spin at 14,000 RPM at room temperature for 2 minutes. Carefully remove 700 µL of supernatant from the tube and place it into a small counting vial. Add 20 µL of the reaction mixture to a separate small counting vial (for determination of specific activity). Add 2 mL of Scintillant to the vial, shake vigorously, and take ^{14}C counts for 2.5 minutes. All data are means of duplicate determinations.

Protein concentration was determined according to the method of Bradford (26) using bovine serum albumin as a standard.

5.2.4 SDS-PAGE

Two volumes of acetone were added to the protein extracts from different purification stages and subsequently stored at - 70 °C for 2 hours. After centrifugation, the protein precipitates were then dissolved in a buffer containing: 62.5 mM Tris-HCl, pH 6.8, 1.25 % SDS, 30 % glycerol, 1.25 % 2-mercaptoethanol and 0.125 % (w/vol) bromophenol blue. The mixture was then heated for 3 minutes in boiling water. After loading the mixtures onto a

gel, the gel was run at a constant voltage of 200 volts for 1 hour. Bands were visualized by Commassie Brilliant Blue R250 followed by destaining in an aqueous solution of methanol : acetic acid : water (10 : 10 : 80 vol/vol/vol). The protein standards used were: myosin, 205 KDa; β-galactosidase, 116 KDa; bovine serum albumin, 66 KDa; ovalbumin, 45 KDa; carbonic anhydrase, 29 KDa; trypsin inhibitor, 20 KDa; α-lactalbumin, 14.2 KDa and aprotinin, 6.5 KDa.

The 15% acrylamide gel consisted of a separating gel (pH 8.8) and a stacking gel (pH 6.6).

The molecular weight of NO synthase monomer can be determined from a calibration curve which is the plot of the log of molecular weight of the standard protein *versus* the relative mobility. The relative mobility is the ratio of the protein migration distance to the migration distance of bromophenol blue.

5.3 RESULTS AND DISCUSSION

Protein concentrations were determined before addition of 20 % glycerol to the enzyme extracts for storage since glycerol interferes with the assay (19). A total of 770 µg of protein was obtained from 1 kg of porcine cerebella.

The NO synthase activity was determined by the sensitive method of ^{14}C-citrulline assay. A total of 2660 units of activity was obtained. One unit of activity is defined as one pmole of citrulline formed per min per µg of protein.

The effects of EGTA, hematin and calmodulin concentrations on the NO synthase activity were examined. As expected, EGTA, a chelator of Ca^{2+}, inhibits NO synthase activity and calmodulin enhances the activity. Hematin enhances the NO synthase activity when its concentration is less than the

enzyme concentration but inhibition was observed when a high concentration of hematin was used. All of these results are shown in Figs. 5.2 to 5.4.

Purified enzyme extract and the eluate from 2',5'-ADP-Sepharose gel were heat-dissociated in the presence of sodium dodecyl sulfate (SDS) and 2-mercaptoethanol and were analyzed on 15 % SDS-polyacrylamide gel (SDS-PAGE) using the discontinuous buffer system (27). Bands were visualized by staining with Coomassie Brilliant Blue R250 as shown in Fig. 5.5. Using the calibration curve of Fig. 5.6, the molecular weight of the purified NO synthase monomer determined by SDS gel electrophoresis is 128 KDa, which is in agreement with other investigators' reports.

The purified enzyme was stored at - 70°C for six days. The NO synthase activity was measured again and it was observed that more than 70 % of the total activity was lost. The original purpose of the purification of NOS was for some kinetic studies on NOS-catalyzed reactions. However, the low yield of the enzyme and the instability of the purified NOS enzyme prevent us from doing some intended further studies.

Some suggestions for future work

After the work on isolation of NO synthase from porcine cerebella was started, following the procedure of Mayer *et al.* (15-17), it became apparent that the complexity of the purification procedure is due in part to the large amount of porcine cerebella used as the starting material and accordingly because of the high content of fat tissue in the porcine cerebella. Schmidt *et al.* (14) purified NO synthase from rat brain using a significantly reduced amount of starting material than that required for porcine cerebella. Because of the small amount of rat brain used, the purification procedure employing rat

brain is simplier than that using porcine cerebella. For the same reason, rat brain should have higher NO synthase activity than porcine cerebella. This was confirmed by NO synthase activity measurements. The NO synthase activities of the cytosols from both porcine cerebella and rat brain were measured. The results show that rat brain has at least a two fold higher NO synthase activity than porcine cerebella (data not shown). Due to the low content of fat the cytosol of rat brain is much clearer than that of porcine cerebella. The facts of the increased enzyme activity and a greatly simplified enzyme purification procedure for NO synthase from rat brain indicate that fresh rat brain is a better source for extraction of NO synthase than porcine cerebella.

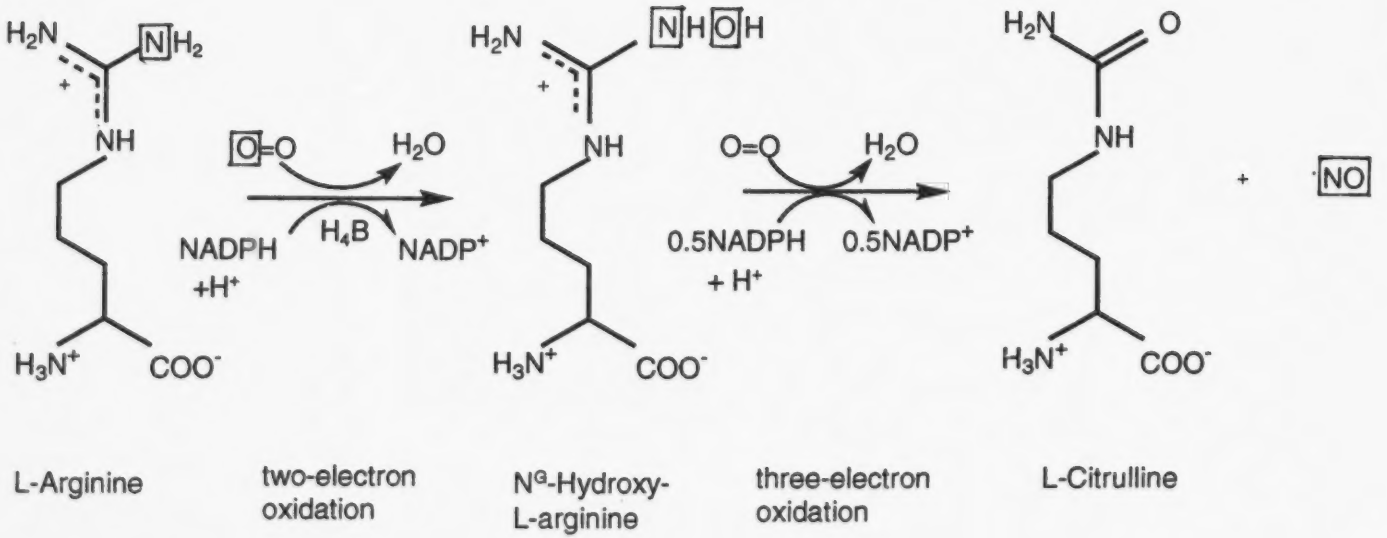

Figure 5.1. Reaction Catalyzed by Nitric Oxide Synthase (NOS). The boxed O and N atoms show the origin of the constituent atoms of NO.

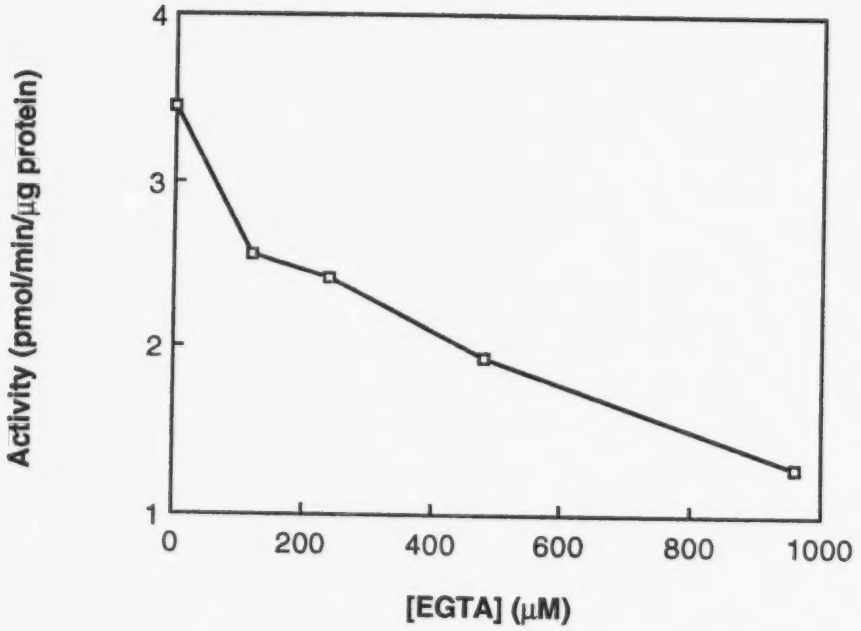

Figure 5.2. Concentration dependence of NO synthase activity on EGTA. The reaction was carried out in phosphate buffer, pH 7.2 and the mixture contains 10 mM of L-arginine, 1 mM of L-citrulline, 50 mM of L-valine, 4 mM of H_4B, 10 mg/ml of PMSF, 0.24 mM of Ca^{2+} and 1.24 mM of Mg^{2+}. 123 nM NO synthase and varied concentrations of EGTA were used.

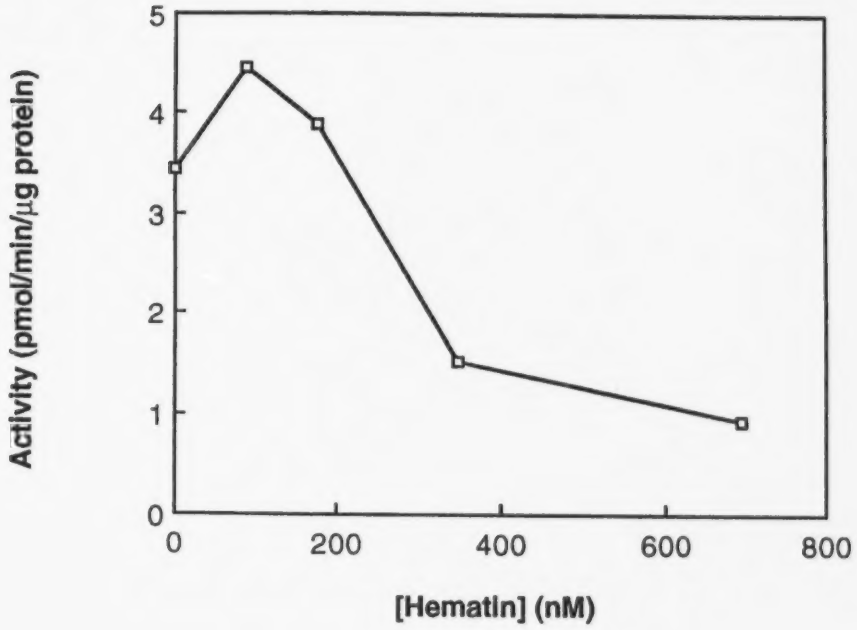

Figure 5.3. Concentration dependence of NO synthase activity on hematin. The reaction conditions are the same as Fig. 5.2.

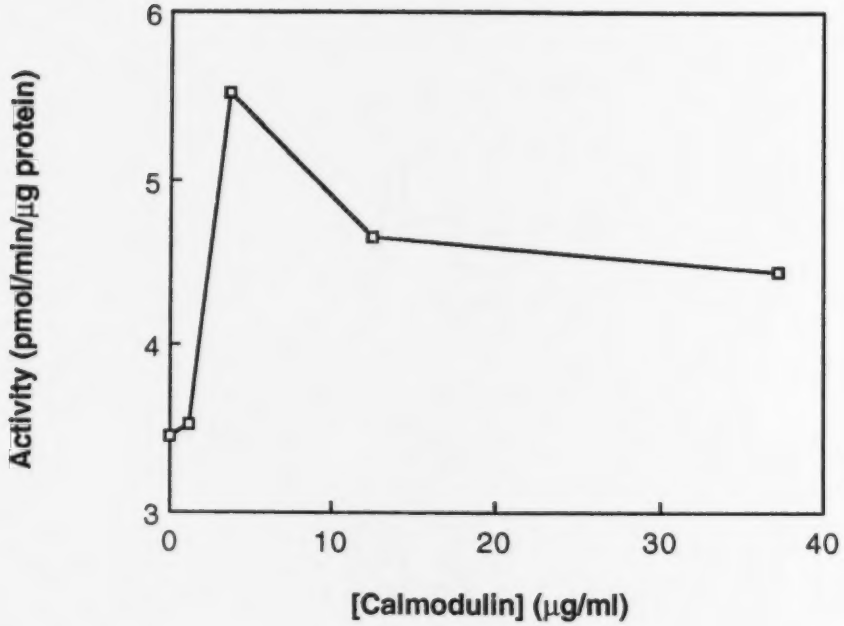

Figure 5.4. Concentration dependence of NO activity on calmodulin. The reaction conditions are the same as Fig. 5.2.

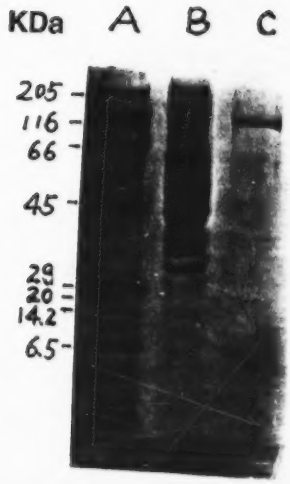

Figure 5.5. SDS-PAGE ayalysis of purified NO synthase. A 15 % polyacrylamide gel was stained with Coomassie blue. Lanes: A, molecular markers; B, 1.0 ml of 2',5'-ADP-sepharose gel eluate; C, 300 µl of calmodulin eluate.

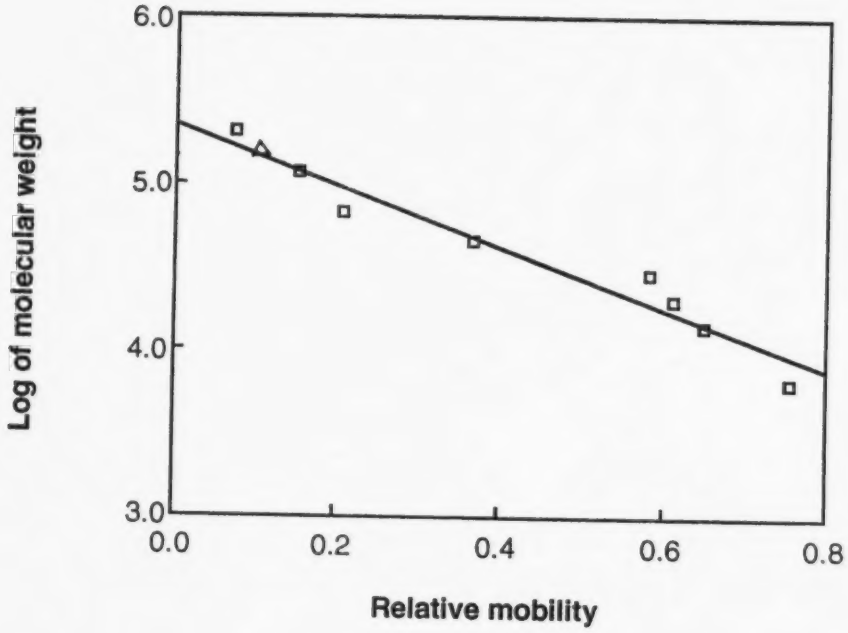

Figure 5.6. Plot of the log of molecular weight of the protein standard *versus* the relative mobility obtained from a 15 % nongradient denaturing (SDS) discontinuous gel electrophoresis.

Δ shows NO synthase.

5.4 REFERENCES

1. Palmer, R. M. J., Ferrige, A. G. and Moncada, S. (1987) *Nature* (London) **327**, 524-526.
2. Ignarro, L. J., Buga, G. M., Wood, K. S., Byrnes, R. E. and Chaudhuri, G. (1987) *Proc. Natl. Acad. Sci. USA* **84**, 9265-9269.
3. Palmer, R. M. J., Ashton, D. S. and Moncada, S. (1988) *Nature* (London) **333**, 664-666.
4. Schmidt, H. H. H. W., Nau, H., Wittfoht, W., Geriach, J., Prescher, K. E., Klein, M. M., Niroomand, F. and Bohme, E. (1988) *Eur. J. Pharmacol.* **154**, 213-216.
5. Garthwaite, J. (1991) *Trends Neurosci.* **14**, 60-67.
6. Marletta, M. A., Tayeh, M. A., and Hevel, J. M. (1990) *BioFactors* **2**, 219-225.
7. Ignarro, L. L. (1990) *Annu. Rev. Pharmacol. Toxicol.* **30**, 535-560.
8. Kwon, N. S., Nathan, C. F., Gilker, C., Griffith, O. W., Matthews, D. E. and Stuehr, D. J. (1990) *J. Biol. Chem.* **265**, 13442-13445.
9. Stuehr, D. J., Kwon, N. S., Nathan, C. F., Griffith, O. W., Feldman, P. L. and Wiseman, J. (1991) *J. Biol. Chem.* **266**, 6259-6263.
10. Leone, A. M., Palmer, R. M. J., Knowles, R. G., Francis, P. L., Ashton, D. S. and Moncada, S. (1991) *J. Biol. Chem.* **266**, 23790-23795.
11. Stuehr, D. J. and Griffith, O. W. (1992) *Adv. Enzymol.* **65**, 287-346.
12. Bredt, D. S. and Snyder, S. H. (1990) *Proc. Natl. Acad. Sci. USA* **87**, 682-685.
13. Bredt, D. S., and Snyder,S. H. (1990) *Annu. Rev. Pharmacol. Toxicol.* **30**, 535-560.

14. Schmidt, H. H. W., Pollock, J. S., Nakane, M., Gorsky, L. D., Forstermann, U., and Murad, F. (1991) *Proc. Natl. Acad. Sci. USA* **88**, 365-369.

15. Mayer, B., John, M., and Bohme, E. (1990) *FEBS Lett.* **277**, 215-219.

16. Mayer, B., John, M., Heinzel, B., Werner, E. R., Wachter, H., Schultz, G., and Bohme, E. (1991) *FEBS Lett.* **288**, 187-191.

17. Heinzel, B., John, M., Klatt, P., Bohme, E., and Mayer, B. (1992) *Biochem. J.* **281**, 627-630.

18. Marletta, M. A., Yoon, P. S., Iyengar, R., Leaf, C. D., and Wishnok, J. S. (1988) *Biochemistry* **27**, 8706-8711.

19. Hevel, J. M., White, K. A., and Marletta, M. A. (1991) *J. Biol. Chem.* **266**, 22789-22791.

20. Hevel, J. M., White, K. A., and Marletta, M. A. (1991) *In* Biology of Nitric Oxide: Physiology, Pathophysiology, Pharmacology and Clinical Significance, Portland Press, London.

21. Bredt, D. S., Hwang, P. M., Glatt, C. E., Lowenstein, C., Reed, R. R., and Snyder, S. H. (1991) *Nature* **351**, 714-718.

22. Feldman, P. L., Griffith, O. W., and Stuehr, D. J. (1993) *C & E News* December 20, 26-38.

23. Hevel, J. M., and Marletta, M. A. (1992) *Biochemistry* **31**, 7160-7165.

24. Baek, K. J., Thiel, B. A., Lucas, S., and Stuehr, D. J. (1993) *J. Biol. Chem.* **268**, 21120-21129.

25. Salter, M., Knowles, R. G. and Moncada, S. (1991) *FEBS Lett.* **291**, 145-149.

26. Bradford, M. M. (1976) *Anal. Biochem.* **72**, 248-254.

27. Laemmli, U. K. (1970) *Nature* **227**, 680-687.

CHAPTER SIX

GENERAL DISCUSSION

6.1 SOME PRELIMINARY WORK ON TWO PROBLEMS

Peroxidase-catalyzed iodination reactions are of special importance in iodine metabolism. It has been reported that peroxidase-catalyzed iodination reactions can be regulated by suitable electron donors such as EDTA (1-3). We have studied the mechanism of the tyrosine iodination reaction catalyzed by HRP and LPO as described in Chapter two (4). It is known that the peroxidase-catalyzed oxidation of iodide is the first step in tyrosine iodination. In order to know the effect of EDTA on tyrosine iodination, it is necessary to first study the effect of EDTA on iodide oxidation. EDTA is not a physiological substrate. The purpose of this investigation was to resolve the controversy which is described later.

As described in chapter 4 of this thesis, the catalatic and peroxidatic activities of chloroperoxidase (CPO) and their interactions were investigated. CPO is important also since it has the ability to use Cl^- as an electron donor for the chlorination of a large array of nucleophilic substrates (5). The mechanism of the chlorination of organic substrates by peroxide or peracid and Cl^- catalyzed by CPO has been studied extensively. Determination of the nature of HOCl, whether it is free in solution or is enzyme-bound, has been a major common theme in previous investigations (6-11). Chlorination was believed to proceed via compound I formation and an enzyme-bound hypochlorite intermediate (6-8). Product analysis studies led to the conclusion that free HOCl is the most likely chlorinating agent (9) and that the reaction

does not occur at the enzyme active site (10). However, there appears to be a difference in the product distribution of uncatalyzed compared to CPO-catalyzed reactions (12, 13). Recently the peroxidatic substrates catechol (CAT) and 2,4,6-trimethylphenol (TMP) were used as probes of the Cl^--dependent reactions catalyzed by CPO (14). The fact that CAT and TMP compete for reaction with the free oxidized halogen species (HOCl or Cl_2) provides evidence for the kinetically significant involvement of a free oxidized halogen species as an intermediate in any CPO-catalyzed reaction. The exact nature of the chlorinating agent remains unknown.

The only other peroxidase existing in nature that can catalyze chlorination reactions is myeloperoxidase (MPO). The kinetic studies of the chlorination of taurine by the MPO/H_2O_2/Cl^- system indicate that the chlorination reaction mediated by the MPO system *in vivo* may involve an enzyme intermediate species (MPO-I-Cl^-) rather than free HOCl (15). The direct reaction of MPO with its product HOCl has been carried out by Floris and Wever (16), in an attempt further understand the chlorination mechanisms. In order to determine the similarities or the differences between MPO and CPO catalyzed chlorination reactions, direct reaction of CPO with free HOCl was examined and the results were compared to those obtained from the MPO study.

The following two sections summarize our results for preliminary investigations of EDTA effect on iodide oxidation by HRP and the reaction of CPO with HOCl. However, the complexity of the reaction system of HRP/H_2O_2/I^-/tyrosine/EDTA was not realized until after the work had been started. Subsequently, this complication that is described later prevented the completion of this work. Furthermore, for the reaction of CPO with HOCl,

more varied techniques, such as product analysis or multi-mixing stopped-flow kinetic studies, are required to unambiguously define the exact nature of the reaction mechanism.

6.1.1 Peroxidase-catalyzed oxidation of iodide in the presence of EDTA

6.1.1.a Introduction

EDTA, a classical chelating agent (17), is generally used for chelation of various bivalent cations present in biological macromolecules. Several enzymes that require bivalent cations are inactivated when the metal ion is chelated by EDTA and subsequently are reactivated upon addition of the metal ion. HRP contains 2 mol of Ca^{2+}/mol of enzyme (18). One tightly bound Ca^{2+} of HRP, which is essential for maintaining the protein structure in the heme cavity for enzyme activity (19-21), could be removed only by very drastic treatment such as incubation with EDTA or EGTA in the presence of guanidinium chloride. Therefore, the presence of EDTA in the system of HRP/H_2O_2/I^- does not inactivate the enzyme through removal of the essential Ca^{2+} ion.

EDTA can also sometimes be used as a reducing agent (22, 23). The ferrous HRP produced by reduction of native HRP with dithionite absorbs at 435 nm (24), whereas EDTA only causes a small hypsochromic change at 402 nm (2, 25). This suggests that EDTA does not reduce native HRP to ferrous HRP.

Banerjee *et al.* (1) have shown that EDTA is an inhibitor of the iodide oxidase activity of HRP. They concluded that this inhibition of iodide oxidase activity of HRP is due to the competition between EDTA and iodide at the

iodide binding site of HRP (2). They recently reported that EDTA inhibits HRP-catalyzed iodide oxidation in a pH-dependent manner (26). The inhibition is more effective at pH 6 than at lower pH values. It has also been demonstrated that among the structural analogues of EDTA, tetramethylethylenediamine (TEMED) is 80 % as effective as EDTA, whereas the EDTA-Zn^{2+} chelate and EGTA are ineffective (26). They concluded that EDTA competes for the same binding sites with iodide and inhibits iodide oxidation by acting as an electron donor.

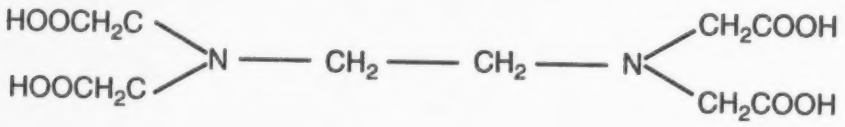

EDTA

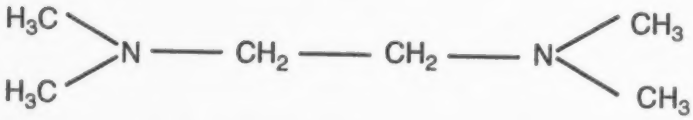

TEMED

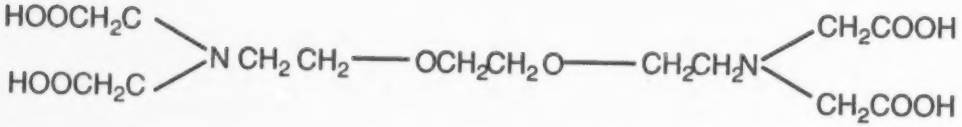

EGTA

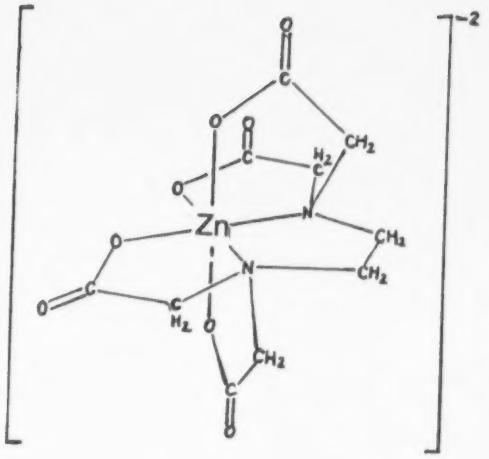

EDTA-Zn^{2+}

However, in a similar reaction system, Shah and Aust claimed that EDTA is non-enzymatically oxidized to the EDTA radical by the primary oxidation product of iodide (3); and recently, by ESR spin trapping studies, they demonstrated that the oxidation of EDTA is mediated by the iodide radical (27). In brief, they concluded that iodide is oxidized to HOI by peroxidases and that this HOI then is reduced by EDTA, hydrogen peroxide or iodide (3, 27).

The related information to the EDTA effect on the iodide oxidation by HRP is the binding of EDTA to HRP. Recently, Modi (28) reported from ^1H NMR studies that EDTA binds at or near the iodide binding site at the heme edge about 0.8 nm away from the ferric centre of HRP, and that the binding is facilitated by protonation of an acid group of pK_a 4.0 in the native enzyme. This value differs from pK_a 5.8 which was reported by Bhattacharyya *et al.* (29). Sakurada *et al.* (30) suggested that EDTA may bind at a higher affinity to the catalytically active HRP than to the native enzyme.

The exact mechanism for the inhibition of iodination reactions by EDTA is not yet fully understood. It is a prime topic for further investigation.

6.1.1.b Some preliminary experiments

Materials and methods

HRP was purchased as a suspension in ammonium sulfate from Boehringer-Mannheim Corp. After dialysis in deionized water from the Milli-Q system, a purity number of 3.46 was determined from the ratio of absorbances at 403 nm and 280 nm. The concentration of the enzyme solution was measured spectrophotometrically at 403 nm where the molar absorptivity is 1.02×10^5 $M^{-1}cm^{-1}$(31).

Lactoperoxidase with a purity number (A_{412}/A_{280}) of 0.83 was purchased from Sigma as a purified, lyophilized powder. A molar absorptivity value of 1.12×10^5 $M^{-1}cm^{-1}$ at 412 nm was used for spectrophotometric determination of its concentration (32).

The concentration of hydrogen peroxide (~30 % solution, BDH Chemicals) was determined, after appropriate dilution, using the horseradish peroxidase assay (33).

Analytical reagent grade EDTA was purchased from BDH Chemicals. Reagent grade KI and crystalline iodine were obtained from Shawinigan Chemicals. All of the chemicals were used without further purification. Solution concentrations were determined by weight and fresh stock solutions were prepared just before use. A solution of I_3^- was prepared by dissolving a small amount of crystalline iodine to a solution of known KI concentration. The concentration of the I_3^- solution was determined spectrophotometrically at 353 nm where the molar absorptivity is 2.64×10^4 $M^{-1}cm^{-1}$ (34).

Chemicals used for the citrate buffers were reagent grade and used without further purification. The total ionic strength of solution was maintained at 0.18 M by addition of KNO_3.

All solutions were prepared using deionized water obtained from the Milli-Q system (Millipore).

Stopped-flow experiments were performed on a Photal (formerly Union Giken) Model RA-601 Rapid Reaction Analyzer equipped with a 1-cm observation cell. Optical absorption measurements on a conventional time scale (> 1 s) were made using a Beckman DU 650 spectrophotometer.

O_2 evolution was determined using a Yellow Spring Instruments Model 53 Oxygen Monitor.

The pH-jump method was used to measure the initial rate of I_2 formation when the final pH was below 4.0 since native HRP is unstable at low pH values. One driving syringe contained HRP and iodide (and EDTA when necessary) in deionized water, ionic strength 0.18 M; the other syringe contained H_2O_2 in the low pH citrate buffer solution, ionic strength 0.18 M. The final pH after mixing the two solutions was the same as the buffer pH, at a total ionic strength of 0.18 M.

The initial I_2 formation rates were obtained by taking the tangents from the starting point of the stopped-flow trace at 460 nm as described in our previous work (4).

A Fisher Accumet Model 25 digital pH meter was used for all pH measurements.

All experiments were performed at (25.0 ± 0.5) °C.

Results

Since EDTA binds to HRP only under acidic conditions (pH < 5) (28), our experiments were therefore performed at pH values lower than 5.0 and at 4.1 in most cases.

In a reaction system of 0.63 μM of HRP, 200 μM of H_2O_2, 100 μM of KI and varied amounts of EDTA at pH 4.1, the initial I_2 formation rates were measured and observed to be constant over the EDTA concentration range from 0 to 30 mM as shown in Fig. 6.1. The rate was unchanged even when the EDTA concentration was increased to as high as 74 mM (data not shown).

Curve a in Fig. 6.2 shows one example of the stopped-flow trace at 460 nm over 1.0 s in the HRP/H_2O_2/I^- system which includes 1.14 μM of HRP, 2.0 mM of H_2O_2, and 1.0 mM of KI. With 15 mM EDTA present in the reaction mixture, it can be clearly seen that the stopped-flow trace at 460 nm (curve b in Fig. 6.2) remains the same as that without EDTA present (curve a). The reactions were all carried out at pH 3.67.

For comparison with the HRP/H_2O_2/I^- system, similar experiments were carried out using the LPO/H_2O_2/I^- system at pH 3.67 as shown in Fig. 6.3. The reaction mixture is 0.63 μM of LPO, 2.0 mM of H_2O_2 and 1.0 mM of KI and 0 (in the absence) or 15 mM (in the presence) of EDTA. In sharp contrast, the stopped-flow trace at 460 nm was observed to be markedly affected by the presence of EDTA. A larger absorbance change at 460 nm with EDTA present (curve b) was observed than that without EDTA present (curve a) in this system.

Since the binding ability of EDTA to HRP increases with decreasing pH (28), the initial I_2 formation rates were measured at different pH values by keeping the reactant concentrations constant with and without the presence of

EDTA. This experiment was designed to observe the pH-dependent inhibition of iodide oxidation due to the binding of EDTA to HRP. The reaction mixture was made up of 0.63 μM of HRP, 200 μM of H_2O_2, 500 μM of KI and 0 (in the absence) or 300 μM (in the presence) of EDTA. The results are shown in Fig. 6.4. Within experimental error, over a pH range of 3.5 to 5.0, the presence of EDTA does not have any effect on the initial I_2 formation rate.

However, the pseudo-catalatic degradation of H_2O_2 by iodide and HRP was observed to be inhibited by the presence of EDTA by measuring the O_2 evolution at pH 4.1 (Fig. 6.5). In a reaction system of 0.42 μM of HRP, 2.00 mM of H_2O_2 and 500 μM of KI, the presence of varied amounts of EDTA clearly shows that inhibition of O_2 evolution increases as the EDTA concentration increases from 0 to 30 mM.

Non-enzymatic reactions were designed to elucidate the role of enzyme in the reaction process. Chemically synthesized HOI was prepared by the reaction of H_2O_2 with iodide (35). The presence of excess iodide leads to generation of I_2 as shown in eq. 6.1:

$$HOI + I^- + H^+ \underset{k_{-1}}{\overset{k_1}{\rightleftharpoons}} I_2 + H_2O \qquad (6.1)$$

The overall rate constant for the forward reaction of eq. 6.1, k_1, is 4.4×10^{12} $M^{-2}s^{-1}$, k_{-1} is 3.0 s^{-1} for the reverse reaction (36). The initial I_2 formation rates were determined in a reaction system of 10 mM of H_2O_2, 10 mM of EDTA and KI concentrations ranging from 50 mM to 150 mM at pH 5.2 and an ionic strength of 0.18 M. The rates were compared with those obtained from the reaction system without EDTA present. The observed results that the I_2

formation rate increases with increasing I^- concentration, but remains unchanged with differing amounts of EDTA are shown in Fig. 6.6. The initial I_2 formation rates were then determined by keeping the initial iodide concentration at 80 mM, H_2O_2 concentration at 10 mM and increasing the EDTA concentration from 5 mM to 30 mM at pH 5.2 and a total ionic strength of 0.18 M. The result that the I_2 formation rate is not affected by the presence of varied amounts of EDTA is shown in Fig. 6.7. These results (Figs. 6.6 and 6.7) indicate that either EDTA does not react with HOI to affect the I_2 formation, or EDTA reacts with HOI but with a much slower rate than the forward reaction of I_2 formation as in eq. 6.1. Nevertheless, the measurement of the I_2 formation rate does not give any evidence for the possibility that EDTA may slowly react with I_2 after its formation.

Triiodide ion is known to be in equilibria with other iodide species in aqueous solution as shown by eqs. 6.1 and 6.2:

$$HOI + I^- + H^+ \rightleftharpoons I_2 + H_2O \qquad (6.1)$$

$$I_2 + I^- \rightleftharpoons I_3^- \qquad (6.2)$$

A non-enzymatic system of I_3^- and EDTA in aqueous solution was developed to verify the existence and the nature of the reaction occurring between EDTA and the oxidizing iodide species I_2 or HOI. The disappearance of I_3^- was observed by monitoring the absorbance at 353 nm ($\varepsilon_{353} = 2.64 \times 10^4$ $M^{-1}cm^{-1}$ (34)) over 10 min (Fig. 6.8) in a mixture of 27 μM of I_3^- and 30 mM EDTA at pH 4.1 and an ionic strength of 0.18 M. The stopped-flow measurements of this reaction were then carried out precisely using the

Photal instrument in a short time of 30 s at pH 3.50 and a total ionic strength of 0.18 M. The reaction mixtures contained 25.6 μM of I_3^- and EDTA concentrations ranging from 5 mM to 30 mM. The initial I_3^- disappearance rate was obtained by taking the tangent to the starting point of the stopped-flow trace at 353 nm as shown in the inset of Fig. 6.9. From the slope of the trace in Fig. 6.9, the first order rate constant of the reaction was obtained and found to be $(2.5 \pm 0.1) \times 10^{-5}$ s^{-1}. From eqs. 6.1 and 6.2, the concentrations of I_2 and HOI can be calculated by use of the known concentrations of I_3^- and I^-. The maximum second order rate constants for the reactions between EDTA with I_2 and HOI can be obtained by assuming that only one of the reactions occurs. The calculated second order rate constants are $(2.6 \pm 0.1) \times 10^5$ M^{-1} s^{-1} for the reaction with HOI and $(1.8 \pm 0.1) \times 10^{-1}$ $M^{-1}s^{-1}$ with I_2. Therefore, HOI is the dominant species in the iodine aqueous solution which reacts with EDTA. At the same pH of 3.50, the second order rate constant of the forward reaction of eq. 6.1 can be calculated to be 1.3×10^9 M^{-1} s^{-1} which is more than three orders of magnitude larger than that for the reaction between EDTA and HOI. Therefore, under our experimental conditions, the effect of EDTA on the I_2 formation rate is negligible.

6.1.1.c Discussion

Our preliminary results presented here show that EDTA does not inhibit the iodide oxidase activity of HRP, but EDTA does react with the iodide oxidation product HOI.

It was reported that the inhibition of iodide oxidase activity of HRP was observed at much higher EDTA concentrations than corresponding concentrations of iodide. This was explained by the observation that EDTA

competitively binds to HRP at the same binding site of iodide and that its binding is much weaker than that for iodide (1, 2). However, by comparing the association constant of the EDTA binding to HRP, which is 12.8 M^{-1} (28), with that of iodide binding which is about 10 M^{-1} (30) at pH 4.0, the binding of EDTA to HRP is stronger than that for iodide. Therefore, it is not necessary to use higher EDTA concentrations than iodide to observe inhibition on the iodide oxidation reaction catalyzed by HRP. We were unable to observe inhibition of the iodide oxidase activity of HRP by EDTA even under the conditions where the EDTA concentrations were in excess of those for iodide at pH 4.1 and an ionic strength of 0.18 M (Fig. 6.1).

The effect of pH on EDTA binding to HRP has been reported and was shown to increase with decreasing pH (28). The experiment of measuring the initial I_2 formation rates in the HRP/H_2O_2/I^- system in the presence of EDTA at various pH values was designed to observe the effect of EDTA binding to HRP on the enzyme iodide oxidase activity. Within experimental error, the I_2 formation rates remain the same over pH values ranging from 3.5 to 5.0 (Fig. 6.4) which indicates that the binding of EDTA to HRP does not cause any inhibition of the enzyme iodide oxidase activity. We thus conclude that the binding of EDTA to HRP occurs at a binding site different from that of iodide and that its binding to the enzyme does not have any influence on the iodide oxidase activity of HRP.

We reported earlier that HOI is formed in the HRP/H_2O_2/I^- system and that HOI reacts with excess I^- to form I_2, and with excess H_2O_2 to produce O_2 (4). The present results show that EDTA inhibits the O_2 evolution in the system (Fig. 6.5). This suggests that EDTA competes with H_2O_2 for HOI.

The I_2 formation measurements do not reveal information for the competitive reaction of EDTA with I^- for HOI. This phenomenon was observed in both enzymatic and non-enzymatic systems (Figs. 6.1 and 6.7). Compared to the I_2 formation from HOI and I^-, the reaction of EDTA with HOI is much slower under our experimental conditions. Our kinetic measurements show that the second order rate constant of the reaction between EDTA and HOI is $(2.6 \pm 0.1) \times 10^5\ M^{-1}s^{-1}$ at pH 3.5 and that EDTA does not react with I_2.

It is known that either HOI, I_2 , or both, are the iodinating agent in the HRP iodination system (4). The maximum second order rate constants of the tyrosine iodination were measured to be $9.3 \times 10^5\ M^{-1}s^{-1}$ by HOI and $1.18 \times 10^4\ M^{-1}s^{-1}$ by I_2 at pH 3.5. Compared to the second order rate constant for the reaction of EDTA with HOI at the same pH, they are of the same order of magnitude. It is, therefore, speculated that EDTA may inhibit the tyrosine iodination in the HRP iodination system by competing for HOI with tyrosine.

We tried to observe the inhibition of EDTA on tyrosine iodination quantitatively by monitoring monoiodotyrosine formation at 290 nm ($\varepsilon_{290} = 2.3 \times 10^3\ M^{-1}cm^{-1}$ (4)) in a reaction system of HRP/H_2O_2/I^-/tyrosine. However, I^- is one of the products of the redox reaction between EDTA and HOI. The generation of I_3^- from the product I^- with excess I_2 was found to interfere with our measurements because of the larger absorbance of I_3^- at 290 nm ($\varepsilon_{290} = 4.0 \times 10^4\ M^{-1}cm^{-1}$ (34)) than that of monoiodotyrosine. Therefore, the initial absorbance increase at 290 nm was greater with EDTA present than in the pure iodination system due to formation of both monoiodotyrosine and I_3^- in the presence of EDTA (data not shown). It was thus not possible to quantitatively measure the inhibition of EDTA on tyrosine iodination directly.

LPO-OI is the dominant tyrosine iodinating agent in the LPO iodination system (4). The fact that EDTA interferes with the formation of HOI and thereby I_2 in the LPO/H_2O_2/I^- system (Fig. 6.3) but not in the HRP/H_2O_2/I^- system (Fig. 6.2), indicates that LPO-OI has the same oxidizing ability as HOI, but not the same as HRP-OI. Formation of I_3^- from the reaction of I_2 with I^-, the product of the reaction of EDTA with LPO-OI, interferes with the measurement of the initial I_2 formation rate at 460 nm due to the greater absorbance of I_3^- at 460 nm ($\varepsilon_{460} = 9.75 \times 10^2\ M^{-1}cm^{-1}$ (34)) than I_2 ($\varepsilon_{460} = 7.46 \times 10^2\ M^{-1}cm^{-1}$ (34)). Therefore, the inhibition of HOI formation and thereby I_2 formation by EDTA in the LPO/H_2O_2/I^- system was unable to be measured quantitatively at 460 nm because of the complication. However, the results shown in Fig. 6.3 indicate that reaction of LPO-OI with EDTA does occur which indicates that EDTA inhibits the formation of HOI from LPO-OI. Therefore, EDTA inhibits the iodide oxidase activity of LPO due to the competitive reaction of EDTA with I^- in contrast to the activity of HRP. EDTA may compete with tyrosine for LPO-OI, it is expected that EDTA inhibits tyrosine iodination in the LPO/H_2O_2/I^-/tyrosine system.

The reaction between EDTA and HOI is a redox reaction; EDTA is decarboxylated when HOI is reduced (3). In our reaction systems, the presence of the oxidizing reagent H_2O_2 had no effect on EDTA determined by monitoring the absorbance of the mixture of H_2O_2 and EDTA at 240 nm, the wavelength at which H_2O_2 absorbs (37) (data not shown).

In conclusion, our preliminary experimental results show that EDTA does not inhibit the iodide oxidation catalyzed by HRP. Nevertheless, EDTA does react with the iodide oxidation product, HOI, but at a much slower rate than the reaction of HOI with I^- to form I_2.

6.1.2 Kinetics and mechanism of the reaction of CPO with hypochlorous acid (HOCl)

6.1.2.a Some preliminary experiments

Materials and methods

Chloroperoxidase from *Caldariomyces fumago* was isolated and purified following established procedures (38). The concentration of the enzyme was determined from the absorbance at 400 nm using a molar absorptivity of 9.12×10^4 M^{-1} cm^{-1} (39). The R.Z. value (A_{400} / A_{280}) of the enzyme used in this study was 1.30.

An aqueous solution of sodium hypochlorite was prepared by dissolving chlorine, generated by reaction of manganese dioxide with concentrated hydrochloric acid, in a 0.1 M sodium hydroxide solution (40). This stock solution of sodium hypochlorite was stored in a cold environment and was protected from light. Its concentration was determined from the absorbance of OCl^- at 290 nm ($\varepsilon_{OCl^-} = 3.5 \times 10^2$ $M^{-1}cm^{-1}$(41)). Reagent grade potassium chloride was purchased from Aldrich and used without further purification. The concentration of the KCl solution was determined by weight.

Chemicals used for the preparation of the phosphate buffer (pH 6.2) were reagent grade and used without further purification. The ionic strength of the buffer was calculated to be 0.03 M. Analytical reagent K_2SO_4, obtained from AnalaR, was used to maintain the total ionic strength of all reaction mixtures at 0.11 M. A Fisher Scientific Accumet pH Meter was used to measure the phosphate buffer pH at 6.2.

All solutions were prepared using deionized water obtained from a Milli-Q water purification system (Millipore).

Stopped-flow and rapid scan experiments were performed on a Photal (formerly Union Giken) model RA-601 rapid reaction analyzer. The 1-cm observation cell was thermostatted at (25.0 ± 0.5) °C for all measurements. For both rapid scan and stopped-flow experiments, one drive syringe was filled with HOCl (pK_a=7.51) by mixing a small volume of NaOCl stock solution with a large volume of phosphate buffer pH 6.2, ionic strength 0.11 M. The other syringe was filled with chloroperoxidase (and KCl when necessary) in the same buffer. The pH after mixing the solutions in the two syringes was therefore controlled to 6.2 and the final ionic strength remained unchanged at 0.11 M.

For rapid scan experiments, both transient state and steady state conditions were employed for observation of the different steps of the reaction. A mixture of 1.0 μM of CPO with 6.0 μM of HOCl clearly displayed compound I formation. A mixture of 0.16 μM of CPO with 47.4 μM of HOCl demonstrated the conversion of compound I to compound II.

In order to measure the rate constant of compound I formation, a minimum of a 10-fold excess of HOCl was used to maintain pseudo-first-order conditions. The concentration of HOCl was not allowed to exceed a 35-fold excess to avoid the added complication of interference from the second reaction (i.e., the conversion of compound I to compound II). The final concentration of CPO was kept at 0.16 μM for all kinetic measurements. The rate of the enzyme reaction was monitored at 400 nm. A non-linear least-squares analysis of the exponential traces at 400 nm resulted in the observed pseudo-first-order rate constants. At 0.16 μM of CPO and 2.83 μM of HOCl,

the formation rate of compound I monitored at 400 nm was examined by adding KCl to yield concentrations ranging from 50 μM to 10 mM. The initial rate was determined by taking the tangent to the linear part of the stopped-flow trace at 400 nm allowing 320 ms for mixing. Six traces were recorded for every determination and the mean of these values of the initial rates was used.

For measuring the formation rate of compound II, high HOCl concentrations need to be used in order to accelerate the conversion of compound I to compound II. The effect of Cl^- concentration on the initial formation rate of compound II was studied. The Cl^- concentrations were varied from 50 μM to 5.0 mM. The final concentration of CPO was kept constant at 0.16 μM and HOCl at 47.4 μM. The initial formation rate of compound II was determined by taking the tangent to the linear part of the stopped-flow traces at 438 nm. Usually 6 traces were recorded for every determination and the mean value of the initial rates was used.

Results

Rapid Scan Measurements

Transient-State Experiments. Fig. 6.10 shows the rapid scan spectra taken over 91 ms for the reaction of 1.0 μM of CPO with 6.0 μM of HOCl at pH 6.2 and an ionic strength of 0.11 M. The partial conversion of native CPO to compound I is observed. The isosbestic points between the native enzyme and compound I were reported to be 369 nm and 444 nm (42, 43). The fact that no clear isosbestic point at 444 nm was observed in Fig. 6.10 implied that not a single conversion of native enzyme to compound I by reaction with HOCl occurred in the mixture. By increasing the time scale to 830 ms, the

conversion of compound I to compound II is observed for the same reaction mixture (Fig. 6.11). The molar absorptivities of compound II and native enzyme are similar for most peroxidases. As can be seen in Fig. 6.11 the intensity of the absorption band at 438 nm, the wavelength of the maximum absorbance of compound II, after the reaction with HOCl is much lower compared to the absorption of native enzyme at 400 nm. This shows that HOCl is able to bleach chloroperoxidase irreversibly as judged by the absorption loss. This phenomenon was observed even on a longer time scale (Data not shown).

Steady-State Experiments. In a reaction mixture of 0.16 μM of CPO and 47.4 μM of HOCl at pH 6.2, the spectra (Fig. 6.12), taken over 9.1 s after mixing, show the absorbance increase at 438 nm which indicates the conversion of compound I to compound II. With a longer time scale of 16.6 s, the spectra (Fig. 6.13) show the conversion of compound II to native enzyme in the same mixture. Fig. 6.14 shows that in the above reaction mixture of 0.16 μM of CPO and 47.4 μM of HOCl with 50 mM of KCl, compound II is still formed and subsequently converted to native enzyme.

Stopped-Flow Measurements

Transient-State Experiments. The rate constant for the formation of compound I from native enzyme and HOCl was measured at 400 nm at a pH value of 6.2 and an ionic strength of 0.11 M under pseudo-first-order conditions. The inset of Fig. 6.15 shows a typical exponential stopped-flow trace at 400 nm fitted by non-linear least-squares analysis in a reaction mixture of 0.16 μM of CPO and 2.83 μM of HOCl. A linear plot of the observed pseudo-first-order rate constants was obtained. The slope from this

plot resulted in the second order rate constant for the reaction of native CPO with HOCl and was found to be (4.0 ± 0.1) x 10^6 $M^{-1}s^{-1}$. The intercept was determined to be (0.6 ± 0.1) s^{-1}. The dissociation constant for HOCl binding to CPO can be calculated from the intercept and slope and is found to be (0.2 ± 0.1) μM which is so small as to be negligible.

The effect of Cl^- concentration on the initial compound I formation rate was examined in a reaction mixture containing 0.16 μM of CPO and 2.83 μM of HOCl and Cl^- concentrations ranging from 0 to 10 mM. The initial formation rate of compound I was obtained from the linear portion of the stopped-flow trace as the change in absorbance at 400 nm per unit time as shown in the inset of Fig. 6.16. The results shown in Fig. 6.16 (and in the inset) indicate that the presence of Cl^- does not affect the initial compound I formation rate.

Steady-State Experiments. Stopped-flow traces were taken over an 80 s sampling period for a reaction mixture containing 0.16 μM of CPO and 47.4 μM of HOCl at 438 nm, the wavelength of maximum absorbance of compound II, as shown in Fig. 6.17 (A). The first phase of the spectrum, with the sharp increase in absorbance, indicates the formation of compound II. The second phase where the absorbance decreases reflects the conversion of compound II to native enzyme as was observed previously in Fig. 6.13. However, we cannot rule out the possibility that the second phase is partly due to the bleaching of the enzyme by HOCl as we found in Fig. 6.11. Fig. 6.17 (A) shows that compound II is formed completely in 10 s and begins to convert to native enzyme at this time. Therefore, after 10 s the absorbance at 400 nm, the wavelength of maximum absorbance of native enzyme, is expected to increase instead of decrease. However, the stopped-flow trace at 400 nm

(Fig. 6.17 (B)) in the same reaction mixture shows a decrease in absorbance after 10 s which is an indication of the bleaching of native enzyme by HOCl. The presence of 50 mM Cl^- is not able to inhibit the bleaching process as shown in Fig. 6.18.

The initial compound II formation rate in a reaction mixture containing 0.16 μM of CPO and 47.4 μM of HOCl and varied amounts of KCl was observed to increase with increasing Cl^- concentrations ranging from 50 μM to 5.0 mM as shown in Fig. 6.19. The rate was determined by taking the tangent to the increasing linear part of the absorbance spectrum at 438 nm as shown in the inset of Fig. 6.19. Compound I formation is indicated because of the unchanged absorbance 200 ms after mixing. Increasing the Cl^- concentration from 5.0 mM to 50 mM did not change the compound II formation rate (data not shown).

6.1.2.b Discussion

Although chloroperoxidase is similar to horseradish peroxidase in many of its chemical and physical properties, it has the ability among peroxidases to catalyze the oxidation of Cl^- (44, 45). The only other peroxidase that can oxidize Cl^- is myeloperoxidase (46, 47). Thus, CPO and MPO can catalyze the chlorination of organic compounds. The chlorinating agents have been reported to be the enzyme-bound hypochlorite (EOCl) for both CPO (20, 21) and MPO (29, 36). In this preliminary study, the reaction pathway occurring between native CPO and the chloride oxidation product HOCl was followed at pH 6.2 and an ionic strength of 0.11 M. The effect of Cl^- concentration on this reaction was also investigated.

It can be seen from Fig. 6.10 that the spectral changes in the Soret region observed during the reaction of 1.0 μM of CPO with 6.0 μM of HOCl are similar to those observed during reaction of CPO with H_2O_2 under transient state conditions (48). The indication of the conversion of native enzyme to compound I is a rapid absorption decrease at 400 nm. The second order rate constant of compound I formation from CPO and HOCl was determined to be $(4.0 \pm 0.1) \times 10^6$ $M^{-1}s^{-1}$ with a negligible reverse reaction (Fig. 6.15). This rate is of the same order of magnitude as that for compound I formation from CPO and H_2O_2 which is $(2.3 \pm 0.1) \times 10^6$ $M^{-1}s^{-1}$ (48). The absence of a clear isosbestic point of native enzyme and compound I at 444 nm (42, 43), as shown in Fig. 6.10, indicates that compound II formation occurred prior to completion of compound I formation. Although the isosbestic points between compound I and compound II have not been reported because of the instability of these intermediates, the last four spectra did show an isosbestic point at about 417 nm taken 335 ms to 830 ms after mixing 1.0 μM of CPO with 6.0 μM of HOCl as shown in Fig. 6.11. This clear isosbestic point indicates single conversion of compound I to compound II in that time range.

As shown in Figs. 6.12 and 6.13, the formation of compound II has been clearly observed under steady state conditions from the rapid scan spectra in which an absorption peak at 438 nm was observed in a reaction mixture of 0.16 μM of CPO and 47.4 μM of HOCl. Since the conversion of compound II to native enzyme is also observed as shown in Fig. 6.13, the stopped-flow trace at 438 nm in Fig. 6.17 (A) can be explained by initial formation of compound II from compound I and then conversion of compound II to native enzyme. As mentioned earlier, Fig. 6.11 shows the absorption

loss of compound II compared to native enzyme which indicates bleaching of the enzyme by HOCl. Therefore, the absorbance decrease phase at 438 nm in Fig. 6.17 (A) may be due to both the partial bleaching of enzyme by HOCl and the conversion of compound II to native enzyme. In the time range required for conversion of compound II to native enzyme, the fact that the absorbance at 400 nm (Fig. 6.17 (B)) decreases rather than increases provides further evidence that bleaching of CPO by HOCl occurs. A large excess of Cl^- (50 mM) in the reaction mixture containing 0.16 μM of CPO and 47.4 μM of HOCl did not protect the enzyme from being bleached by HOCl (Fig. 6.18).

The Soret spectrum of CPO is not affected by the presence of Cl^- (data not shown). Also, the presence of KCl in the mixture of 0.16 μM of CPO and 2.83 μM of HOCl does not affect the initial formation rate of compound I as shown in Fig. 6.16. This indicates that the reaction of HOCl with CPO to form compound I is considerably faster than the reaction of HOCl with Cl^- to form Cl_2 as shown in eqs.6.3 and 6.4.

$$Fe^{III} + HOCl \xrightarrow{k_3} Fe^{V}=O + Cl^- + H^+ \qquad (6.3)$$

$$HOCl + Cl^- + H^+ \underset{k_{-4}}{\overset{k_4}{\rightleftharpoons}} Cl_2 + H_2O \qquad (6.4)$$

The second order rate constant of k_3 was determined to be $(4.0 \pm 0.1) \times 10^6$ $M^{-1}s^{-1}$ at pH 6.2. The overall rate constant of k_4 is 1.8×10^4 $M^{-2}s^{-1}$ and k_{-4} is 11.0 s^{-1} (24). The equilibrium constant K_4 of eq. 6.4 is $(2.54 \pm 0.02) \times 10^3$ M^{-2} at 25 °C (49). Since our experiments were carried out at pH 6.2, the second

order rate constant for the forward reaction of eq. 6.4 is 1.1×10^{-2} $M^{-1}s^{-1}$ at that pH value. The second order rate constants provide quantitative evidence that Cl^- has almost no affect on the compound I formation rate in a reaction mixture containing CPO and HOCl.

In the reaction mixture containing 0.16 μM of CPO and 47.4 μM of HOCl in the presence of a large excess of Cl^- (50 mM), the formation of compound II from compound I indicates that this occurs via a one-electron transfer process (Fig. 6.14). Also, it was observed that the initial formation rate of compound II increased with increasing Cl^- concentration and eventually reached a saturation (Fig. 6.19). The chloride species that exist in this reaction mixture are HOCl, Cl^- and their product Cl_2 as given by eq. 6.4. The exact manner in which these species are involved in the process of conversion of compound I to compound II requires further investigation.

In contrast to the results obtained for the reaction system of HOCl with MPO, which shows that reaction of MPO with HOCl is inhibited by excess Cl^-, and that Cl^- protects the enzyme from bleaching by HOCl (30); our present study of the reaction of HOCl with CPO shows that Cl^- has no affect on compound I formation although, it accelerates compound II formation but does not protect the enzyme from bleaching by HOCl.

We speculate that the difference between the reaction of HOCl with CPO and MPO in the presence of Cl^- may be caused by different Cl^- binding to the enzymes. The fact that Cl^- binds to the native enzyme of MPO at the heme iron which is shown in the absorption spectrum (50-52) but not CPO supports our speculation. Binding of Cl^- to the native enzyme at the heme iron prevents the binding of HOCl and therefore inhibits the reaction with HOCl for MPO.

6.2 SUGGESTIONS FOR FUTURE WORK

Since the peroxidase-catalyzed iodination reactions were reported to be regulated by suitable substrates of electron donors, the study of the peroxidase-catalyzed iodination reaction with a physiological substrate present is an open topic for investigation. The choice of EDTA as such substrate might not explain the regulation mechanism of the iodination reaction that might occur *in vivo*. Therefore, a suitable substrate should be used for further investigation of the regulation mechanism.

As mentioned in the last section of this chapter, the reaction of CPO with HOCl can only be studied under steady state conditions because both CPO-I and CPO-II are short-lived species. As such the conventional stopped flow technique cannot be used to examine the individual steps of the reaction cycle. Some details of the reaction mechanism can be explored by use of a multi-mixing apparatus wherein CPO-I can be reacted rapidly with HOCl. Future work pertaining to study of the reaction of CPO-I with HOCl can therefore be carried out under transient state conditions. The measurement of the second order rate constant of the reaction of CPO-I with HOCl could be carried out by multi-mixing stopped flow measurements at 438 nm, the wavelength at which CPO-II has its maximum absorbance. The effect of Cl^- concentration on the rate of this reaction should also be examined. The results of measurements from the transient state kinetic studies could then be compared with those obtained from previous steady state kinetic studies. The multi-mixing rapid scan spectral study may provide evidence to show that CPO-II does not have an intermediate, namely compound III, when HOCl reduces it back to the native form.

We have investigated the catalatic activity of CPO under steady state conditions by the measurements of O_2 generation and H_2O_2 disappearance (Chapter 4). However, the presence of a large excess of H_2O_2 might lead to formation of compound III. Unlike myeloperoxidase (MPO) little work has been done on CPO compound III. CPO compound III can be generated by the reaction of native CPO with superoxide $O_2^{-\cdot}$ from xanthine/xanthine oxidase (53, 54). A study of CPO compound III with suitable physiological substrates could yield valuable information on CPO-catalyzed reactions. It is interesting to note that ascorbic acid has been reported to react with MPO compound III and accelerate the MPO-catalyzed chlorination reactions. An investigation of the CPO-catalyzed chlorination reactions with ascorbic acid present could also lend insight into the reaction mechanism.

Another area suitable for further investigation is the mechanistic study of catalase reactions. It is apparent that not much work on catalase has been done since the 1970's. However, the details of the catalase reaction still require further investigation as discussed in Chapter 4.

6.3 CONCLUSIONS

One of the requirements for life is the maintenance of molecules in a reduced state even though they are exposed to an oxidizing atmosphere. Another requirement is the generation of energy, commonly accomplished by respiration, in which an essential step is the reduction of oxygen to water:

$$O_2 + 4H^+ + 4e \longrightarrow 2H_2O \qquad (6.1)$$

This reaction can be catalyzed by a single enzyme, cytochrome oxidase. However, the partial reduction of oxygen is also a widely occurring biological process. Among the inorganic compounds of oxygen in oxidation states intermediate between those of oxygen and water are the superoxide anion, $O_2^{-}\cdot$, and hydrogen peroxide, H_2O_2. These highly reactive species are a threat to life, but they can be efficiently removed by the enzymes superoxide dismutase, catalase and peroxidase. The peroxidases not only remove H_2O_2, but utilize its oxidizing ability in a variety of interesting ways.

A sharp increase in oxygen consumption is always found to accompany phagocytosis. O_2 is first reduced to $O_2^{-}\cdot$ which is then converted to H_2O_2 and O_2 (46). H_2O_2 can oxidize Cl^- ion to give HOCl by CPO (44, 45) and MPO (46, 47). HOCl is highly reactive, being able to oxidize many biological molecules and in this way is considered to exert its bactericidal action (55). HOCl in itself is a strong oxidizing agent but it can also be a precursor to some toxic agents. As mentioned in Chapter 1, besides their roles in the synthesis of the thyroid hormones, peroxidase-catalyzed iodination reactions play important roles in the biological defense system as well. However, there was some disagreement regarding the exact mechanism of the peroxidase-catalyzed iodination reactions in terms of the iodinating agent. This puzzle has clearly been resolved as described in Chapter 2. The iodination agent in the plant HRP catalyzed iodination system is either HOI, I_2 or both of them, i.e.: non-enzymatic iodination occurs. In contrast, enzymatic iodination occurs in the mammalian LPO catalyzed iodination system and enzyme-bound hypoiodite (LPO-OI) is the dominant iodinating agent. The conclusion of this study is that a picture of the simplest

evolutionary progression has been shown: from the use of HOI free in solution to the use of enzyme-bound hypoiodite as the iodinating agent.

Reactions catalyzed by peroxidases are general acid-base catalysis. The pH dependence of the reaction of LPO-II with Trolox C (Chapter 3) indicates a mechanism in which the protonated form of the enzyme intermediate and the ionized Trolox C are the reactive species. Protonation of a distal amino acid (pK_a = 2.3) is required for LPO-II to react. Thus the reactivity of LPO-II is decreased with increasing pH. In its reactive form, which exists below pH 2.3, it accepts both a proton and an electron from the reducing substrate Trolox C. Fe^{IV}=O is reduced to Fe^{III}, the proton from the substrate is added to the ferryl oxygen atom as is the proton from the distal acid group, and produce water leaves from the sixth coordination position of Fe^{III}.

The kinetic and mechanistic study of the oxidation of ascorbic acid by LPO-II was studied by Zhang and Dunford (not yet published). The second order rate constant for Trolox C oxidation by LPO-II is three orders of magnitude bigger than that for ascorbic acid. As described in Chapter 1, direct observations of the interaction of α-tocopherol and ascorbic acid have been reported and they have been shown to act synergistically (56). Our kinetic studies have further supported the synergistical interaction of Trolox C, a water soluble vitamin E derivative, and ascorbic acid. Trolox C, an antioxidant, reduces LPO-II to native enzyme. Ascorbic acid, a radical scavenger, then rapidly reduces the Trolox C radical formed from the preceding reaction to the neutral Trolox C species, thus enhancing the antioxidant activity of Trolox C.

Since the discovery of chloroperoxidase in 1961, much interest has been focussed on this enzyme because of its versatile properties. However, its catalatic activity has hampered the investigation of its peroxidatic activity. The interaction of the catalatic and peroxidatic activities was therefore examined (Chapter 4). It was found that the interaction of catalatic activity with peroxidatic activity is attributed to the competition of H_2O_2 and reducing substrate for CPO compound I. Furthermore, the catalatic activity of CPO is demonstrated to have a different mechanism from that of catalase. CPO compound I forms a complex with H_2O_2 and it is the dissociation of this complex that is the rate-determining step in the overall reaction to generate O_2 from H_2O_2. This study may also trigger further investigation of catalase reactions.

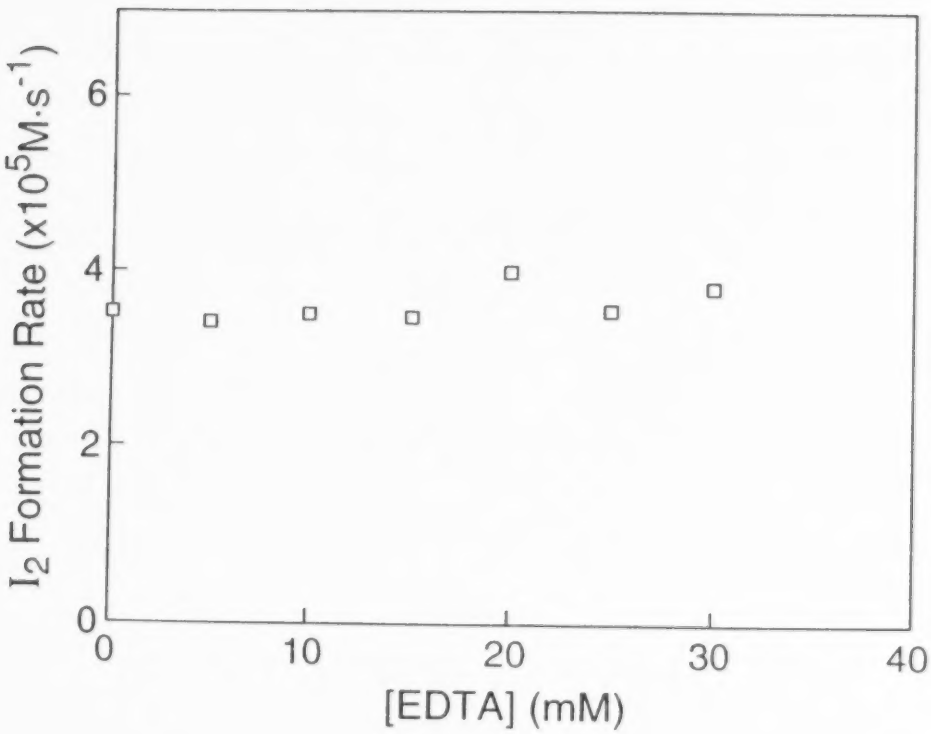

Figure 6.1. The plot of initial formation rates of I_2 monitored at 460 nm *versus* EDTA concentration in HRP systems. One driving syringe contained HRP, KI (and EDTA when necessary) in citrate buffer, pH 4.1, ionic strength 0.18 M; the other contained H_2O_2 in the same buffer, ionic strength 0.18 M. After mixing, final concentrations are: [HRP], 0.63 μM; [H_2O_2], 200 μM; [KI], 100 μM; [EDTA] ranging from 0 to 30 mM; pH 4.1, ionic strength 0.18 M.

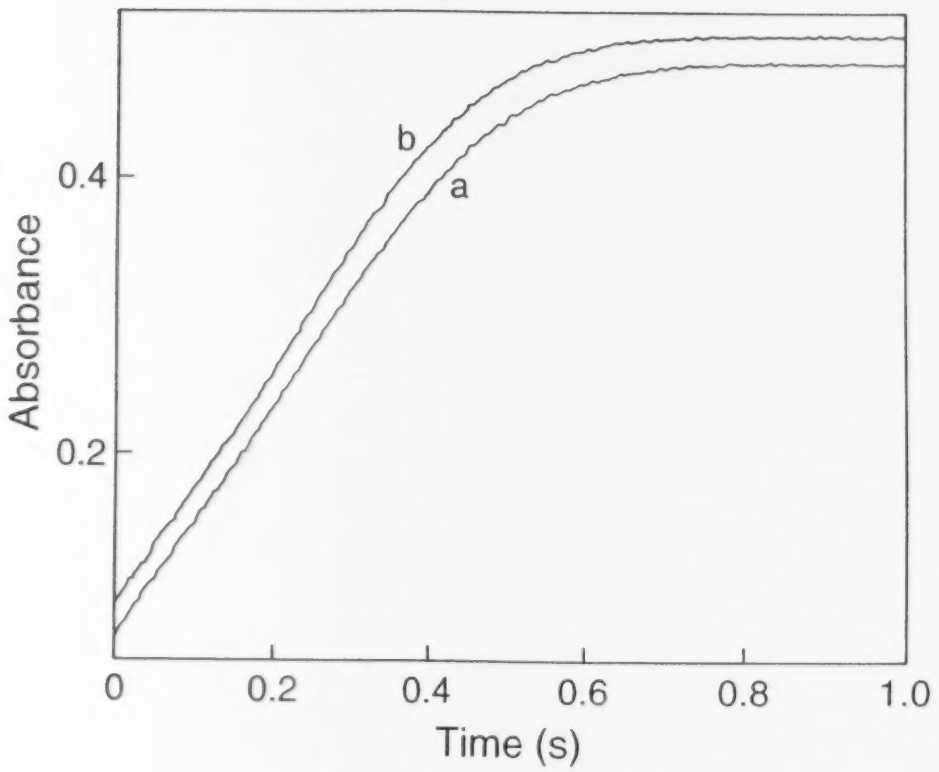

Figure 6.2. Stopped-flow traces at 460 nm over 1.0 s in a reaction mixture of 1.14 μM HRP, 1.0 mM KI and 2.0 mM H_2O_2 without EDTA present (curve a) and with 15 mM EDTA present (curve b) in the system. One driving syringe contained HRP and KI (and EDTA when necessary) in deionized water, ionic strength 0.18 M; the other contained H_2O_2 in citrate buffer, pH 3.67, ionic strength 0.18 M. The final pH is 3.67, ionic strength 0.18 M.

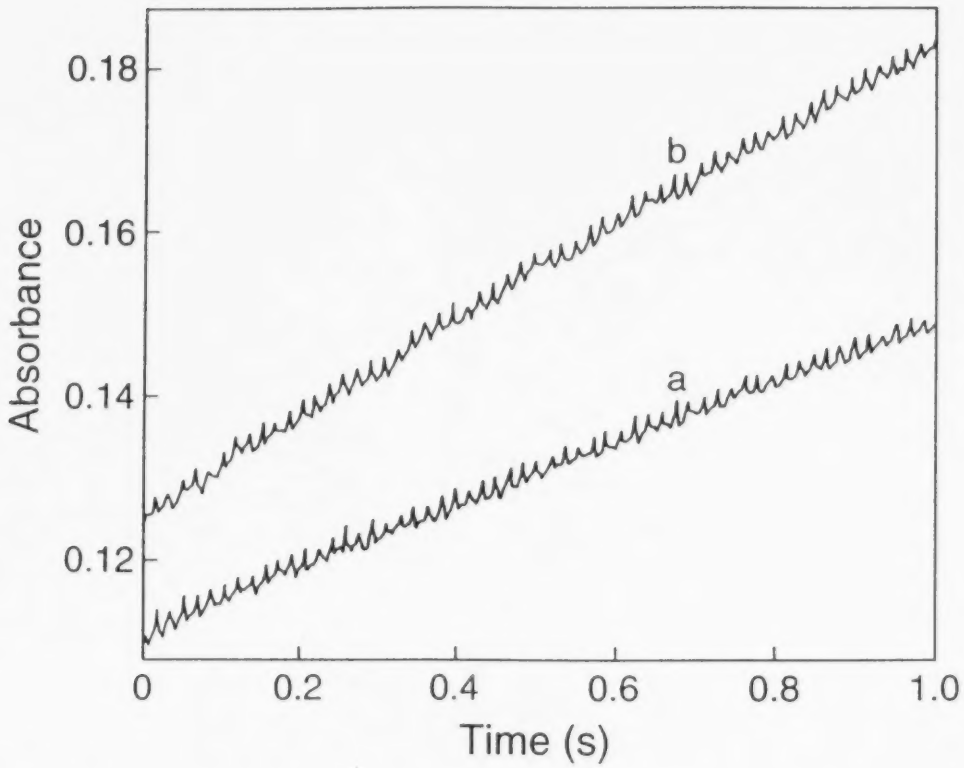

Figure 6.3. Stopped-flow traces at 460 nm over 1.0 s in a reaction mixture of 0.63 μM LPO, 1.0 mM KI and 2.0 mM H_2O_2 without EDTA present (curve a) and with 15 mM EDTA present (curve b) in the system. One driving syringe contained LPO and KI (and EDTA when necessary) in deionized water, ionic strength 0.18 M; the other contained H_2O_2 in citrate buffer, pH 3.67, ionic strength 0.18 M. The final pH is 3.67, ionic strength 0.18 M.

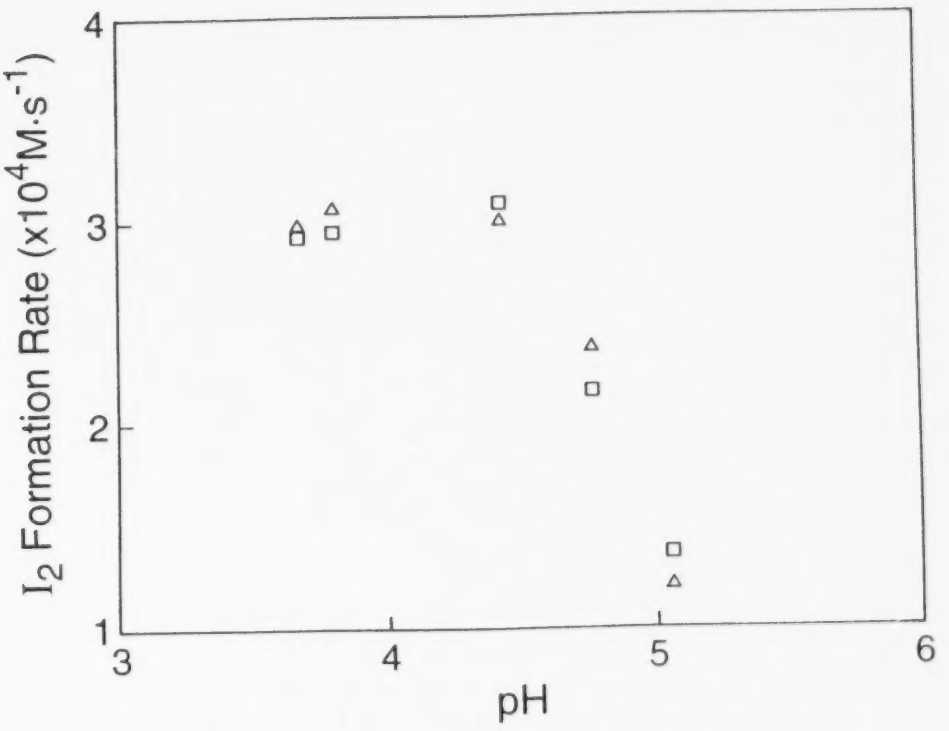

Figure 6.4. Comparison of the initial formation rates of I_2 monitored at 460 nm *versus* the pH values with and without EDTA present. One driving syringe contained H_2O_2 in citrate buffer, pH range from 3.5 to 5.0, ionic strength 0.10 M; the other contained HRP, KI (and EDTA when necessary) in deionized water, ionic strength 0.10 M. After mixing, final concentrations are: [HRP], 0.63 μM; [H_2O_2], 200 μM; [KI], 500 μM and [EDTA], 300 μM. (□) without EDTA present, (△) with EDTA present in the system.

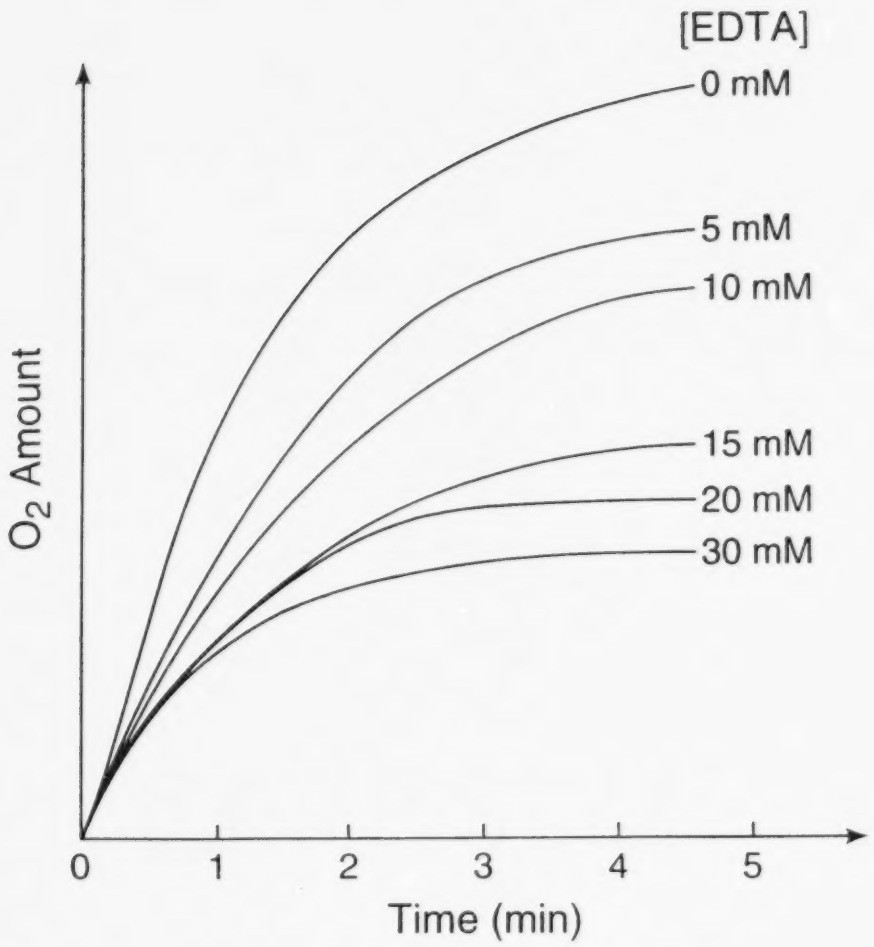

Figure 6.5. Relative O_2 evolution in a reaction mixture of 500 μM KI, 2.00 mM H_2O_2, 0.42 μM HRP with EDTA concentration changed from 0 to 30 mM. Citrate buffer pH 4.1 and total ionic strength 0.18 M.

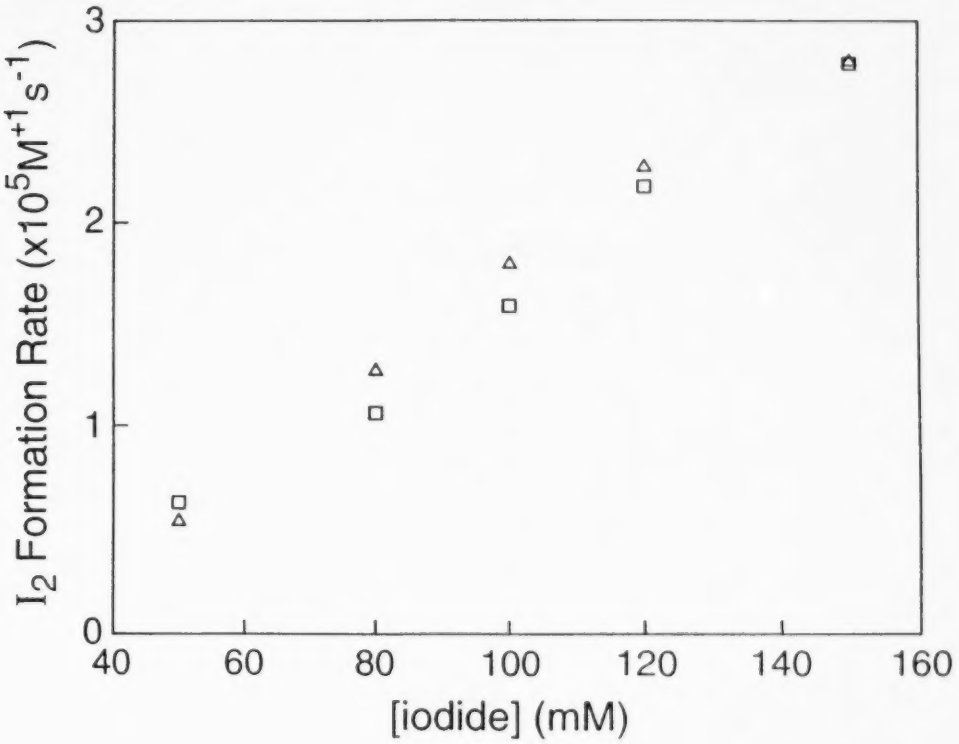

Figure 6.6. Comparison of the initial formation rates of I_2 monitored at 460 nm *versus* the iodide concentration with and without EDTA present in nonenzymatic systems. One driving syringe contained H_2O_2 in citrate buffer, pH 5.2, ionic strength 0.18 M; the other contained KI (and EDTA when necessary) in the same buffer solution, total ionic strength 0.18 M. After mixing, final concentrations are: [H_2O_2], 10 mM; [EDTA], 10 mM; [KI] ranging from 50 mM to 150 mM; pH 5.2, ionic strength 0.18 M. (□) without EDTA present, (Δ) with EDTA present in the system.

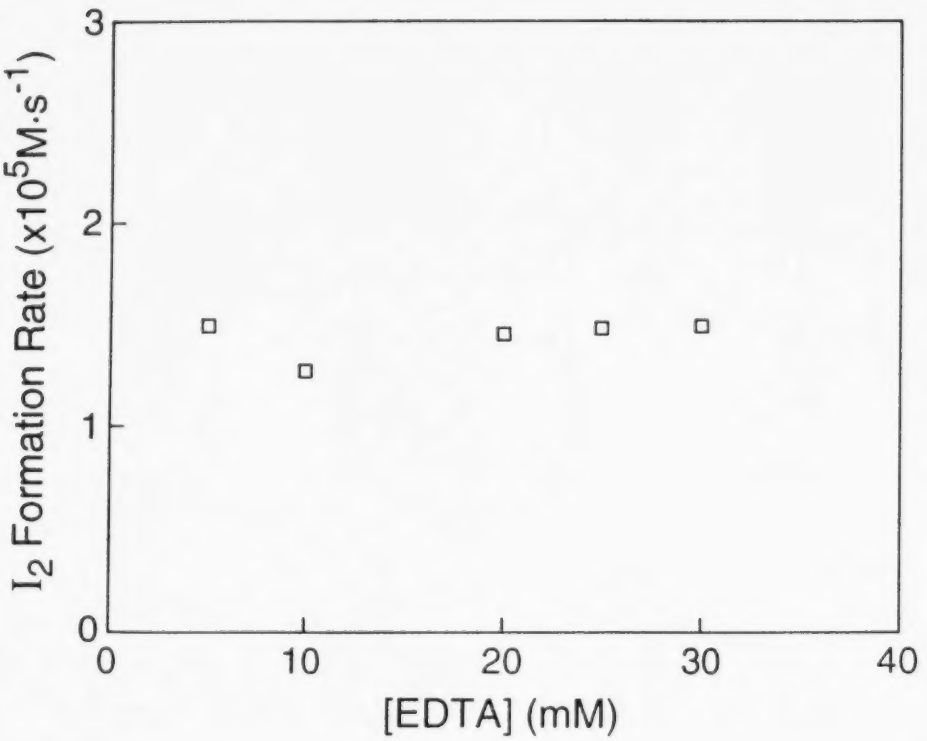

Figure 6.7. The plot of initial formation rates of I_2 monitored at 460 nm *versus* EDTA concentration in nonenzymatic system. One driving syringe contained H_2O_2 in citrate buffer, pH 5.2, ionic strength 0.18 M; the other contained KI and EDTA in the same buffer solution, ionic strength 0.18 M. After mixing, final concentrations are: [H_2O_2], 10 mM; [KI], 80 mM; [EDTA] ranging from 5 mM to 30 mM; pH 5.2, ionic strength 0.18 M.

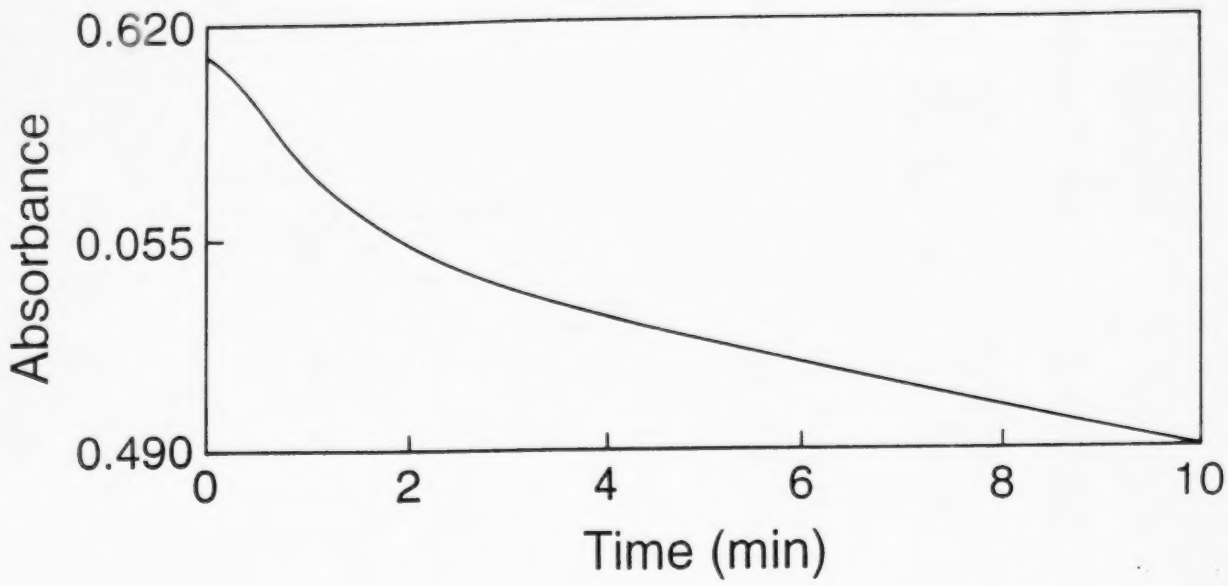

Figure 6.8. I_3^- disappearance monitored at 353 nm over 10 min in a reaction mixture of 30 mM EDTA and 27 μM I_3^- in citrate buffer, pH 4.1, ionic strength 0.18 M.

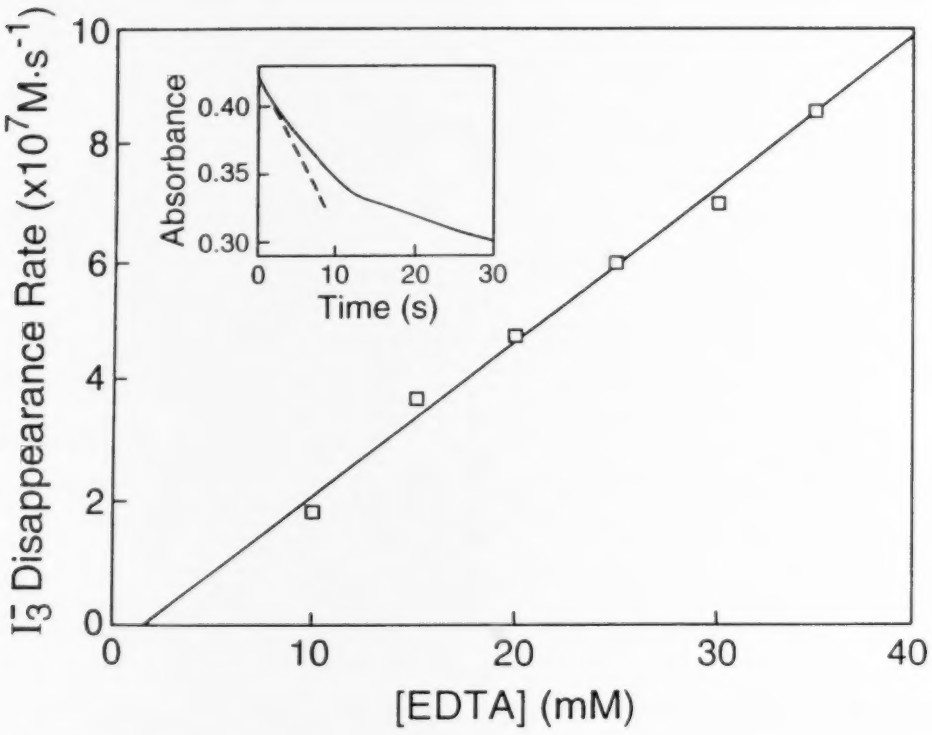

Figure 6.9. The plot of initial disappearance rates of I_3^- *versus* EDTA concentration. The initial disappearance rates of I_3^- were obtained as shown in the inset. One driving syringe contained I_3^- in citrate buffer, pH 3.5, ionic strength 0.18 M; the other contained EDTA in citrate buffer, pH 3.5, ionic strength 0.18 M. After mixing, final concentrations are: [I_3^-], 25.6 μM; [EDTA] ranging from 5 mM to 30 mM. The inset shows an example of a trace (15 mM EDTA) monitored at 353 nm from which the initial disappearance rate of I_3^- was obtained.

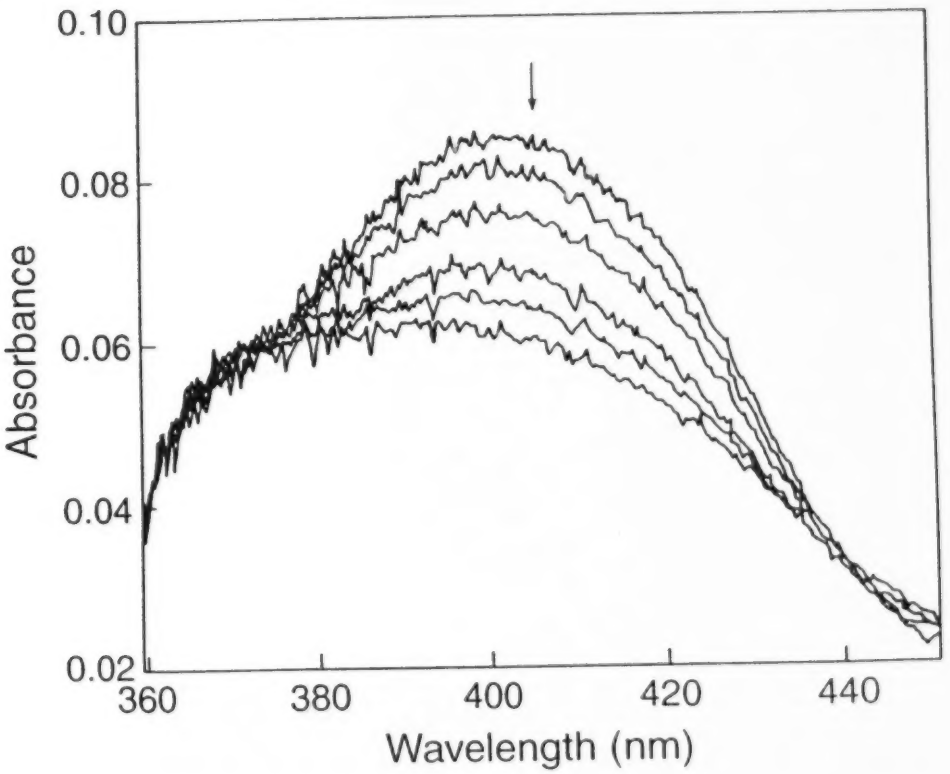

Fig. 6.10. Rapid scan spectra over 91 ms for the reaction of 1.0 μM CPO with 6.0 μM HOCl at pH 6.2, total ionic strength 0.11 M. One drive syringe contained CPO in phosphate buffer, pH 6.2, ionic strength 0.11 M; the other contained HOCl in the same phosphate buffer, ionic strength 0.11 M. The spectra were taken 13, 19, 31, 49, 67 and 91 ms after mixing. The partial conversion of native enzyme to compound I is clearly shown. The arrow indicates the direction of absorbance change with increasing time.

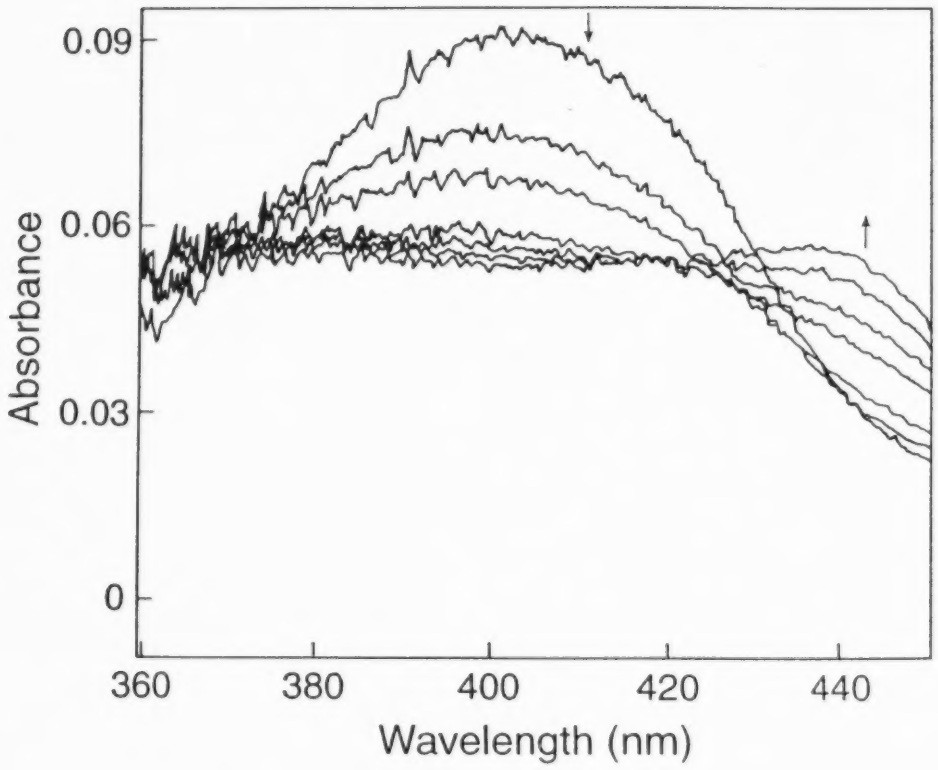

Fig. 6.11. Rapid scan spectra over 830 ms for the reaction of 1.0 μM CPO with 6.0 μM HOCl at pH 6.2, ionic strength 0.11 M. The experimental conditions are the same as given in the legend to Fig. 6.10. The spectra were taken 60, 115, 170, 335, 445, 610 and 830 ms after mixing. The results indicate that compound I is converted to form compound II. The arrows indicate the direction of absorbance change with increasing time.

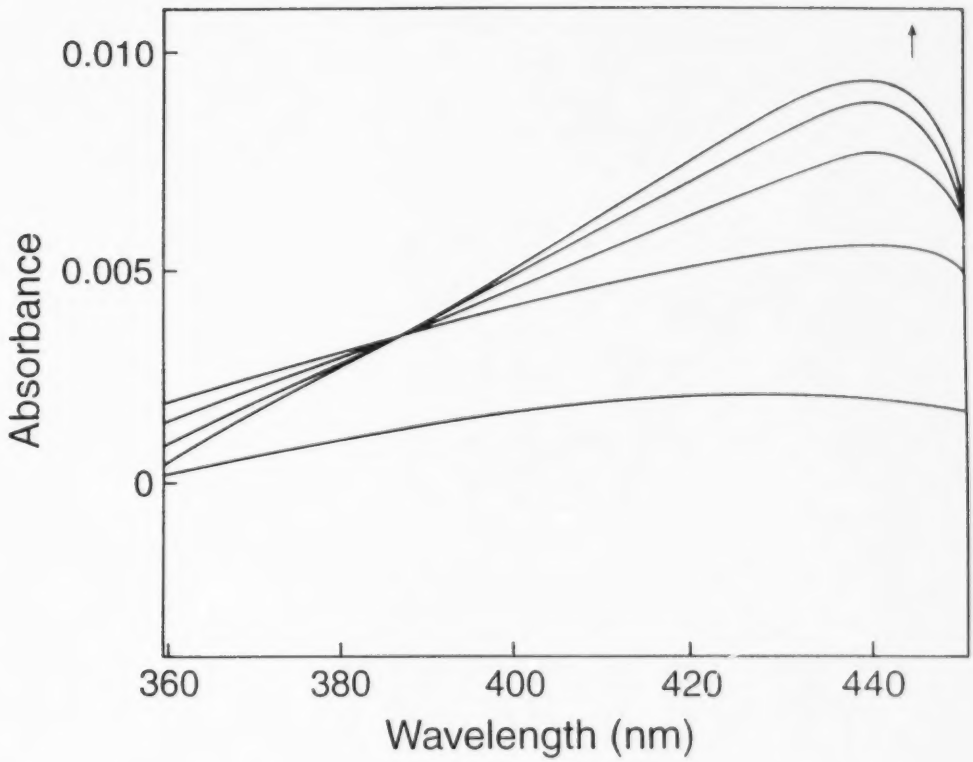

Fig. 6.12. Rapid scan spectra over 9.1 s for the reaction of 0.16 μM CPO with 47.4 μM HOCl at pH 6.2, ionic strength 0.11 M. The maximum absorbances occur at 438 nm. The arrow indicates the direction of absorbance change with increasing time.

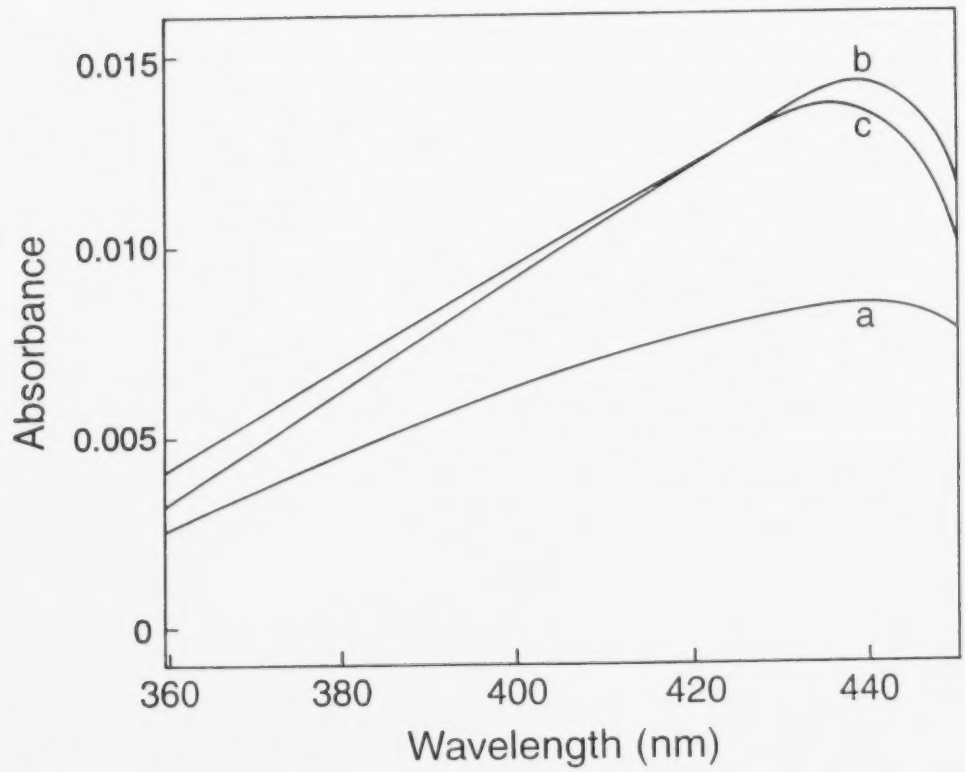

Fig. 6.13. Rapid scan spectra over 16.6 s for the reaction of 0.16 μM CPO with 47.4 μM HOCl at pH 6.2, ionic strength 0.11 M. The spectra were taken 1.2 s (a), 5.6 s (b) and 16.6 s (c) after mixing. The results indicate that compound II is formed and then converted to native enzyme slowly.

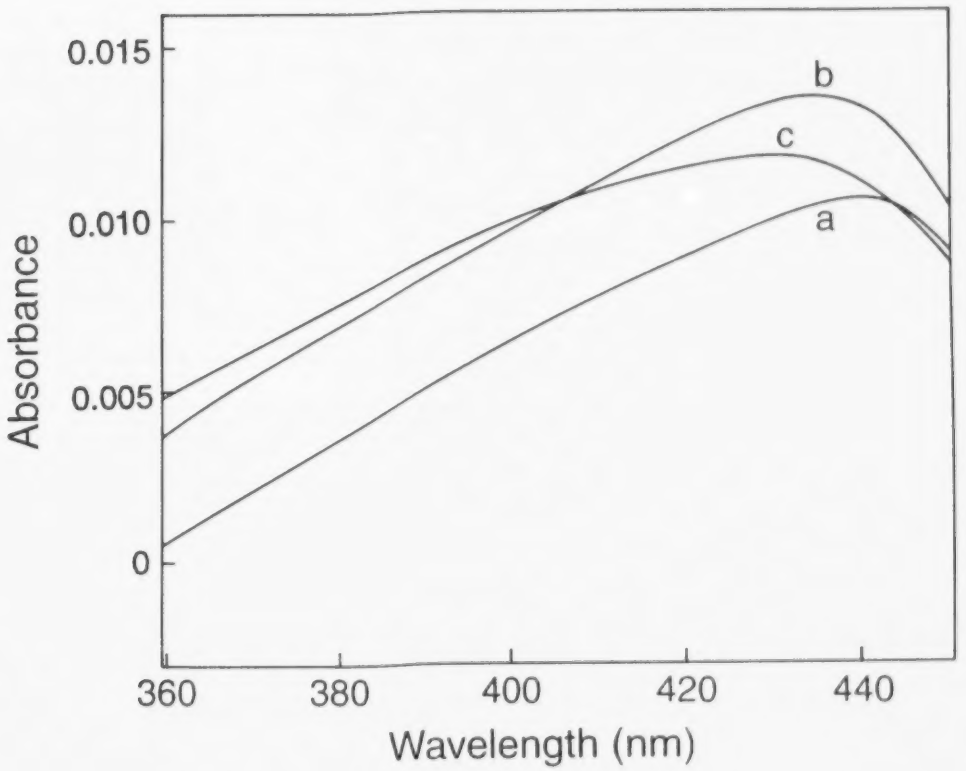

Fig. 6.14. Rapid scan spectra over 16.6 s for the reaction mixture of 0.16 μM CPO and 47.4 μM HOCl in the presence of 50 mM KCl. The spectra were taken 1.2 s (a), 2.3 s (b) and 16.6 s (c) after mixing. The results indicate that compound II is still formed and then converted to native enzyme.

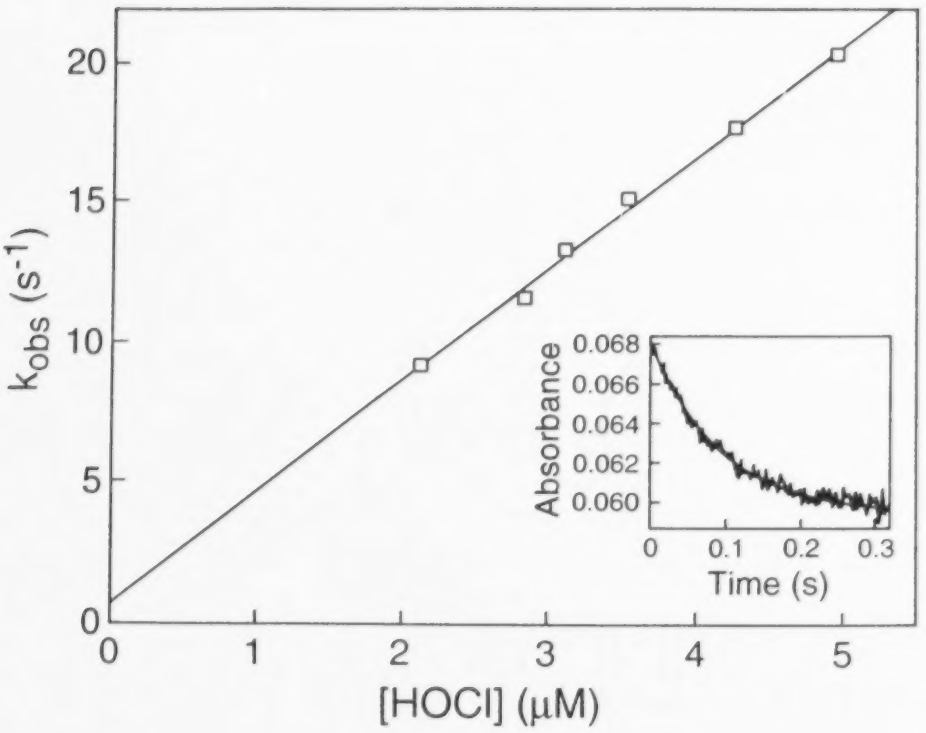

Fig. 6.15. Plot of k_{obs} *versus* HOCl concentration for the reaction of HOCl with native enzyme. The reactions were carried out in buffer solutions of pH 6.2, ionic strength 0.11 M. The inset shows an example of a first order exponential trace (2.83 μM HOCl) followed by a nonlinear least-square analysis from which k_{obs} was obtained.

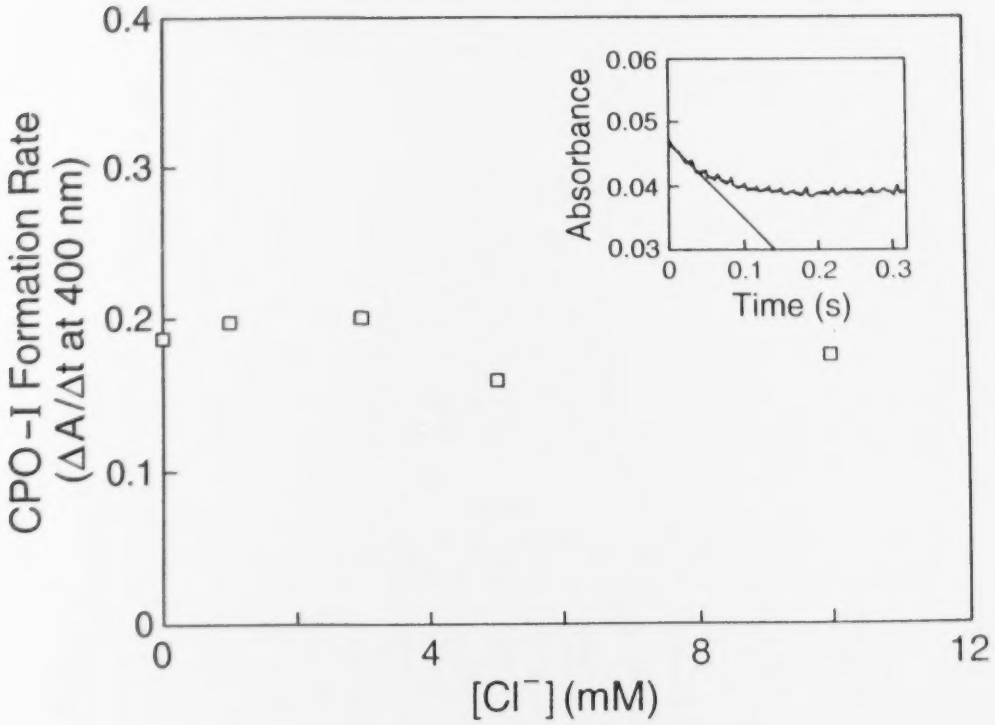

Fig. 6.16. Plot of the initial formation rate of compound I (ΔA / Δt at 400 nm) *versus* Cl^- concentration in a reaction mixture of 0.16 μM CPO, 2.83 μM HOCl and varied KCl concentration at pH 6.2, ionic strength 0.11 M. The inset shows an example of a first order exponential trace. The initial formation rate of compound I can be obtained from the linear part.

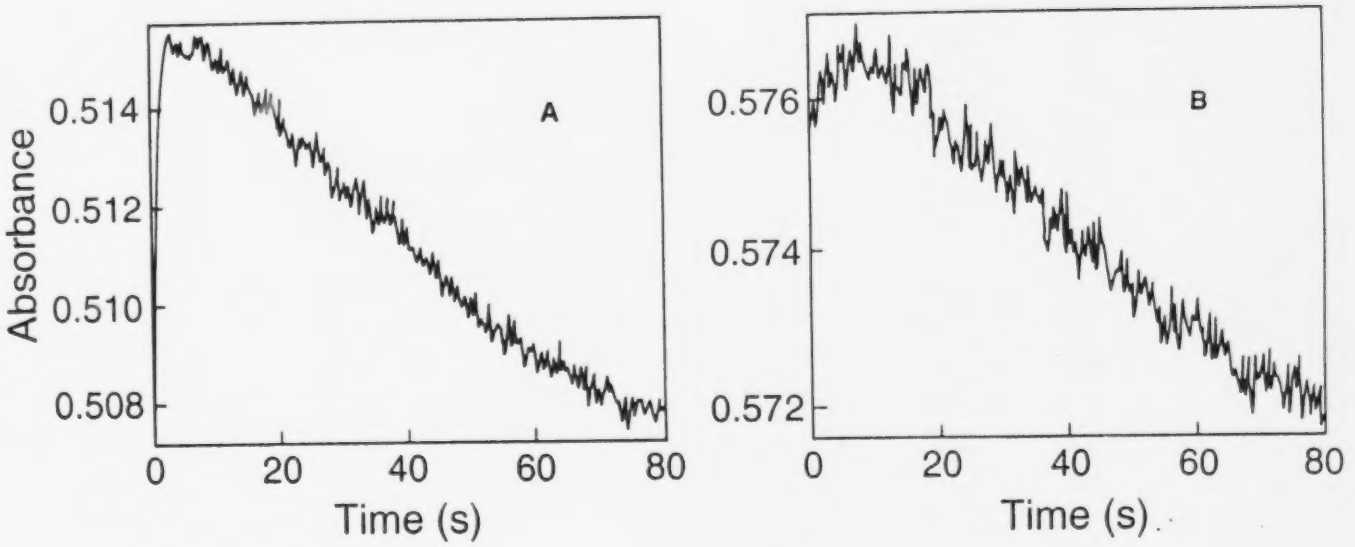

Fig. 6.17. Stopped-flow trace at 438 nm (A) and 400 nm (B) over 80 s in a reaction mixture of 0.16 μM CPO and 47.4 μM HOCl at pH 6.2, ionic strength 0.11 M.

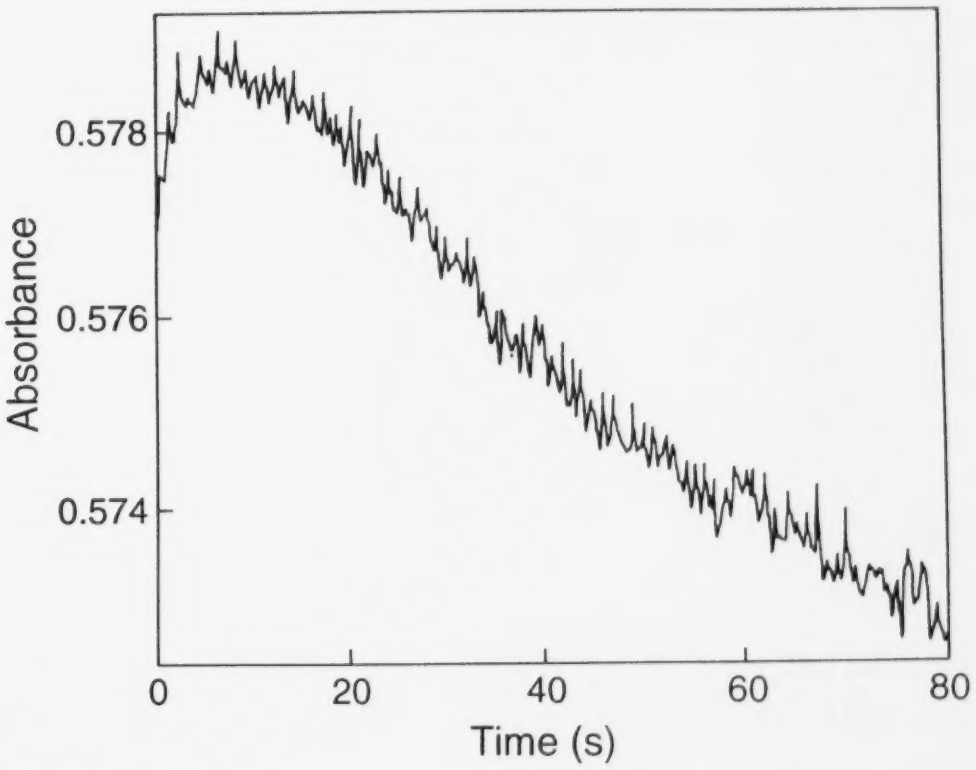

Fig. 6.18. Stopped-flow trace at 400 nm over 80 s in a reaction mixture of 0.16 μM CPO and 47.4 μM HOCl with 50 mM KCl present at pH 6.2, ionic strength 0.11 M.

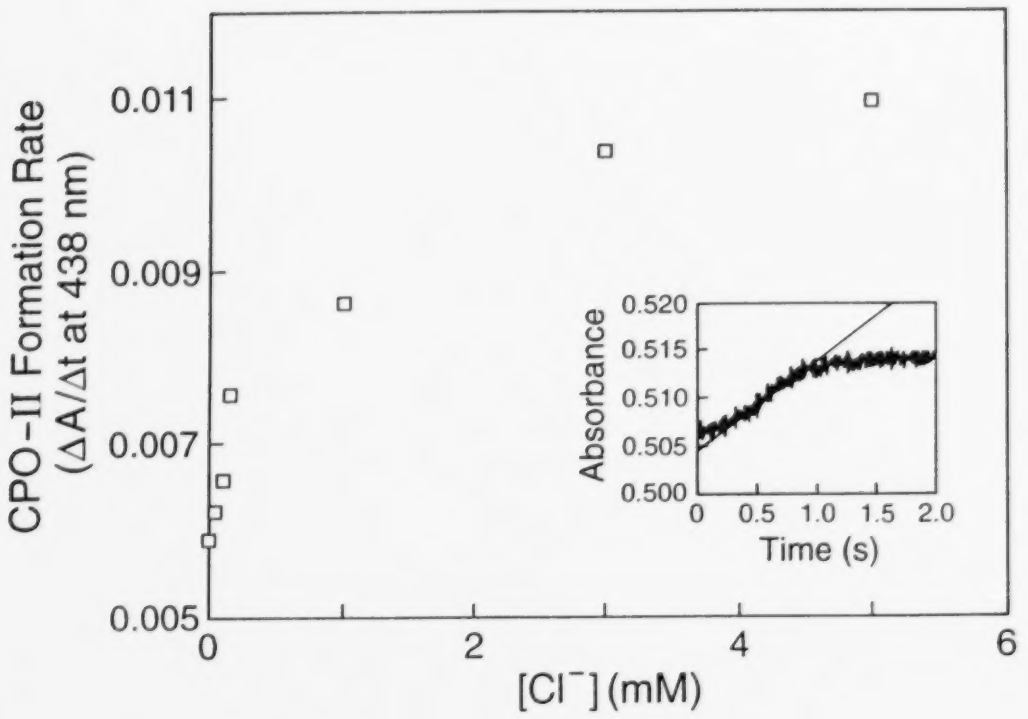

Fig. 6.19. Plot of the initial formation rate of compound II (ΔA / Δt at 438 nm) *versus* Cl^- concentration in a reaction mixture of 0.16 μM CPO, 47.4 μM HOCl and varied KCl concentration at pH 6.2, ionic strength 0.11 M. The inset shows an example of the stopped-flow trace from which the initial formation rate of compound II can be obtained.

6.4 REFERENCES

1. Banerjee, R. K., De, S. K., Bose, A. K., and Datta, A. G. (1986) *J. Biol. Chem.* **261**, 10592-10597.
2. Banerjee, R. K. (1989) *J. Biol. Chem.* **264**, 9188-9194.
3. Shah, M. M., and Aust, S. D. (1993) *Arch. Biochem. Biophys.* **300**. 253-257.
4. Sun, W., and Dunford, H. B. (1993) *Biochemistry* **32**, 1324-1331.
5. Thomas, J. A., Morris, D. R., and Hager, L. P. (1970) *J. Biol. Chem.* **245**, 3129-3134.
6. Libby, R. D., Thomas, J. A., Kaiser, L. W., and Hager, L. P. (1982) *J. Biol. Chem.* **257**, 5030-5037.
7. Lambeir, A. -M., and Dunford, H. B. (1983) *J. Biol. Chem.* **258**, 13558-13563.
8. Dunford, H. B., Lambeir, A. -M., Kashem, M. A., and Pickard, M. (1987) *Arch. Biochem. Biophys.* **252**, 292-302.
9. Geigert, J., Neidleman, S. L., and Dalietos, D. J. (1983) *J. Biol. Chem.* **258**, 2273-2277.
10. Ramakrishnan, K., Oppenhuizen, M. E., Saunders, S., and Fisher, J. (1983) *Biochemistry* **22**, 3272-3277.
11. Griffin, B. W. (1983) *Biochem. Biophys. Res. Commun.* **116**, 873-879.
12. Sono, M., Dawson, J. H., Hall, K., and Hager, L. P. (1986) *Biochemistry* **25**, 347-356.
13. Brown, F. W., and Hager, L. P. (1967) *J. Am. Chem. Soc.* **89,** 719-720.
14. Libby, R. D., Shedd, A. L., Phipps, A. K., Beachy, T. M., and Gerstberger, S. M. (1992) *J. Biol. Chem.* **267**, 1769-1775.
15. Leah, A. M., and Dunford, H. B. (1994) *J. Biol. Chem.* **269**, 7950-7956.

16. Floris, R., and Wever, R. (1992) *Eur. J. Biochem.* **207**, 697-702.

17. Bell, C. F. (1977) *in* Principles and application of metal chelations. Oxford University Press (Clarendon), London and New York.

18. Haschke, R. H., and Friedhoff, J. M. (1978) *Biochem. Biophys. Res. Commun.* **80**, 1039-1042.

19. Ogawa, S., Shiroto, Y., and Morishima, I. (1979) *Biochem. Biophys. Res.Commun.* **90**, 674-678.

20. Morishima, I., Ogawa, S., Inubushi, T., Jonezawa, T., and Izuka, T. (1977)*Biochemistry* **16**, 5109-5115.

21. Booth, K. S., Shioko, K., Lee, H. C., Ikeda-Saito, M., and Chaughey, W. S. (1989)*Biochem. Biophys. Res. Commun.* **160**, 897-902.

22. Fife, D. J., and Moore, W. M. (1989) *Photochem. Photobiol.* **29**, 43-47.

23. Heelis, P. F. (1982) *Chem. Soc. Rev.* **11**, 15-39.

24. Keilin, D., and Hartree, E. F. (1961) *Biochem. J.* **49**, 88-104.

25. Banerjee, R. K. (1989) *Biochim. Biophys. Acta* **992**, 392-396.

26. Bhattacharyya, D. K., Adak, S., Bandyopahdyay, U., and Banerjee, R. K. (1994)*Biochem. J.* **298**, 281-288.

27. Shah, M. M., and Aust, S. D. (1993) *J. Biol. Chem.* **268**, 8503-8506.

28. Modi, S. (1993) *Biochim. Biophys. Acta* **1162**, 121-126.

29. Bhattachayya, D. K., Bandyopahdyay, U., Chatterjee, R., and Benerjee, R. K. (1993) *Biochem. J.* **289**, 575-580.

30. Sakurada, J., Takahashi, S., and Hosoya, T. (1987) *J. Biol. Chem.* **262**, 4007- 4010.

31. Ohlsson, P.-I., and Paul, K. -G. (1976) *Acta Chem. Scands.* **B30**, 373-375.

32. Paul, K. -G., and Ohlsson, P. -J. (1985) *In* The lactoperoxidase system, Edited by Pruitt, K. M., and Tenovuo, Y. O., 27, pp. 15-30, Dekker, New York.

33. Cotton, M. L., and Dunford, H. B. (1973) *Can. J. Chem.* **51**, 582-587.

34. Awtrey, A. D., and Connick, R. E. (1951) *J. Am. Chem. Soc.* **73**, 1842-1843.

35. Leibhafsky, H. A. (1932) *J. Am. Chem. Soc.* **52**, 3499-3508.

36. Eigen, M., and Kustin, K. (1962) *J. Am. Chem. Soc.* **84**, 1355-1361.

37. Beers Jr., R. F., and Sizer, I. W. (1952) *J. Biol. Chem.* **195**, 133-140.

38. Carmichael, R. D., Jones, A., and Pickard, M. A. (1986) *Appl. Environmental Microbiol.* **51**, 276-280.

39. Hollenberg, P. F., Hager, L. P., Blumberg, W. E., and Peisach, J. (1980) *J. Biol.Chem.* **255**, 4801-4807.

40. Brauer, G. (1960) *In* Handbook of Preparative Inorganic Chemistry, 2nd ed., **Vol. 1**, pp. 272, Academic Press, New York.

41. Zgliczynski, J. M., Stelmaszynska, T., Domanski, J., and Ostrowski, W. (1971)*Biochim. Biophys. Acta* **235**, 419-424.

42. Palcic, M. M., Rutter, R., Araiso, T., Hager, L. P., and Dunford, H. B. (1980)*Biochem. Biophys. Res. Commun.* **94**, 1123-1127.

43. Nakajima, R., Yamazaki, I., and Griffin, B. W. (1985) *Biochem. Biophys. Res.Commun.* **128**, 1-6.

44. Morris, D. R., and Hager, L. P. (1966) *J. Biol. Chem.* **241**, 1763-1768.

45. Hager, L. P., Morris, D. R., Brown, F. S., and Eberwein, H. (1966) *J. Biol. Chem.* **241**, 1769-1777.

46. Klebanoff, S. J., and Clark, R. A. (1978) *in* The neutrophil: function and clinical disorders, pp. 409-488., Elsevier/North-Holland, Amsterdam.

47. Klebanoff, S. J. (1968) *J. Bacteriol.* **95**, 2131-2138.

48. Sun, W., Kadima, T., Pickard, M., and Dunford, H. B. (1994) Submitted to *Biochem. Cell Biol.*

49. Connick, R. E., and Chia, Y. -T. (1959) *J. Am. Chem. Soc.* **81**, 1280-1284.

50. Ikeda-Saito, M. (1987) *Biochemistry* **26**, 4344-4349.

51. Stelmaszynska, T., and Zgliczynski, J. M. (1974) *Eur. J. Biochem.* **45**, 305-312.

52. Ikeda-Saito, M. (1985) *J. Biol. Chem.* **260**, 11688-11696.

53. Kettle, A. J., and Winterbourn, C. C. (1988) *Biochem. J.* **252**, 529-536.

54. Metodiewa, D., and Dunford, H. B. (1989) *Arch. Biochem. Biophys.* **272**, 245-253.

55. Halliwell, B., and Gutteridge, J. M. C. (1985) *in* Free radicals in biology and medicine, pp 258-259, Clarendon Press, London.

56. Packer, J. E., Slater, T. F., and Willson, R. L. (1979) *Nature (London)*, **278**, 738.

APPENDIX I

Transient-State Equation for Compound I Formation

$$CPO + H_2O_2 \underset{k_{-4}}{\overset{k_4}{\rightleftharpoons}} CPO\text{-}I + H_2O \quad (4.4)$$

The substrate is in large excess,

$$[H_2O_2] >> [CPO]_0 \quad (4.23)$$

Therefore k_4 can be replaced by a pseudo-first-order constant k_4'

$$k_4' = k_4[H_2O_2] \quad (4.24)$$

$$-d[CPO]/dt = k_4'[CPO] - k_{-4}[CPO\text{-}I] \quad (4.25)$$

Conservation relation

$$[CPO]_0 = [CPO] + [CPO\text{-}I] \quad (4.26)$$

Therefore

$$-d[CPO]/dt = (k_4' + k_{-4})\{[CPO] - k_{-4}[CPO]_0 / (k_4' + k_{-4})\} \quad (4.27)$$

At equilibrium $k_4'[CPO]_{eq} = k_{-4}[CPO\text{-}I]_{eq}$

$$[CPO\text{-}I]_{eq} = [CPO]_0 - [CPO]_{eq}$$

Therefore

$$[CPO]_{eq} = k_{-4}[CPO]_0 / (k_4' + k_{-4}) \quad (4.28)$$

Eq. 4.27 becomes eq. 4.29:

$$-d[CPO]/dt = (k_4' + k_{-4})([CPO] - [CPO]_{eq}) \quad (4.29)$$

$$-d[CPO]/([CPO] - [CPO]_{eq}) = (k_4' + k_{-4})\,dt$$

$$\ln[([CPO]_0 - [CPO]_{eq})/([CPO] - [CPO]_{eq})] = (k_4' + k_{-4})t \quad (4.30)$$

$$k_{obs} = k_4' + k_{-4} \quad (4.31)$$

Combining eqs. 4.24 and 4.31

$$k_{obs} = k_4[H_2O_2] + k_{-4} \quad (4.6)$$

APPENDIX II

Steady-State Equations Which Fit a Rectangular Hyperbola

Mechanism:

$$CPO + H_2O_2 \xrightarrow{k_4} CPO\text{-}I + H_2O \qquad (4.4)$$

$$CPO\text{-}I + H_2O_2 \underset{k_{-5}}{\overset{k_5}{\rightleftharpoons}} CPO\text{-}I\text{-}H_2O_2 \qquad (4.10)$$

$$CPO\text{-}I\text{-}H_2O_2 \xrightarrow{k_6} CPO + O_2 + H_2O \qquad (4.11)$$

Stoichiometry: $2H_2O_2 = O_2 + 2H_2O$ (4.32)

Rate: $v_{(O_2)} = d[O_2] / dt = k_6[CPO\text{-}I\text{-}H_2O_2]$ (4.33)

Steady State:

$$d[CPO\text{-}I] / dt = k_4[CPO][H_2O_2]$$

$$-k_5[CPO\text{-}I][H_2O_2] + k_{-5}[CPO\text{-}I\text{-}H_2O_2] = 0 \qquad (4.34)$$

$$d[CPO\text{-}I\text{-}H_2O_2] / dt = k_5[CPO\text{-}I][H_2O_2] - k_{-5}[CPO\text{-}I\text{-}H_2O_2] - k_6[CPO\text{-}I\text{-}H_2O_2] = 0 \qquad (4.35)$$

$$-\frac{d[CPO]}{dt} = k_4[CPO][H_2O_2] - k_6[CPO\text{-}I\text{-}H_2O_2] = 0 \qquad (4.36)$$

Conservation relation:

$$[CPO]_0 = [CPO] + [CPO\text{-}I] + [CPO\text{-}I\text{-}H_2O_2] \qquad (4.37)$$

Combination of eqs. 4.34-4.37 yields:

$$[\text{CPO-I-H}_2\text{O}_2] = \frac{k_4k_5[H_2O_2]^2[\text{CPO}]_0}{(k_5k_6 + k_4k_{-5} + k_4k_6)[H_2O_2] + k_4k_5[H_2O_2]^2} \quad (4.38)$$

Substitution of eq.4.38 into 4.33 gives the expression for v:

$$v = d[O_2] / dt = k_6[\text{CPO-I-H}_2\text{O}_2]$$

$$= \frac{k_4k_5k_6[H_2O_2]^2[\text{CPO}]_0}{(k_5k_6 + k_4k_{-5} + k_4k_6)[H_2O_2] + k_4k_5[H_2O_2]^2} \quad (4.12)$$

Eq. 4.12 can be put into the form by assuming k_{-5} is much smaller than k_6

$$\frac{v_{(O2)}}{[\text{CPO}]_0} = \frac{k_6[H_2O_2]}{(k_4 + k_5)k_6 / k_4k_5 + [H_2O_2]} \quad (4.13)$$

The experimental result is $$\frac{v}{[\text{CPO}]_0} = \frac{B_1[H_2O_2]}{B_2 + [H_2O_2]} \quad (4.9)$$

By comparison of eqs. 4.9 and 4.13: $B_1 = k_6$ (4.14)

$$B_2 = \frac{k_4k_6 + k_5k_6 + k_4k_{-5}}{k_4k_5} \quad (4.39)$$

The flux of enzyme which passed through the intermediate CPO-I-H_2O_2 can be quantitated assuming $k_{-5} = 0$, so that B_2 becomes

$$B_2 = \frac{(k_4 + k_5)k_6}{k_4k_5} \quad (4.15)$$

Since k_4 was determined independently and k_6 is obtained from eq. 4.14, k_5 is readily calculated.

APPENDIX III

Fraction of Enzyme in the Complex CPO-I-H_2O_2

Eq. 4.38 becomes

$$\frac{[\text{CPO-I-H}_2\text{O}_2]}{[\text{CPO}]_0} = \frac{[\text{H}_2\text{O}_2]}{\frac{(k_4k_6 + k_5k_6 + k_4k_{-5})}{k_4k_5} + [\text{H}_2\text{O}_2]} \tag{4.40}$$

and with substitution of eq. 4.39 it becomes

$$\frac{[\text{CPO-I-H}_2\text{O}_2]}{[\text{CPO}]_0} = \frac{[\text{H}_2\text{O}_2]}{B_2 + [\text{H}_2\text{O}_2]} \tag{4.16}$$

Therefore the percent of enzyme existing as the complex CPO-I-H_2O_2 can be calculated for any value of $[H_2O_2]$.

APPENDIX IV

Reversibility of Formation of CPO-I-H_2O_2

In the catalatic cycle there is a net flux of enzyme which passes through the step

$$CPO\text{-}I + H_2O_2 \underset{k_{-5}}{\overset{k_5}{\rightleftharpoons}} CPO\text{-}I\text{-}H_2O_2 \qquad (4.10)$$

The rate constant k_{-5} appears in the parameter B_2 determined experimentally from the rectangular hyperbolae

$$B_2 = \frac{k_4k_6 + k_5k_6 + k_4k_{-5}}{k_4k_5} \qquad (4.39)$$

$$B_2 = \frac{k_6}{k_4} + \frac{k_6}{k_5} + \frac{k_{-5}}{k_5} \qquad (4.41)$$

The dissociation constant of the CPO-I-H_2O_2 complex to CPO-I and H_2O_2 is given by

$$K_{Diss} = \frac{k_{-5}}{k_5} \qquad (4.42)$$

Therefore

$$B_2 = \frac{k_6}{k_4} + \frac{k_6}{k_5} + K_{Diss} \qquad (4.43)$$

Since k_4 is determined from independent transient state experiments and $k_6 = B_1$, there are two unknown constants in the single eq. 4.43. There are two possibilities. One is

$$k_{-5} = 0$$

which is the assumption made in the text. The other is to assume k_5 occurs at the diffusion-controlled limit

$$k_5 = 10^9\ M^{-1}s^{-1}$$

Substituting known values into eq. 4.43:

$$3.3 \times 10^{-3} = \frac{9.3 \times 10^2}{2.3 \times 10^6} + \frac{9.3 \times 10^2}{10^9} + K_{Diss}$$

$$\therefore \qquad K_{Diss} = 2.9 \times 10^{-3}\ M$$

and from eq. 4.42

$$k_{-5} = 2.9 \times 10^{-3} \times 10^9 = 2.9 \times 10^6\ s^{-1}$$

It is impossible to ascertain which of the two extreme assumptions is more correct. The simplest assumption is that $k_{-5} = 0$.

APPENDIX V

Combined Mechanism For Reactions Catalyzed by CPO

Mechanism:

$$CPO + H_2O_2 \xrightarrow{k_4} CPO\text{-}I + H_2O \quad (4.4)$$

$$CPO\text{-}I + H_2O_2 \xrightarrow{k_5} CPO\text{-}I\text{-}H_2O_2 \quad (4.10)$$

$$CPO\text{-}I\text{-}H_2O_2 \xrightarrow{k_6} CPO + O_2 + H_2O \quad (4.11)$$

$$CPO\text{-}I + TMPD \xrightarrow{k_7} CPO\text{-}II + TMPD^{\cdot} \quad (4.17)$$

$$CPO\text{-}II + TMPD \xrightarrow{k_8} CPO + TMPD^{\cdot} + H_2O \quad (4.18)$$

Steady State:

$$d[CPO\text{-}I]/dt = k_4[CPO][H_2O_2] - k_5[CPO\text{-}I][H_2O_2] - k_7[CPO\text{-}I][TMPD] = 0$$

$$[CPO] = \frac{k_5[H_2O_2] + k_7[TMPD]}{k_4[H_2O_2]}[CPO\text{-}I] \quad (4.44)$$

$$d[CPO\text{-}I\text{-}H_2O_2]/dt = k_5[CPO\text{-}I][H_2O_2] - k_6[CPO\text{-}I\text{-}H_2O_2] = 0$$

$$[CPO\text{-}I\text{-}H_2O_2] = \frac{k_5[CPO\text{-}I][H_2O_2]}{k_6} \quad (4.45)$$

$$d[CPO\text{-}II]/dt = k_7[CPO\text{-}I][TMPD] - k_8[CPO\text{-}II][TMPD] = 0$$

$$[CPO\text{-}II] = k_7[CPO\text{-}I]/k_8 \quad (4.46)$$

Conservation relation:

$$[CPO]_0 = [CPO] + [CPO\text{-}I] + [CPO\text{-}II] + [CPO\text{-}I\text{-}H_2O_2] \quad (4.47)$$

Combination of eqs. 4.44-4.47 yields:

$$[CPO\text{-}I] = \frac{k_4k_6k_8[H_2O_2][CPO]_0}{(k_5k_6k_8 + k_4k_6k_8 + k_4k_6k_7)[H_2O_2] + k_4k_5k_8[H_2O_2]^2 + k_6k_7k_8[TMPD]} \quad (4.48)$$

$$[\text{CPO-II}] = \frac{k_4k_6k_7[H_2O_2][\text{CPO}]_0}{(k_5k_6k_8 + k_4k_6k_8 + k_4k_6k_7)[H_2O_2] + k_4k_5k_8[H_2O_2]^2 + k_6k_7k_8[\text{TMPD}]} \quad (4.49)$$

Peroxidatic Activity:

From Eqs. 4.17 and 4.18

$$v_{(\text{TMPD})} = -d[\text{TMPD}]/dt = k_7[\text{CPO-I}][\text{TMPD}] + k_8[\text{CPO-II}][\text{TMPD}]$$

$$v_{(\text{TMPD})} = \frac{2[\text{CPO}]_0}{\frac{1}{k_4}\frac{1}{[H_2O_2]} + \left(\frac{1}{k_7} + \frac{1}{k_8} + \frac{k_5}{k_4k_7}\right)\frac{1}{[\text{TMPD}]} + \frac{k_5}{k_6k_7}\frac{[H_2O_2]}{[\text{TMPD}]}} \quad (4.50)$$

$$\frac{2[\text{CPO}]_0}{v_{(\text{TMPD})}} = \frac{1}{k_4}\frac{1}{[H_2O_2]} + \left(\frac{1}{k_7} + \frac{1}{k_8} + \frac{k_5}{k_4k_7}\right)\frac{1}{[\text{TMPD}]} + \frac{k_5}{k_6k_7}\frac{[H_2O_2]}{[\text{TMPD}]} \quad (4.19)$$

Catalatic Activity:

$$v_{(O_2)} = d[O_2]/dt = k_6[\text{CPO-I-}H_2O_2] = k_5[\text{CPO-I}][H_2O_2]$$

$$= \frac{[\text{CPO}]_0}{\left(\frac{1}{k_4} + \frac{1}{k_5} + \frac{k_7}{k_5k_8}\right)\frac{1}{[H_2O_2]} + \frac{1}{k_6} + \frac{k_7}{k_4k_5}\frac{[\text{TMPD}]}{[H_2O_2]^2}} \quad (4.51)$$

$$\frac{[\text{CPO}]_0}{v_{(O_2)}} = \left(\frac{1}{k_4} + \frac{1}{k_5} + \frac{k_7}{k_5k_8}\right)\frac{1}{[H_2O_2]} + \frac{1}{k_6} + \frac{k_7}{k_4k_5}\frac{[\text{TMPD}]}{[H_2O_2]^2} \quad (4.20)$$